Free volume properties of semi-crystalline polymers

By

Muhamed Amer Sweed

Dissertation is presented in partial fulfillment of the requirements for the degree of PhD in Polymer Science at the University of Stellenbosch

Promoter: Prof. Peter Mallon

Department of Chemistry and Polymer Science

March 2011

Declaration

I, the undersigned, hereby declare that the work contained in this thesis is my own original work and that I have not previously in its entirety or in part, submitted it at any university for a degree.

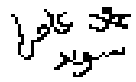

_____
Signature

Muhamed Amer Sweed
_____
Name in full

___15___/___02__/__2011_
Date

Abstract

Positron annihilation lifetime spectroscopy (PALS) is well established as a novel method currently available for the study of polymers at a molecular level because of its sensitivity to the microstructural changes in the polymer matrix. The technique provides unique, but limited, information of the solid state structure – primarily on the nature of the free volume (or unoccupied space) in the polymer due to the less dense packing of polymer chains relative to in other solid materials.

In the case of completely homogeneous polymer materials the measurement and interpretation of the positron annihilation parameters is relatively simple. However, in the case of polymers with more complex morphologies the situation becomes less clear. This is due to the possibility of the formation, localization and subsequent annihilation of o-Ps (ortho-positronium) within different areas of the complex morphology. This can result in more than one o-Ps lifetime component being present, and each of the different components corresponds to areas with differing types and amounts of 'open spaces'.

In this study a detailed and systematic approach was taken to study the positron annihilation parameters in various semi-crystalline polymers and to correlate these to the chain structure and morphology of the materials. The study focused specifically on polyolefin polymers as these are the most widely used semi-crystalline materials, but more importantly, they offer the possibility to produce a variety of morphological complexity by simple manipulation of the chain structure – while there is essentially no difference in the chemical composition of the materials. The copolymers were selected to study the influence of short-chain branching (amount and length), short-chain branching distribution and tacticity on the morphology, and subsequent positron annihilation lifetime parameters.

Three separate topics were addressed. First, preparative temperature rising elution fractionation was used to isolate polymer samples that are homogeneously crystallisable and to produce a series of polymers with differing chain structure and resultant morphologies. Second, additional series were produced by removing specific crystallisable fractions from the bulk materials. Third, the temperature variation of the samples as they approach and go through the crystalline melting point was studied.

All the raw positron data were found to be best fitted with a four-component positron annihilation lifetime analysis. The longest lifetime (which is attributed to annihilation of o-Ps in the amorphous phase of the materials) showed systematic variations with the degree and nature of the short-chain branding, tacticity variation, a combination of both short-chain branching and tacticity, and changes in the amorphous phase as a result of heating. The third lifetime component (which is attributed to o-Ps annihilation in or around the crystalline areas of the materials) showed less variation across the sample series. Typically, greater variations were observed in the propylene copolymers than in the ethylene copolymers, which are reflective of the more complex chain structure and corresponding morphology in the propylene copolymer series. Direct evidence for a contribution from the nature of the amorphous phase to the bulk microhardness of the sample was also found.

Opsomming

Positronvernietigingsleeftydspektroskopie (PALS) is goed gevestig as ‘n nuwe metode vir die studie van polimere op molekulêrevlak agv die sensitiwiteit van die metode vir mikrostrukturele veranderings in die polimeermatriks. Hierdie tegniek verskaf unieke, maar beperkte, inligting aangaande die vastetoestandstruktuur – veral aangaande die aard van die vryevolume (of onbesette spasie) in die polimeer as gevolg van die minder digte verpakking van polimeerkettings relatief tot in ander vastestowwe.

In die geval van volledig homogene polimeriese materiale is die meet en interpretasie van die positronvernietigingsparameters relatief eenvoudig. Maar in die geval van polimere met meer komplekse morfologieë is die situasie minder duidelik. Die rede hiervoor is die moontlikheid vir die formasie, lokalisering en gevolglike vernietiging van o-Ps (orto-positronium) in die verskillende areas van die komplekse morfologie. Dit kan tot gevolg hê dat meer as een o-Ps komponent teenwoordig is en waar elk van die verskillende komponente ooreenstem met areas met verskillende tipes en hoeveelhede 'oop spasies'.

In hierdie studie is ‘n sistematiese, in-diepte benadering gebruik om die positronvernietigingsparameters in verskeie semikristallyne polimere te bestudeer en hulle te korreleer met dié van die kettingstruktuur en die morfologieë van die materiale. Hierdie studie het spesifiek gefokus op poliolefiene aangesien hulle die mees algemene semikristallyne materiale is wat gebruik word en, nog meer belangrik, hulle bied die geleentheid om verskeie komplekse morfologieë te lewer dmv eenvoudige manipulasie van die kettingstrukture – terwyl daar basies geen verandering in die chemiesesamestelling van die materiale is nie. Die kopolimere is gekies om die invloed van kort-ketting vertakking (lengte en hoeveelheid), kort-ketting vertakking verspreiding en taktisiteit op die morfologie en vervolgens die positronvernietigingsleeftyd parameters te bestudeer.

Drie onderwerpe is aangespreek. Eerstens, preparatiewe temperatuurstygingelueringsfraksionering (prep-TREF) is gebruik om polimeermonsters wat homogeenkristalliseerbaar is te isoleer om sodoende 'n reeks polimere met verskillende kettingstrukture, en gevolglike morfologieë, te lewer. Tweedens, 'n

addisionele reekse monsters is berei deur die verwydering van spesifieke kristalliseerbare fraksies vanaf die grootmaatmonsters. Derdens, die temperatuurverandering van die monsters wanneer die monsters naby aan die kristallyne smeltpunt is en wanneer hulle deur die kristallyne smeltpunt gaan is bestudeer.

Daar is bevind dat alle rou positrondata ten beste gepas het in 'n vier-komponent positronvernietigingsleeftydanalise. Die langste leeftyd (wat toegeskryf is aan vernietiging van o-Ps in die amorfe fase van die materiaal) het sistematiese variasies getoon met die volgende: hoeveelheid en aard van die kort-kettingvertaking, verandering in taktisiteit, 'n kombinasie van beide kort-kettingvertakking en taktisiteit en veranderings in die amorfiesefase as gevolg van verhitting. Die derde leeftyd komponent (wat toegeskryf is aan die o-Ps vernietiging in of rondom die kristallyne areas van die materiale) het minder variasie in hierdie reeks monsters getoon. Daar is tipies meer variasie waargeneem in die propileenkopolimere as in die etileenkopolimere, wat ’n weerspieëling is van die meer komplekse kettingstruktuur en ooreenstemmende morfologie in die propileenkopolomeerreeks. Direkte bewys vir 'n bydrag van die aard van die amorfe fase tot die grootmaat mikrohardheid van monsters is ook bevind.

This thesis is dedicated to my parents (ZAZIA & AMER) for their love, trust and support through my study career, to my wife for here support and to my family.

Acknowledgements

-Would like to extend my heartfelt thanks to the following people and companies for their help in making this project possible:

- Prof Peter Mallon (study leader) for his leadership during my study and for his interest in the field.

-Libyan government / Center for macromolecular chemistry and technology Tripoli-LIBYA, for allowing me the opportunity to do studies in South Africa to acquire the necessary skills and knowledge, and for their financial support during my study.

-SASOL Polymer for material supply.

-Dr. Margie Hurndall for her help with editing this thesis.

- Prof Mallon's group for their support and help.

-All my friends and colleagues for their support- especially Ali Rashed, Sami Ouda and Abd Almonmem Baleg.

- To my parents - for their continuing support throughout my studies, to my brothers and sisters for their constant, unwavering support throughout my studies.

Table of Contents

List of Figures

Chapter 2:

Chapter 3:

Chapter 4:

Chapter 5:

Chapter 6:

List of Tables

Chapter 3:

Chapter 4:

Chapter 5:

Chapter 6:

List of Abbreviations

ΔH_f	Enthalpy of fusion
ΔH_{fc}	Enthalpy of fusion of ideal 100% crystalline polypropylene
ΔT	Difference in temperature
^{13}C	Carbon thirteen
σ_e	Free surface energy
A-TREF	Analytical temperature rising elution fractionation
CRYSTAF	Crystallisation analysis fractionation
DSC	Differential scanning calorimetry
GFC	Gel filtration chromatography
GPC	Gel permeation chromatography
HDPE	High density polyethylene
HT-GPC	High temperature gel permeation chromatography
I_i	Intensity of τ_t lifetime
l_w	Weight average lamellar thickness
LDPE	Low density polyethylene
M_n	Number average molar mass
MFR	Melt flow rate
M_w	Weight average molar mass
MMD	Molar mass distribution
MSL	Methylene sequence length
NMR	Nuclear magnetic resonance spectroscopy
PALS	Positron annihilation lifetime spectroscopy
PE1	Linear low density polyethylene (octane comonomer)

PE2	Linear low density polyethylene (hexane comonomer)
PD	Polydispersity
PP	Polypropylene
RI	Refractive index
SEC	Size exclusion chromatography
SCB	Sort chain branching
T_c	Crystallisation temperature
TCB	Trichlorobenzene
T_e	Elution temperature
T_g	Glass transition temperature
T_m	Melting temperature
TREF	Temperature rising elution fractionation
WAXD	Wide-angle x-ray diffraction
W_i	Weight fraction
W_i%	Weight fraction percentage
τ_1	Shortest lived component
τ_2	Intermediate component
τ_3	Third component
τ_4	Longest lived component

Chapter 1
Introduction and objectives

1.1 General introduction

The use of positron annihilation lifetime spectroscopy (PALS) in the study of polymer properties has seen a remarkable increase. This is due to the unique information that can be provided about the local free volume (holes) that appear in a polymer microstructure due the structural disorder. These holes can reduce the density of the amorphous polymer by about 10% compared with the crystalline state of the same material, resulting in a great effect on the thermal and mechanical properties of polymers.

The successful application of PALS as a technique to study the structural characteristics of amorphous polymers has been proved in many studies [1-4]. It has been shown that the positron (Ps) is formed in subnanometre size holes of the excess free volume in amorphous polymers [5].

In semi-crystalline polymers the situation appears to be much more complex, where at least three different regions must be considered: the amorphous, crystalline and interfacial or defects in crystalline regions. The crystallite segments in semi-crystalline polymers are connected to the surrounding amorphous material through chain segments in which the crystalline order is partially maintained into the amorphous phase. Because of the defects in the crystallites themselves, which arise from the extensive chain entanglements of molecules, a definite point of discontinuity between the crystalline and amorphous regions is not possible. When these materials are probed using positron annihilation spectroscopy, there is a probability of o-Ps forming within the open spaces of both the amorphous regions and possibly within the intermediary regions as well. It is generally accepted that no o-Ps formation occurs in the perfectly crystalline regions

themselves due to the close packing. Because of the possibility of o-Ps formation in different regions of the morphology, the interpreting of PALS data is not as simple as in the case of homogenously amorphous material. This accounts for the fact that there is no clear consensus in the literature as to how many lifetimes can be resolved in semi-crystalline polymers [6].

Many studies have been reported in the literature concerning this topic [7-10]. However, many of these studies lack information on the detail of the microstructure of the material, and in many cases use poorly defined commercial polymers. In the present study, it was considered important to study the positron annihilation parameters as measured by positron annihilation lifetime spectroscopy on semi-crystalline polymers in order to achieve a better understanding of the relationship between the molecular structure, the measured positron annihilation parameters and final material properties. The overall aim of the present study is, therefore, to add insight and understanding of the influence of the polymer microstructure on the measured free volume properties of semi-crystalline polymers with the ultimate goal of contributing to the understanding of the structure-property relationship in these materials. It is also hoped to provide some clarity as to the interpretation of the various positron annihilation parameters and how they relate to real physical structures or differences in the often complex morphology of semi-crystalline materials.

In this study several different semi-crystalline polymers were selected on the basis of their structural variables. The study focused specifically on polyolefin polymers since these are the most widely used semi-crystalline materials but more importantly they offer the possibility to produce a variety of morphological complexity by simple manipulation of the chain structure but essentially have no difference in the chemical composition of the materials. Specifically is well known that the type and nature of short chain branching as well as tacticity (specifically in the case of polypropylene) to a large degree controls the degree and nature of the crystalline or ordered structure in these materials. The relationship between the measured positron annihilation parameters, free volume properties and microstructural variables are investigated in a systematic approach. This study will by its nature be complex because of the multiplicity of structural species

present. Characterization of the selected copolymers is by no means easy, since there is more than one factor (tacticity, comonomer, crystallinity) that may affect the microstructure.

In the present study, a novel approach to that used in many previous studies on semi-crystalline polymers was undertaken. In previous studies reported, microstructurually heterogeneous materials were used and studied. In many case these studies were done on poorly defined commercial materials. The present study takes a different approach in that it makes use of preparative fractionation of bulk copolymers to isolate microstructurually homogenous fractions (at least with respect to one property). This allows for a systematic study of the relationship between the chain microstructure and the measured positron annihilation parameters. This approach also produces a systematic series of samples of differing crystallinities and morphologies. Such systematic series are essential to the development of an understanding of positron annihilation parameters in polymers with complex morphologies and are needed to provide insight as to the interpretation of the various annihilation parameters.

As has been mentioned previously, the PALS technique provides unique, but very limited, information on materials. It can certainly be considered as an information poor spectroscopic technique when compared to other techniques such as FTIR and NMR. Because of such limited information, and the need in the case of complex morphologies to interpret the information obtained, it is only when a systematic series of samples are studied that this technique is useful and provides insight into the structure property relationships.

The first part of this study focuses on the relationship between the measured free volume and the short chain branching in metallocene linear low density ethylene copolymers (LLDPE). In this study the degree and type of short chain branches are investigated. The study is then extended to study the effect of tacticity as well as short chain branching in propylene and propylene copolymers. In each of the studies the morphologies and composition of the materials are varied by preparative fraction as well as by using preparative fractionation to remove certain fractions from the bulk materials.

In the last part of the study, the morphology of the various samples is varied by studying the materials at different temperatures, primarily at temperatures reaching the melting points in the materials. This study was done to provide further insight into the variation in the different positron annihilation parameters close to or in the melting range.

1.2 Objectives

The main objectives of the study can be summarized as follows:

a) Select suitable series of semi-crystalline polymers which will allow for a systematic study of the relationship between chain structure, morphology, positron annihilation lifetime parameters and the resultant measured free volume properties.

b) The materials will be selected in order to study the effects of, i) short chain branching, ii) variation of tacticity iii) variation in both tacticity and short chain branching.

c) Use preparative fractionation to isolate crystallizably homogeneous fractions from the bulk material.

d) Use the fractions to produces systematic series of samples of varying chain structure and resultant morphologies.

e) Perform the positron annihilation measurements on very well characterized polymer fractions in order to study the variation in the positron lifetime parameters across the systematic series.

f) Correlate the measured positron lifetime parameters with the bulk physical properties of each of the polymer series.

g) Extend the investigation by producing polymer series where selected crystallizable fractions are removed from the bulk polymer samples and in

so doing produce different polymer series with different crystal morphologies from the same bulk polymer.

h) Investigate the variation in the measured positron annihilation parameters as the various copolymers approach the crystalline melting point.

i) Ultimately the objectives set out above aim to provide better insight into the measurement and ultimate interpretation of the measured positron annihilation lifetime parameters in morphologically complex semi-crystalline materials and correlate these measured parameters to specific morphological and structural variables. In so doing it is hoped to shed light on the application of the positron annihilation lifetime spectroscopy technique as a tool for measurement of free volume in semi-crystalline materials as well contribute to an understanding of the fundamental structure-property relationship in commercially important semi-crystalline materials. .

1.3 Layout of the document

This dissertation comprises eight chapters. Chapter 1 includes a brief introduction, which sets out the overall objectives of the study.

Chapter 2 provides a literature review including a brief background on polyolefins (arguably the most important class of semi-crystalline polymers) and free volume properties, and the related work done on various semi-crystalline polymers by others in the field.

Chapter 3 contains the experimental details of the study.

Chapter 4 focuses on the effect of comonomer length on the measured free volume properties of linear low density polyethylene, followed by the affect of removal of the TREF fraction on the overall properties of the linear low density polyethylene.

Chapter 5 discusses the influence of tacticity and short chain branching on the measured free volume parameters in polypropylene and propylene copolymers, followed by the affect of removal TREF fraction on the overall properties of propylene copolymers.

Chapter 6 discusses the variation in the measured free volume properties as the copolymers approach their melting point. A brief discussion of the effects of exposure time to the positron source on the measured annihilation parameters is also included in this chapter.

Chapter 7 provides the overall conclusions of the study and presents suggestions as to the interpretation and reliability of the positron annihilation parameters and their relationship to real physical structures within the materials.

1.5 References

1. Zelkó, R., Orbán, Á. and Süvegh, K. Journal of Pharmaceutical and Biomedical Analysis 2006, 40, 249-254.
2. Consolati, G., Kansy, J., Pegoraro, M., Quasso, F. and Zanderighi, L. Polymer 1998, 39, 3491-3498.
3. Lu, W., Yang, L., Yan, B. and Huang, W-H. Materials Science and Engineering: B 2006, 128, 179-183.
4. Mohamed, H F M., Abdel-Hady, E E. and Mohamed, S S. Radiation Physics and Chemistry 2007, 76, 160-164.
5. Baugher, A H., Kossler, W J. and Petzinger, K G. Macromolecules 1996, 29, 7280-7283.
6. Jean, Y C., Mallon, P E. and Schrader, D M. Principles and Applications of Positron & Positronium Chemistry; World Scientific: New Jersey, 2003.
7. Sudarshan, K., Rath, S K., Patri, M., Sachdeva, A. and Pujari, P K. Polymer 2007, 48, 6434-6438.
8. Nahid, F., Beling, C D. and Fung, S. Physica Status Solidi (c) 2007, 4, 3751-3754.

9. Abdel-Hady, E E., Mohamed, H F M. and Fareed, S S. Radiation Physics and Chemistry 2007, 76, 138-141.
10. Djourelov, N., Suzuki, T., Shantarovich, V P., Dobreva, T. and Ito, Y. Radiation Physics and Chemistry 2005, 72, 13-18.

Chapter 2
Theoretical background

2.1 Semi-crystalline polymers

Polymers can be classified as crystalline, semi-crystalline or amorphous depending on their degree of crystallinity. A crystal can in a broad sense be defined as an orderly arrangement of atoms in space on what is called a crystal lattice [1]. Polymers that are able to crystallize under suitable temperature conditions are called crystallizable polymers. The primary transition temperature, when a crystalline polymer transforms from a solid to a "liquid", is the melting temperature designated T_m. The phase transition for this type of polymer occurs from the glassy state to the rubbery state at a temperature termed the glass transition temperature, often designated T_g. Most thermoplastics have both a T_g and T_m. This is because it is relatively difficult to get to the extreme case of a completely crystalline polymer, with an ideal formation of single crystals, having the relative arrangement of atoms strictly the same throughout the volume. In fact, deviations from the completely ordered arrangement as well as the completely disordered arrangement always exist. Thus, it is the degree of crystallinity that actually determines whether a polymer can be classified as a crystalline, amorphous or a semi-crystalline polymer. Most polyolefins are semi-crystalline. Their morphologies are governed by molecular characteristics and preparation conditions [2].

Semi-crystalline polymers constitute one of the most rapidly growing areas in materials science research. Semi-crystalline polymers are essentially composite materials with alternating crystalline and amorphous regions. Most semi-crystalline polymers are able to undergo both large strains and high stresses over a wide temperature range, while still retaining their good chemical stability. Controlling the crystallization conditions allows one to control the semi-crystalline morphology, and consequently the material

properties of the final product. This has made semi-crystalline polymers such as polyethylene, PP, polyethylene tetrephthalate and polyamides some of the most widely used industrial and commodity polymers [3].

2.2 Polyolefins

Polyolefins have the simplest chemical structure of all polymers. They have been used as the choice of materials for a broad spectrum of applications, with low cost and ease of processing, due to their properties. Their variety of properties is largely due to the branch concentration and distribution, which provides a diversity of chain structures that is reflected in their morphology and miscibility. Polyolefins are environmentally friendly hydrocarbon materials, produced in energy-efficient catalytic processes without the formation of by-products.

Today polyolefins hold first place (55%), in the world's production of synthetic materials; where the global production of polyolefins has grown to about 46 million metric tons per year [4, 5]. There are several reasons for this; the availability of raw material, their versatility with respect to physical and mechanical properties, their non-toxicity, their energy efficient and economic production, their excellent combination of mechanical and chemical properties, and recyclability. Among the commodity polymers, polypropylene (PP) has shown the highest growth rates. Its unique combination of mechanical properties, ease of processing, and low cost have enabled this polymer to be used in such diverse applications as films, injection molding of household goods, fibres, coatings and adhesives [6-8] . The properties of PP depend largely on the microstructure, the molecular weight and the molecular weight distribution which can be tuned over a wide range to fit the desired application [9-11].

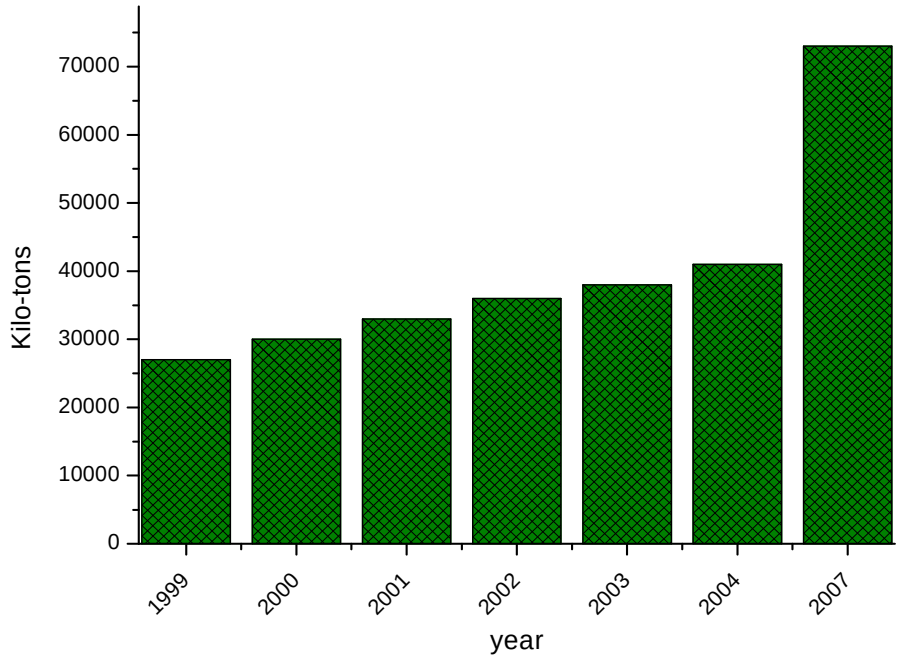

Figure 2.1 Historical world wide polypropylene consumption [12, 13].

Polyolefins are produced commercially using free radical initiators, Phillip's type catalysts and Ziegler-Natta catalysts. Ziegler-Natta catalysts, the most important catalyst type, have evolved significantly since their inception in the 1950s, with large improvements in activity, stereo-selectivity and versatility [14-16]. These catalysts are used extensively in gas phase and slurry phase reactions for the production of a wide range of polyolefins. Polymers produced with Ziegler-Natta catalysts inevitably have broad molecular weight distributions and, in the case of copolymerizations, broad chemical composition distributions. This phenomenon is generally attributed to multiple active sites of the catalysts, each with distinct polymerization properties [14, 17].

The increasing use of PP for different applications requires a good combination of properties over a wide temperature range[12]. Although isotactic PP (i-PP) has many outstanding thermal, physical and mechanical properties, one of its disadvantages is its reduced low-temperature impact strength. One method for improving the impact properties of i-PP is by copolymerization with other olefins, such as ethylene or pentene. The introduction of a small amount of comonomer units into the macromolecular chain of

i-PP will decrease the length of the isotactic segments, leading to a reduced melting temperature and degree of crystallinity [18]. Random propylene copolymers with low ethylene content are commercially important materials because they have improved properties, such as improved clarity, flexibility, toughness, and melt flow rate, without their desirable properties being significantly reduced [19, 20].

2.2.1 Polyethylene

PE is the simplest synthetic polymer. The basic structure of PE is the chain –$(CH_2–CH_2)_n$–, which has no substitute groups, i.e., branches on the backbone [21-24].

PE was synthesised for the first time in 1933 in the laboratories of ICI (Imperial Chemical Industries), where Fawcet and Gibson performed the reaction between ethylene and benzaldehyde in a high-pressure autoclave and reported that "a waxy solid was found in the reaction tube"[25-28]. The "waxy solid" was PE, presently referred to as low density PE (LDPE). During this polymerisation reaction, intra- and intermolecular chain transfer reactions occurred, leading to short- and long-chain branches respectively. Due to the high content of the branches, the chains are unable to pack closely inside the crystals, resulting in a material possessing a rather low density. This material is still extensively used, e.g. for packaging purposes, due to its ease of processing because of its long chain branching. The polymerisation of ethylene under low pressure became possible 20 years later, when Ziegler and Natta reported the importance of the stereo-regulating catalyst in synthesis of various monomers at relatively lower pressures and low temperatures compared to the synthesis of LDPE [29]. The resulting ethylene based polymer, synthesised using the novel stereoregulating catalyst system, was high density PE (HDPE), which has more linear chains, and consequently possessed a much higher density. The low pressure processes, using specific catalyst systems, were not restricted to the production of the linear polymer systems. Lower density products of PE could also be obtained by incorporating higher olefins, like propylene, 1-butene, 1-hexene, 1-octane, etc., which led to chains possessing short-chain branches. The copolymers synthesised in

this way are usually referred to as linear low density PE (LDPE), or with increasing the comonomer content, very low density PE (VLDPE) [30].

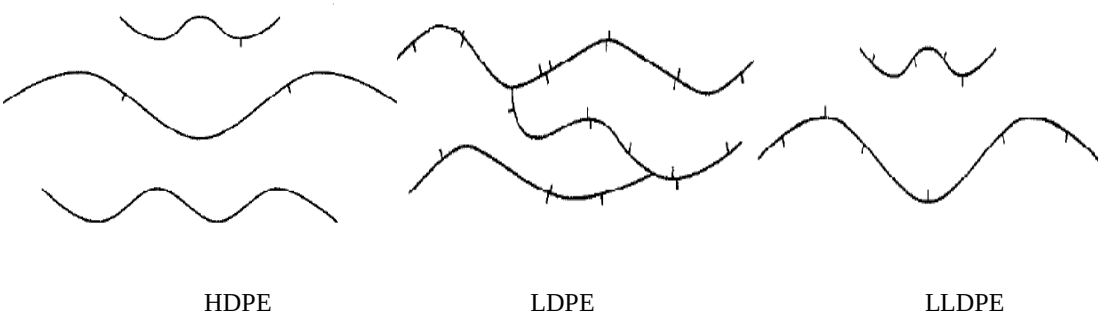

Figure 2.2 Structures of LDPE, HDPE and LLDPE.

2.2.2 Polypropylene

PP is a thermoplastic material that is produced by polymerizing propylene molecules (the monomer units), into very long polymer molecules or chains [12]. There are a number of different ways to link the monomers together, but PP as a commercially used material in its most widely used form is made with catalysts that produce crystallizable polymer chains. These afford a product that is a semi-crystalline solid with good physical, mechanical, and thermal properties. Another form of PP, produced in much lower volumes as a by-product of semi-crystalline PP production and having very poor mechanical and thermal properties, is a soft, atactic material used in adhesives, sealants, and caulk products [31].

Semi-crystalline PP is a thermoplastic material containing both crystalline and amorphous phases. The relative amount of each phase depends on structural and stereochemical characteristics of the polymer chains and the conditions under which the resin is converted to final products such as fibers, films and various other geometric shapes, during fabrication by extrusion, thermoforming or molding.

PP has excellent chemical, and good physical, mechanical and thermal properties when used in room temperature applications [32]. It has a relatively high melting point (about 140 °C), it is stiff, hard and resistant to abrasion and a comparatively good resistance to impact. These properties can be varied in a relatively simple manner by altering the chain regularity (tacticity) content and distribution, as well as changing the average chain lengths, the incorporation of a comonomer such as ethylene into the polymer chains, and the incorporation of an impact modifier into the resin formulation [12].

PP (PP) was first produced by G. Natta, following the work of K. Ziegler, by the polymerization of propylene monomer in 1954. A typical macromolecule of PP contains l0, 000 to 20,000 monomer units. The steric arrangement of the methyl groups attached to every second carbon atom in the chain may vary [33-35].

In industry, the term PP is generally meant to refer to the following types of compounds:

1. Homopolymers – Polymers of propylene only

2. Copolymers

- Random copolymers – small quantities of comonomer are inserted randomly in the polymer chain.

- Impact copolymers – also referred to as hetero-phase copolymers. They include Ethylene Propylene Rubber (EPR) dispersed in the PP matrix.

Each of the different types of polymers is briefly discussed in the following section.

2.2.2.1 Homopolymers

Homopolymer PP is made by polymerizing propylene in the presence of a stereo-specific catalyst. Homopolymers are more rigid and have better resistance to high temperatures than copolymers, but their impact strength at temperatures below zero is limited [12, 19, 36].

Homopolymers differ only in their molecular weights and defect content. Sometimes certain additives are mixed with the polymer to attain desirable properties. Homopolymers are generally injection moulded into small items, where low temperature impact strength is not critical, such as for bottle caps and syringes [37].

2.2.2.2 Copolymers

The properties of PP copolymers depend on the type and amount of comonomer. There are two basic types: random copolymers and block copolymers. The random polymers contain 1.5 to 6% by weight of ethylene or higher alkenes (such as butene-1 in random distribution and in a single chemical phase). The essential difference between a random and a block copolymer is that the block copolymer contains comonomer in the form of a dispersed rubber phase. Typical applications of copolymerised PP are battery cases, bumper tiller supports, interior trim, glove boxes, etc.[22, 33]

A. Random copolymers

Random copolymers are α-olefins propylene copolymers that are made in a single reactor by copolymerizing propylene and small amounts of ethylene (usually 7% and lower). The copolymerized ethylene changes the properties of the polymer chains significantly and results in thermoplastic products that have slightly better impact properties, improved clarity, a wider range of heat sealability, decreased haze, decreased melting point, and enhanced flexibility [19]. The ethylene monomer in the PP chain manifests itself as a defect in the chain regularity, thus hindering the chains crystallizability. As the ethylene content increases, the crystallite thickness gradually decreases, and this manifests itself in a lower melting point. The amount of ethylene incorporated into the chain is usually dictated by the balance between thermal, optical, and mechanical properties [33].

Random copolymers have generally lower melting points, improved optical properties and lower modulus. Because of their improved optical properties, they find use

as packaging materials [38]. These copolymers are also used in auto bumpers for their energy absorbing capacity and low density.

B. Block copolymers

Block copolymers are a special type of polymer in which each molecule consists of two or more segments of simple polymers (blocks) joined in some arrangement. PP homopolymer is copolymerized with ethylene. In block copolymers the ethylene content is much higher than in random copolymers. The copolymerized part of the material is rubbery and forms a separate dispersed phase within the PP matrix. As a result, block copolymerized PP is much tougher than homopolymerised PP and can withstand higher impact, even at low temperatures, but at the expense of transparency and the softening point. The main applications of block copolymerised PP are similar to those of elastomer-modified PP, but where the impact property requirement is not that critical [39-41].

The two most critical features of a base PP are its molecular weight and its tacticity (polymer chain configuration). Molecular weight has the strongest influence on processing characteristics, and the main influence of tacticity is on the physical properties [9, 33, 42] of the materials.

2.2.3 Tacticity of polypropylene

Tacticity is the term used to describe the stereoregularity in a polymer chain structure. It is best defined using PP as an example. PP consists of propylene connected in three different ways. Propylene is similar to ethylene except that a methyl (CH_3) group replaces one of the hydrogen. Propylene monomers are combined in the same way as ethylene monomers to form the polymer [43-45]. There are three types of PP: see Figures 2.3-2.5.

2.2.3.1 Atactic polypropylene (PP)

This type of PP has random placement of the CH_3 groups along the backbone [44]. This type of PP has not been traditionally useful in industry: however, today there are growing markets for hot melt adhesives and low molecular weight processing aids

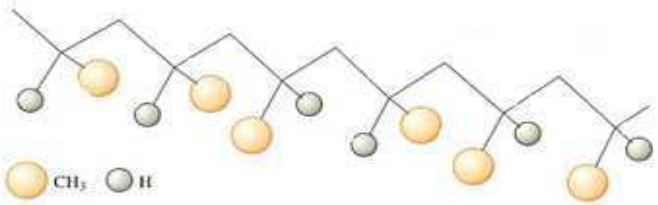

Figure 2.3 Atactic polypropylene.

2.2.3.2 Syndiotactics polypropylene

In syndiotactic PP (s-PP) the methyl group alternate from one side to the other and produces chains that can be easily packed to form a highly crystalline, harder plastic. This is a flexible structure with good impact resistance and clarity [10].

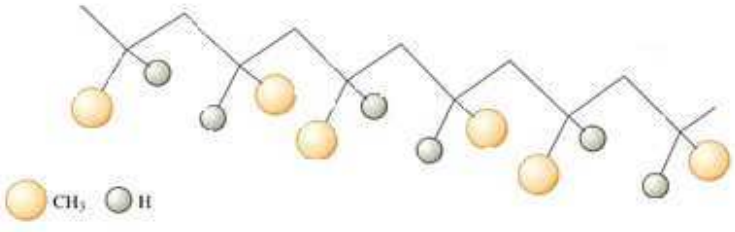

Figure 2.4 Syndiotactic polypropylene.

2.2.3.3 Isotactic polypropylene

Isotactic PP (i-PP) consists of the carbon backbone with the -CH_3 groups attached predominately in the same relative configuration (same side). i-PP is one of the most important commercial polymers. Since the discovery of Ziegler-Natta catalyst systems and their subsequent industrial application, i-PP has received increasing scientific and commercial attention.

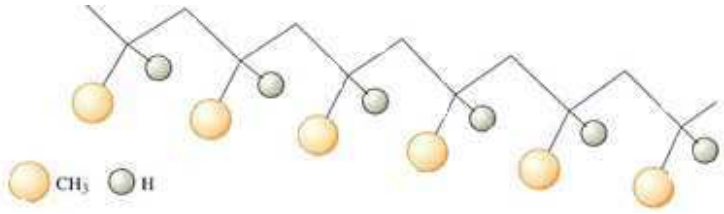

Figure 2.5 Isotactic polypropylene.

In both isotactic and syndiotactic configurations, the polymer chains pack more closely and more uniformly, leading to a high degree of crystallinity. For example, i-PP has a melting range of 110-160°C, whereas s-PP melts at 138°C. This leads to a greater strength and rigidity in PP which result in a wide range of applications.

2.3 Ziegler-Natta and metallocene catalysts

Transition metal catalyzed olefin polymerisation is playing a key role in the development of new versatile and environmentally friendly polymeric materials, including both commodity and specialty polymers [46].

Ziegler-Natta polymerisation is a widely used industrial process for olefin polymerization in both a homogeneous and a heterogeneous system. It produces linear polyolefins of variable molecular weights and tacticities. The catalyst system, developed by Ziegler-Natta in 1953, is still being used for the production of common polyolefins [47]. This catalyst is based on titanium tetrachloride and tri-methyl-aluminium co-

catalyst. A Ziegler-Natta catalyst has several active centres, each of which creates a different polymer (different in terms of molecular weight, comonomer content or tacticity). PP is a good example of stereo-specificity [29].

Although PE can be made by several methods, propylene and higher olefins can only be polymerized to high molecular weight, linear polymers by the use of transition metal catalysts, usually Ziegler-Natta catalysts. In addition, Ziegler-Natta catalysis is one of the few methods capable of stereo-regularly polymerizing of α-olefins [48].

Polyolefin development dates back to the early 1930s with the production of LDPE by free radical initiations [29, 49]. In 1953, the first actual Ziegler polymerisation used zirconium acetylacetonate and $AlEt_{3,}$ to form high molecular mass linear PE. The process was soon improved by the use of $TiC1_4$ and $AlEt_3$. The transition metal coordination polymerisation can take place at ambient temperature and under low pressure conditions. The PE (HDPE) produced has a linear molecular structure with a very low concentration of branches, high density, high crystallinity and high melting point.

In 1954, Natta and Montecatini realized that the Ziegler catalyst is capable of stereo-regularly polymerizing α-olefins, such as 1-propene, into a polymer with stereoregular repeating units[29, 50].

In 1957 PP was taken into commercial production [9, 51]. Since then major developments in the production and applications of PPs have occurred. The polymer yield of this catalyst has increased enormously, from 0.8 kg/(gram catalyst) to more than 100 kg/(gram catalyst), along with a significant increase in isotacticity, over four different generations of the Ziegler-Natta catalyst system [47].

Metallocenes are soluble and well defined. They are termed ‘single-site’ catalysts, as opposed to the conventional heterogeneous Ziegler-Natta catalyst that has a multiplicity of reaction sites that differ in activity [14]. Where as the Ziegler-Natta based polymers have broad molecular weight distributions and uneven comonomer distributions (for ethylene-hexene copolymerization, for example), the metallocene based polymers

have much better controllable, narrow molecular weight distributions and uniform comonomer distributions. The reason for this is that the metallocene catalysis is homogeneous in contrast to the heterogeneous Ziegler-Natta catalysts.

2.4 Relationship between molecular structure and properties of semi-crystalline polymers

The properties of a polymer in both the solid state and molten state depend on its chain molecular structure [52]. Specifically, the properties of semi-crystalline polymers depend on such molecular parameters as molar mass, molar mass distribution, short chain branching (SCB), short chain branch distribution (SCBD) and tacticity. These parameters affect chain movements and thus chains crystallization. As an example, the high flexibility of LLDPE stems from its short chain branches. For a given average SCB content, a broad SCBD indicates a greater amount of low SCB molecules with low flexibility. As a result a metallocene LLDPE with narrow SCBD has higher flexibility than a Ziegler-Natta LLDPE. Many authors have discussed the relationship between structure and properties of semi-crystalline polymers [53-64]. Bubeck in his review [65], discussed recent work done on the relationship between the structure and properties of semi-crystalline polymers. He concluded that the type of chain branch architecture largely determine the polymer properties.

The relationship between molecular structure and physical properties of LLDPEs produced with Ziegler-Natta and metallocene catalysts has been discussed by Todo [66]. He concluded that the comonomer content of Ziegler-Natta LLDPE varies according to the length of the main chain of the polymer. Small LLDPE molecules tend to have a higher concentration of comonomers than large LLDPE molecules. The small molecules are undesirable fractions that decrease performance, such as high blocking characteristics and low clarity of the film. In comparison, metallocene LLDPE shows very narrow molar mass distribution and composition distribution, and exhibits improved properties, such as high impact strength, high stress crack resistance, high clarity, and low heat seal temperature. On the other hand, tacticity plays a large role determining the properties of PP, especially the ability of the chains to crystallize [67].

Kim et al. [68] investigated the processability of various types of commercial PEs with respect to their molecular structure by measuring their melt rheology and thermodynamic properties. They show that SCB mainly controls the density and thermodynamic properties, but it has little effect on the melt rheology properties. On the other hand, long chain branching (LCB) has little influence on the density and thermodynamic properties, but has a large affect on the melt rheology properties - viscosity is reduced- thus improving the processability. They concluded that a very small amount of LCB in metallocene LLDPE can effectively reduce the viscosity and improve the flow stability during processing.

The physical, thermodynamic and rheological properties of LLDPE are a strong function of its molecular structure. Two LLDPEs could exhibit widely different properties even if they have similar melt flow indexes (MFI), densities, or average SCB contents [69]. That is primarily due to the fact that other molecular parameters, such as SCBD, may have a significant impact on the properties. Hence, the interpretation of the structure-property relationship would largely depend on a detailed characterization of the molecular structure of polyolefins.

2.5 Polymer crystallization

2.5.1 Amorphous and semi-crystalline polymer

There are mainly two important types of polymers: amorphous and semi-crystalline. Amorphous polymers have no order with respect to their internal arrangement; their constituent chains are tangled up in various ways. Semi-crystalline polymers usually have a lamellar structure in which thin ribbon-like crystals are constructed from molecule segments in the manner shown in Figure 2.6. The molecules fold at the surface but do not necessarily re-enter at the adjacent site. Molecules pass through the crystal phase and the surrounding amorphous phase, providing strong adhesion between the two phases. Long range mechanical integrity is provided by “tie molecules” that enter more than one of the crystal lamellae, connecting them across the intervening amorphous material, and by molecular entanglements within the amorphous

phase. A rough distinction can be made between the two types of polymers by plotting the specific volume against temperature. In the case of amorphous, there is only the glass transition temperature, T_g, separating the glassy and rubbery phases. In case of semi-crystalline polymer, there is T_g and also the melting temperature T_m, associated with the crystalline fraction of the polymer.

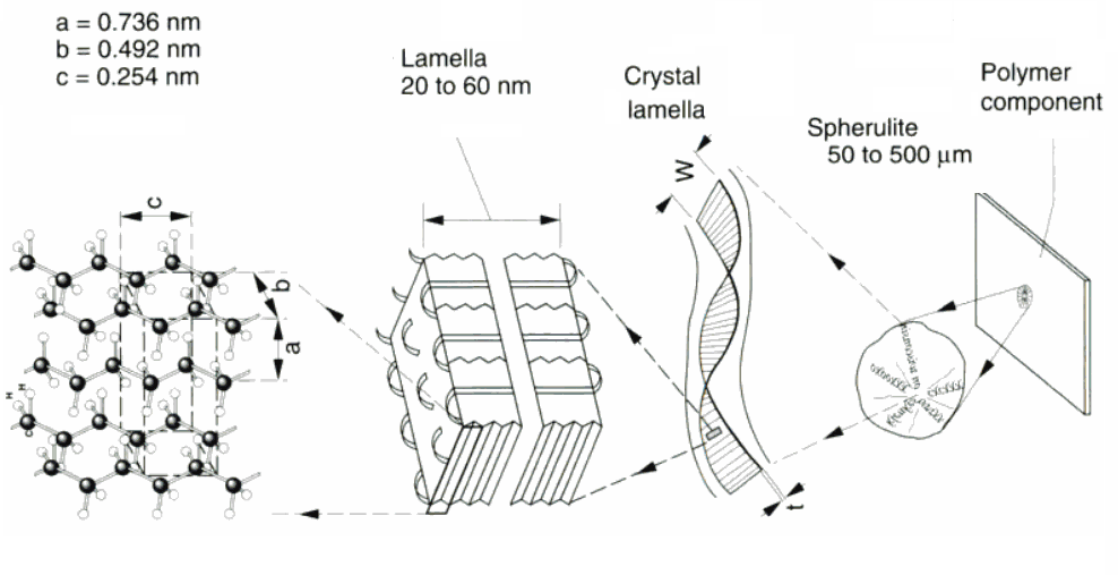

Figure 2.6 Schematic representation of the general molecular structure and arrangement of typical semi-crystalline polymers [70, 71].

Polymer crystallization is controlled by various factors, such as the regularity of the polymer structure, presence of substituents, comonomers, branching, molecular weight and chain flexibility. The crystallization process is also affected by experimental conditions, such as temperature, pressure, nucleating agents, and stress [72].

2.5.2 Requirement for polymer crystallization

For crystallization to occur in a polymer, the requirement is the presence of a regular chain structure, combined with a high mobility of chains at the crystallization temperature. This means that the polymer has a higher capability to orient itself, thus rendering a structure with a high percentage of crystallinity. A main issue is the number

of branches along the chain, which is strongly related to the industrial method of polymerization. Another important factor is the steric isomerism and stereo-regularity, which influence the mechanism of crystallization and hence the properties of the end product.

2.5.3 Effect of molecular structure, crystallization, and processing on the end product

The properties and performance of polymeric materials depend not only on their chemical composition, but also on their structure and morphology that develops during processing. As it can be seen in Figure 2.7, there is a strong relationship between the molecular structure and the properties of the end product. Understanding the effect of these structures and processing variables on the polymer morphology is essential, because it is the morphology that largely determines the polymer properties.

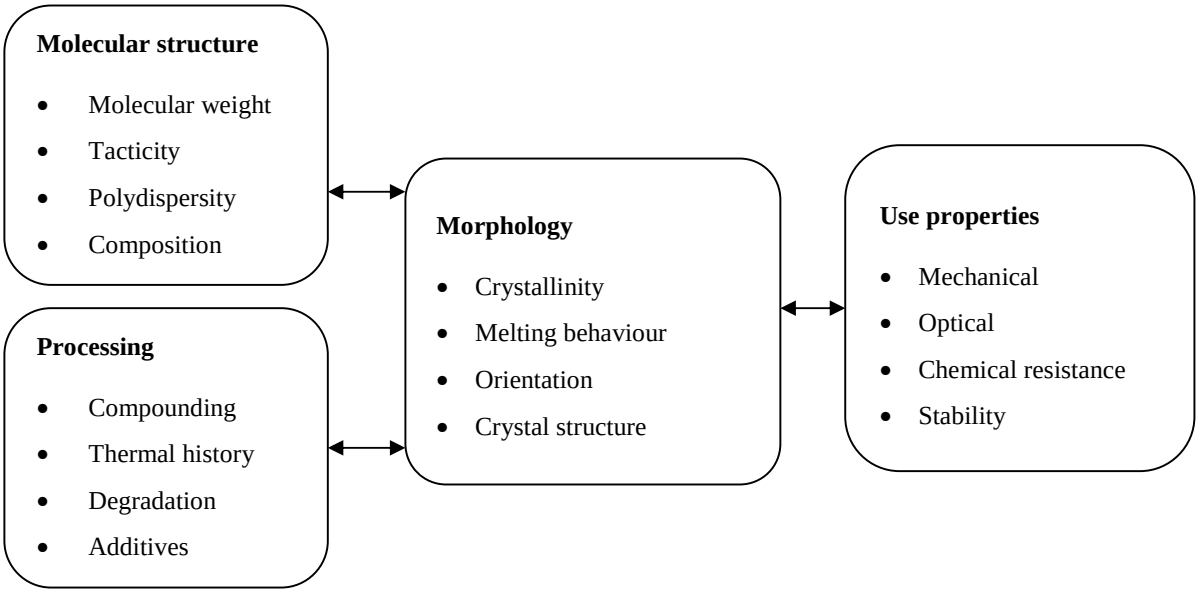

Figure 2.7 The influence of molecular structure, morphology, crystallization, and processing of the end product.

The degree of crystallinity and crystal structure in a polymer depends on its thermal history. The annealing or slow cooling of a product leads to a rather brittle and hazy product; however, rapid quenching produce a tough clear product as it suppresses the formation of crystals. Increased crystallinity increases polymer strength, hardness, modulus, abrasion and wear resistance, harrier properties, shrinkage and density. Low crystallinity offers the advantages of good processability, better transparency, good thermoforming capability, and economical melt processing [19].

The crystalline and amorphous phases have very different properties and the mechanical properties depend strongly on the fraction of material in each phase. Thus, it is of importance to have methods to measure the crystallinity. This can be done using DSC, and density measurements, but also by other methods such as WAXD, and various spectroscopic techniques [73].

2.5.4 PE crystallization

PE is among the most readily crystallizable polymers. It has a relatively flexible backbone that allows the chain ample rotational freedom to configure itself into the preferred trans planar conformation for crystallization. The crystal structure of PE is shown in Figure 2.8.

PE primarily crystallizes to form an orthorhombic unit dimensions a = 0.742, b = 0.495 and c =0.225 nm, and the angle between the zigzag backbone and b axes is 45º. By convention, the c-axis of the unit cell is defined to be parallel to the chain axis. It has been found that for PE crystallization, addition of unit cells occurs most rapidly along the b crystallographic axis [74].

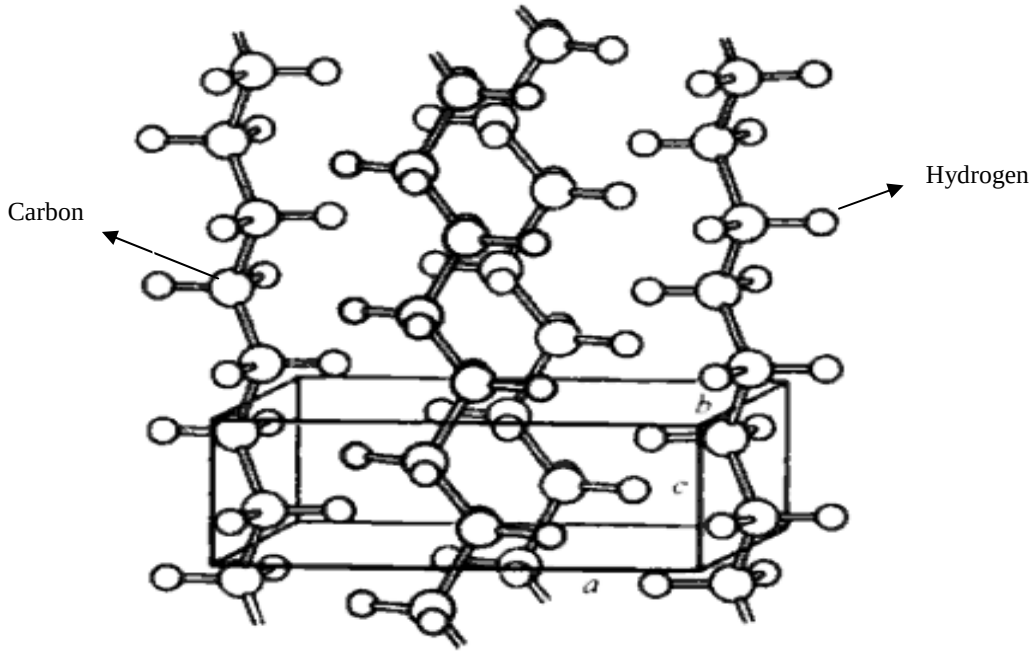

Figure 2.8 Crystal structure in polyethylene [74].

2.5.5 PP crystallization

The crystal structure of PP is much more complicated than that of PE. PP chains exhibit three different configurations: the regular isotactic and syndiotactic, and the irregular atactic configurations, which are defined by the position of the methyl group in relation to the polymer backbone. The position of the methyl groups determines not only the configuration but also the preferred conformation of the PP chain. i-PP chains form three helixes [75]. These helixes pack into crystallite unit cells. The monoclinic α-modification, the hexagonal β-modification, the so-called smectic or mesomorphic modification and the γ-modification. The α -form is the most common crystal form observed in both solution and melt crystallized samples prepared at atmospheric pressure. The metastable β-form is obtained sporadically at high supercoolings or in the presence of selective β-nucleating agents. The γ-form can be produced by using several different methods, such as crystallization of low molecular weight fractions of i-PP, high pressure crystallization, as well as the crystallization of random propylene copolymers with low comonomer content [18].

An extensive study on the γ-form of high molecular weight i-PP with high isotacticity crystallized under high pressures, was done by Mezghani and Phillips [76, 77]. It was found that the formation of the γ-form is preferred at high pressures and low supercoolings (high crystallization temperatures). Figure 2.9 is a representation of the crystal structure in PP.

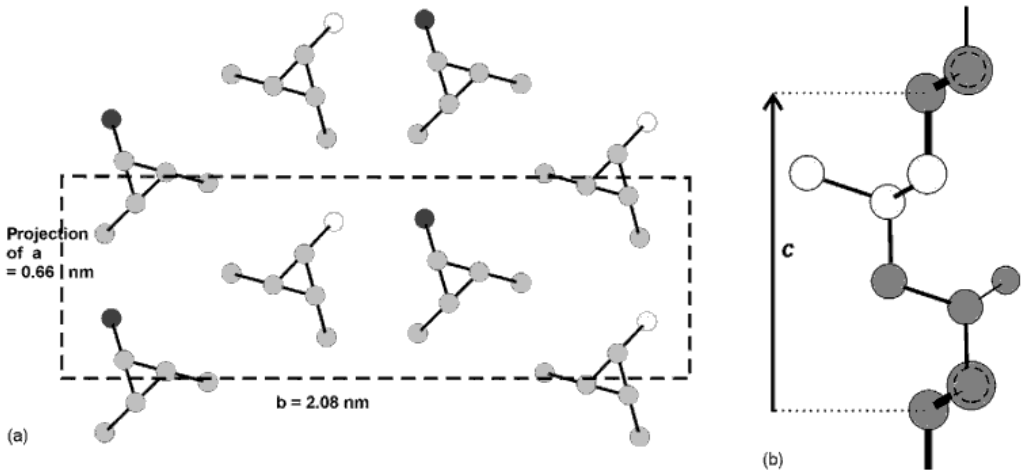

Figure 2.9 Crystal structure in polypropylene [78].

The formation of a particular polymorph depends on crystallization conditions (crystallization temperature and temperature gradient, molecular chain orientation in melts) and on the presence of additives. Many basic studies have been carried out on the formation of PP products with different crystalline modifications and on the development of PP crystallinity and orientation during processing [79-85].

2.5.6 Melt crystallization

Polymer crystallization from the melt takes place in two stages: primary crystallization and secondary crystallization. Primary crystallization involves the nucleation and growth of spherulites, up to the point of spherulite impingement.

The crystallization process in both cases for PE and PP initiate from quiescent melt which is spherulites. The spherulite is not a single crystal, but an extremely complex

spherical aggregate of lamellae, ranging in size from about 0.1μ to a few millimeters in diameter. The nature of the spherulite nucleus can be heterogeneous through impurity or nucleating agent or homogeneous (spontaneous). In primary crystallization the homogeneous nucleus is considered to be composed of a sheaf-like stack of lamellae which achieves spherical shape at some finite size. The radial spreading continues uniformly in all directions by the growth, branching and splaying of individual lamella until neighboring spherulites impinge on each other. Figure 2.10 shows schematic representation of the growth path of homogeneous nucleated spherulite. Secondary crystallization occurs within the spherulite, transforming a portion of the interlamellar material into crystalline material. Depending on the chain structure, the secondary crystallization may involve the processes of lamellar thickening and/or the formation of new lamellae in gaps between existing lamellae [86, 87].

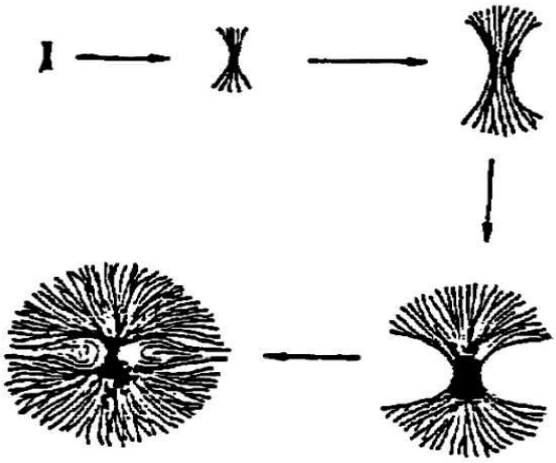

Figure 2.10 Schematic representation growth path of spherulite.

2.5.7 Crystal interface

Semi-crystalline polymers consist of crystalline and amorphous regions that are interconnected by molecular chains (tie molecules) that participate in both regions within the same polymer matrix. The region close to the lamellar surfaces between the

crystalline and amorphous phase is referred to as the interface, where the tie-molecule appears in both phases. The coupling between both phases will produce an intermediate fraction that is present at the interface between the crystals and amorphous. The intermediate fraction is non-crystalline, and includes portions of macromolecules whose mobility is hindered by the near crystalline structures [88-90]. In the current study, PALS is used to determine if this interfacial or intermediary phase can be probe by the technique.

2.5.8 Crystal Defects

Crystals can be arranged regularly with respect to one anther. The regularity of this arrangement can control the thermal and physical properties of the polymer. Semi-crystalline polymers have a regular chain structure, specific preferred chain conformation.

The presence of chain defects (local irregularities) lead to a reduced overall degree of crystallinity and a reduction in crystal thickness. These defects can be as a result of irregularities packing caused by chain folding, chain ends and other molecular irregularities [91] and exist with in the ordered crystal structure. There are two types of defects: point defects and extended defects. Point defects are associated with a single crystal lattice site, while extended defects occur over a greater range [92]. The chain ends of molecules can be regarded as point defects because they differ in chemical character from the chain proper. Figure 2.11 shows a schematic representation of different types of defects that are possible.

Predecki and Statton have studied the defects in polymer crystal structure [93]. They demonstrated that chain ends in crystalline polymer is the main cause for the chain defects in polymer crystals.

The defects can also be associated with the crystalline regions themselves as the spherulites are composed of folded chain molecules and discrepancies in folding can and do occur.

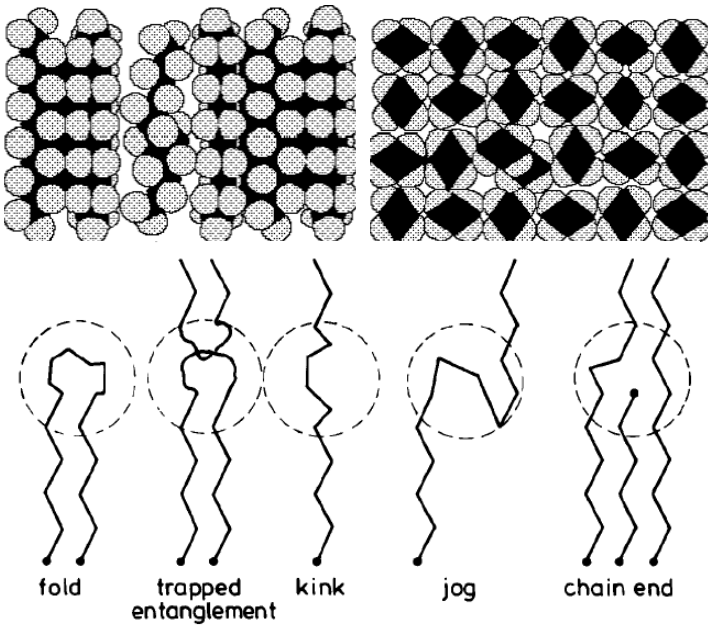

Figure 2.11 Schematic representation of different type of defects

2.5.9 Degree of crystallinity

Crystallinity within a polymer can be described as the arrangement of molecular chains that results in an ordered structure. Most polymers display little crystallinity and are either amorphous or semicrystalline. Crystallinity in a polymer never reaches 100% [94]. Semi-crystalline polymers contain crystalline regions as well as disordered amorphous regions. The crystalline and amorphous components influence polymer properties as much as the molecular weight of a polymer is influenced by that of the various fractions which the polymer consists of. Actually, crystallinity of a polymer sample is expressed in terms of that fraction of the sample which is crystalline [95]. The crystallinity can be measured using a variety of methods including density, DSC, and X-ray measurements.

2.6 Polymer modification

As part of this project we have investigated the effect of fraction removal on the overall properties of the copolymer, this can be considered as a general field of polymer modification. In the 1990s, polymer modification has become a major route to improve polymer properties and wide the applicability [96, 97]. The high cost of developing a completely new polymer and the many long-turn performance objectives a new polymer must meet, have pushed industry to be innovative, in the sense that they rather should explore modification and blending methods to improve polymer properties than exploring the synthesis of new polymers.

For a polymer to be useful, it must be able to function properly in a given application. The performance of a polymer is determined primarily by the composition and structure of the polymer molecule. These factors control the physical, chemical, and other characteristics of the polymer material. Therefore modifications of the composition of the structural units represent one of the main approaches to the modification of polymer behaviour. In addition to the chemical nature and composition of the structural units that constitute the polymer backbone, molecular architecture also contributes to the ultimate properties of polymeric products.

2.7 Mechanical properties

Any improvement in the mechanical properties of a polymer demands a better understanding of the interdependence between its molecular structure, morphology and processing methods on the one hand, and ultimately the mechanical properties on the other, i.e., structure-property correlations. The mechanical properties of a specimen are controlled by its processing history within the limits imposed by its molecular characteristics.

The mechanical properties of a semi-crystalline polymer can be defined as those attributes that involve the physical rearrangement of its component molecules or distortion of its initial morphology in response to an applied force. The nature of a

specimen's response to applied stress can be correlated with its morphological and molecular characteristics and it is these relationships that are emphasized in this work.

2.7.1 Microhardness

Hardness is defined as the resistance of a material against local surface deformation and it is usually computed as the ratio of indentation load to the projected area of contact between the indenter and the material in the plane of the deforming surface. The deformation caused by the indenter involves rearrangement of the initial morphology and hence depends on structural parameters. The microhardness of a sample is thus strongly correlated with its tensile yield stress and elastic modulus, and hence its degree of crystallinity [98-102].

The influence of structural and morphological factors on the mechanical properties of semi-crystalline polymers has been studied by many authors. La Mantia *et al.* [103] studied the influence of structure of the LLDPE on the rheological and mechanical properties of blends with LDPE. They reported that the influence of comonomer was negligible, but the molecular weight had an important effect on properties. Rakesh and Leo [104] reported that the influence of molecular weight manifested itself in the structure of the interlamellar zone, which had major influence on the initial modulus and the ultimate properties.

Balta-Calleja and co-workers [105-108] have done an in depth study of the influence of microstructural parameters on the microhardness. They studied parameters such as the dimensions of the crystalline unit cell for different commercial samples of PE with differing degrees of branching. It was found that the unit cell expansion and lattice distortions increase in parallel as a consequence of increasing incorporation of chain defects within the lattice which will lead to a decrease in the microhardness of the crystals.

2.8 Free volume

The utilization of polymers in industrial applications requires a basic understanding of their material properties. A key problem in this regard is relating the macroscopic mechanical properties (e.g. impact strength, elastic modules, etc.) to atomic-scale free volume holes.

The existence of free volume holes in polymers has been postulated for more than three decades. Many of the visco-elastic properties of polymeric materials can be based on free volume theory [109]. Nowadays it is possible to understand the kinetic and dynamic behaviour of polymeric molecules under varying conditions, if we can understand how free volume holes in the polymer matrix behave.

The basis for free volume can be understood from the theory of Cohen and Turnbull as been reported by Dupasquier and others [110, 111]. According to them, motion of a molecule can occur only when a void having a volume greater than a certain critical value is available for it to move into. As shown in Figure 2.12, the voids are created by fluctuations or the redistribution of free volume originating from the collective or cooperative motion of molecules. Thus, mobility depends on the distribution of free volume and not solely upon the total free volume [112-114].

Free volume arises from three principal sources including the motion of chain ends, side chains and the main chain. These motions, and therefore, the free volume of the polymer can be affected by many factors such as changing the number of end groups, or length of side chains. Also it can be affected by changing the temperature “As the temperature is raised, the kinetic energy of the polymer chains increases, causing the material to expand and enhancing the enhancing free volume” [115].

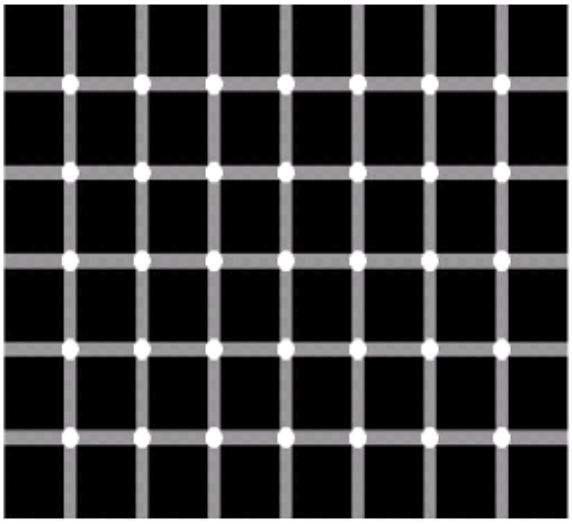

Figure 2.12 The motion of the polymer molecules.

Free volume is usually determined from group additive correlations or it must be inferred indirectly from experimental measurements, such as Positron Annihilation Lifetime Spectroscopy (PALS), Small Angle X-Ray Scattering (SAXS), spin probe methods, photochromic probes, and inverse gas chromatography [116-119]. Of these methods, PALS gives the most detailed characterization of free volume. PALS has been identified as the most successful technique for the direct examination of local free volume holes in polymers. Due to the small size of the positronium probe (1.59 Å) compared to other probes, PALS is particularly sensitive to small holes and free volume of the order of angstrom magnitude [120, 121].

Because of the relatively short lifetime of the o-Ps (typically about 2-4 ns in polymers) PALS can probe holes due to molecular motion from 10^{-10}s or longer [120]. In addition, unlike other methods, PALS is capable of determining the local hole size and free volume in a polymer without being significantly interfered with by the bulk. PALS has also been developed to be a quantitative probe of free volume for polymers. Not only does it probe the free volume size and fractions of free volume, but it also gives detailed information on the distribution of free volume hole sizes in the range from 1 to 10 Å.

2.8.1 Positron and positronium annihilation in polymers

2.8.1.1 Introduction

Positron annihilation is the most efficient, sensitive and reliable method of studying free volumes in polymers [122-126] . The prediction, and subsequent discovery, of the existence of the positron, e^+, constitutes one of the great successes of the theory of relativistic quantum mechanics and of twentieth century physics. The positron as the antiparticle of the electron was predicted by Dirac (1930) as reported by Fraser and others [127-130]. First experimental indications of an unknown particle were found in cloud-chamber photographs of cosmic rays by Anderson (1932) [127, 131]. This particle was identified later as the positron, which was thus the first antiparticle in physics. This was soon confirmed by Blackett and Occhialini, who also observed the phenomenon of pair production as reported by Fraser and others [127, 132]. The annihilation of the positron with electrons in matter was first studied in the 1940s [133]. It was soon discovered that the energy and momentum conservation during the annihilation process could be utilized to study the properties of solids. The bound state of a positron and an electron, as the lightest known atom to be formed, is analogous to a hydrogen atom, where the proton is replaced by the positron. This e^+- e^- state is called Ps. It was predicted by Mohorovicic (1934) and eventually discovered in 1951 by Deutsch. Its properties were investigated in an elegant series of experiments based around positron annihilation in gases [134, 135].

In 1946 Wheeler undertook a theoretical study of the stability of various systems of positrons and electrons, which he termed polyelectrons [135, 136]. He found, as expected, that positronium was bound, but that so too was its negative ion ($e^-e^+e^-$). This entity, Ps^- was not observed until much later after the development of positron beams [136].

As has been mentioned above PALS is powerful to probe free-volume holes that appear in polymers due to irregular molecular packing. This technique provides information on the mean hole size and on the hole size distribution [120, 137].

The lifetime of a positron inside a polymer is normally very short in the order of a fraction of a nanosecond. This is a very short time on a human scale, but is long enough to allow the positron to visit the free volume and to sense the structure of the polymer. Thus we can inject a positron into a sample to draw from it some signal that gives us information on the microscopic properties of the material.

A positron is a subatomic particle that is produced when radioactive material decays; this particle has the same mass as the electron but with a positive charge [138, 139]. When this subatomic particle is irradiated within condensed matter it loses all of its kinetic energy by electrons–positron collisions and ions–positron collisions that are naturally present in the sample to be studied. The positron is thermalized in a sample within a few picoseconds of its injection. This positron can then either bond to an electron to form a neutral atom called positronium (Ps), or becomes part of a chemical complex with a polymer chain [140]. When a positron and electron combine and they annihilate, electromagnetic radiation is given off. Those energies, momentum and times of emission can be measured with high precision. These observable characteristics of the annihilation process depend on the positron finding an electron near to it, and also on the overlap of the positron and electron wave functions. Therefore, the specific values of the positron annihilation parameters (namely, mean life time and probability of formation of the different Ps species) in a particular polymer composite are closely related to the corresponding morphology, because the free spaces in which the Ps can travel without annihilation depends on the geometrical arrangement, on a quasi–molecular level, of the different phases of the sample [141, 142].

2.8.1.2 Positron

A positron is the antiparticle of an electron. As any other antiparticle, the positron reflects its particle counterpart in every respect– their physical properties are equivalent. The masses of the two particles are identical and so are the absolute values of electric charges, spins and magnetic moments. However, the electric charge of the positron is positive, causing its magnetic moment to point in the direction of its spin.

It is rare to find a stable positron naturally due to its very small population and short lifetime compared to its antiparticle. The positron can be generated via nuclear reactions such as decays of neutron deficient radioisotopes, and pair production by γ-rays with energy greater than $2mc^2$. where m is the mass and c is the speed of light.

When the positron encounters an electron, annihilation may take place, and the energy of $2mc^2$ is emitted in the form of γ-ray radiation.

$$e^+ + e^- \longrightarrow n\,\gamma$$

where *n* is the number of photons created by the annihilation process.

2.8.1.3 Positronium

Positronium has a similar structure to that of a hydrogen atom, and is of the same size, but it is 1000 times lighter. Figure 2.13 shows a schematic comparison between hydrogen and Ps atoms. The formation of the Ps atoms occurs mainly in molecular media that usually have a relatively open structure [143]. There exists two ground states of Ps, designated as 'ortho' and 'para', of greatly different lifetimes. In the ortho state the electron and positron spins are coupled into a triplet, and in the para state into a singlet. The p–Ps state annihilates predominantly into two photons, each of 511 keV, with a lifetime of 0.125 ns. o-Ps cannot decay into two photons but instead annihilates predominantly into three photons, with a much longer lifetime of 142 ns. With present technology, only o-Ps is sufficiently long–lived to be useful for studying the free volume in polymers.

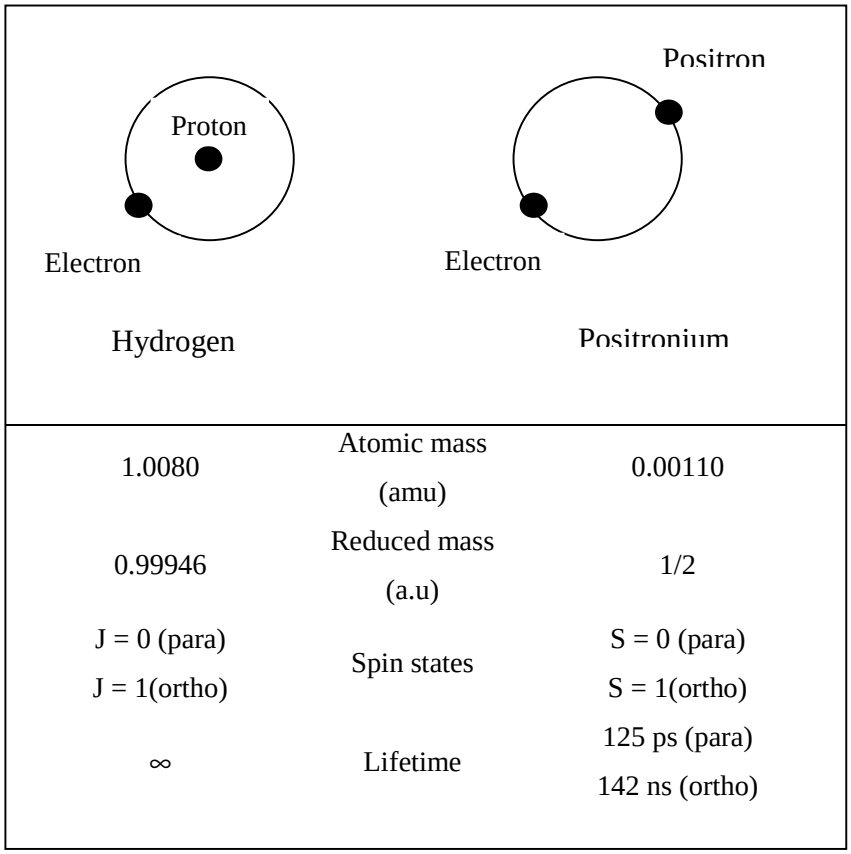

1.0080	Atomic mass (amu)	0.00110
0.99946	Reduced mass (a.u)	1/2
J = 0 (para) J = 1(ortho)	Spin states	S = 0 (para) S = 1(ortho)
∞	Lifetime	125 ps (para) 142 ns (ortho)

Figure 2.13: Comparison between a hydrogen atom and the positronium [120].

2.8.1.4 Principles of PALS

PALS is based upon the interaction of positrons (the antiparticles of electrons) and electrons in condensed matter. The PALS technique involves placing a radioactive source such as ^{22}Na between two small pieces of the sample. This source ejects positrons (the antiparticles of electrons) which, when they enter the sample, release a characteristic energy in the form of a detectable burst of γ-radiation. The positron decays within the sample or forms other subatomic species (positronium) by combination with an electron. The Ps annihilation lifetime is correlated with the free volume in a polymer.

Because of the two possible spin orientations of the two particles, the Ps exists in an ortho and a para form, corresponding to the parallel or anti-parallel orientations of electron and positron spins. These two positronium forms annihilate in quite different ways. The para-positronium (p-Ps) annihilates with the emission of two 511-keV photons, with the mean lifetime of about 125 ps (in vacuum). The ortho-positronium (o-Ps) lives in vacuum for 142 ns and decays via emission of three photons. In matter, however, the o-Ps positron lifetime is reduced to 10^3-10^4 ps due to interaction with surrounding electrons by the so-called "pick-off" process. The o-Ps represents a bonded species of an electron and a positron. This seeks, and becomes trapped in regions of low electron density (spaces between chains), and eventually annihilates with electrons on the surface of the free volume. When these positrons and other species decay they emit a different, detectable γ -radiation energy signature. Both bursts of radiation are detected and a lifetime spectrum results. This spectrum can be translated into three lifetimes, or depending on the complexity of the morphology, four lifetimes.

The first lifetime τ_1 is related to the positron annihilation of p-Ps, with a short lifetime: the second component (τ_2) to annihilation of free positrons, which diffuse though intermolecular spaces. The longest lifetime relates to o-Ps annihilation and is given by the lifetime parameter τ_3, which is of the order of 1 to 3 ns. The size of the voids in which the positronium species reside corresponds to molecular dimensions in the range of a few angstroms, and the larger the size the longer (the greater the value of) the τ_3.

The free-volume hole size calculated from PAL experiments using the Tao-Eldrup equation as has been reported by Lightbody and others [144-147]

$$\tau = \frac{1}{2}\left[1 - \frac{R}{R_0} + \frac{1}{2\pi}\sin\left(\frac{2\pi R}{R_0}\right)\right]^{-1} \qquad 2.1$$

Where R is the radius of the spherical void and

$$R_0 = R + \Delta R \qquad 2.2$$

ΔR= 1.656 Å (an empirical parameter).

The free volume cavity size, V_f, can then be determined by

$$V_f = \frac{4\pi R^3}{3} \qquad 2.3$$

The fractional free volume, f, can be calculated

$$f = CV_f I_3 \qquad 2.4$$

where C is an empirically scaling factor constant, which is 1.5 for spherical cavities [120].

2.8.1.5 Collecting and fitting PALS spectra

All PALS experiments are conceptually the same. Positrons are embedded into a material where, within picoseconds, they thermalize, and either annihilate directly or form either p-Ps or o-Ps. A PALS apparatus uses a very fast timer to measure the time between the positron entering the material and the subsequent annihilation. A spectrum of decay lifetimes is generated by measuring in the order of a million annihilations. A typical Ps annihilation lifetime spectrum is shown in Figure 2.14. Some features are prominent in a PALS lifetime spectrum including the prompt peak, a decay tail, and a constant background.

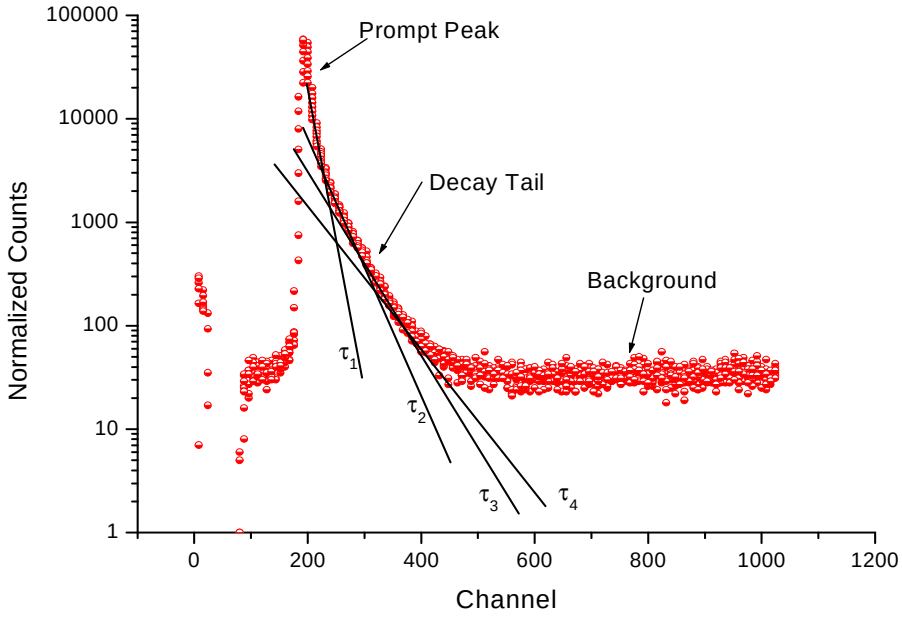

Figure 2.14 Typical PALS lifetime spectrum for copolymer materials where a four component analysis is used.

2.8.1.6 PALS in semi-crystalline polymers

The measurement of parameters relating to free volume within semi-crystalline polymers is an important aspect of their characterization. In l960s it was realized that the annihilation parameters are sensitive to lattice imperfections. MacKenzie *et al*. discovered that the positron may be trapped in crystal defects, where the wave function of the positron is localized in the defect site until annihilation [133].

In 1969 Madey [136] reported his observation of the re-emission of positrons with a relatively broad energy spectrum (peaked at about 20eV) from the surface of PE. Madey's work has largely been overlooked since then.

The o-Ps annihilation component has been associated with the amorphous free volume in polymers. However, in semi-crystalline polymers the crystallinity also contributes to the o-Ps annihilation parameters [125, 126, 148-152], where the situation appears to be much more complex than in the amorphous due to the presence of

crystallites and of amorphous regions of different mobilities. In 1972 Stevens and Lichtenberger resolved four lifetimes for positrons annihilating in PE [151]. They proposed that the τ_3 component is due to free positrons annihilating in the less ordered regions between the folded chains.

Suzuki *et al.* [153] summarised all possibilities for these short time decays in PE. They concluded that the short time decay via a decay of positrons forming a bound system with molecules, and decay of Ps trapped at the crystal–amorphous interface, and finally a decay of a bound positron or a Ps-like system.

In 1989 Nakanishi *et al.* showed that the Ps formation probability in semi-crystalline polymers is proportional to the degree of the crystallinity and that Ps forms at free-volume sites in the amorphous regions of two-phase PEEK [123]. Two years later together with Jean, they studied the dynamical behaviour of the free-volume creation and its relaxation in the amorphous regions of two-phase PEEK. It was found that the crystallinity of the PEEK during the annealing process was obtained from the positronium formation intensities[154].

Brusa *et al.* [155, 156] reported measurements of positron mobility in PE. Their measurements were carried out by improving the acquisition and analysis of Doppler-broadening annihilation spectra.

In 1999 van Prooijen *et al.* [122] studied intensities and lifetimes of positrons annihilating in LDPE and HDPE. He concluded that the shortest lifetime component is caused by a combination of (p-Ps) decay and the annihilation of free positrons in the crystalline regions, and that the second longest lived component can also be associated with crystalline regions, especially the crystalline/amorphous boundary.

A number of recent studies have illustrated the importance of the positron lifetime in probing the free volumes of semi-crystalline polymers [64, 157-164]. Dlubek *et al.* [165] used four lifetimes in their positron lifetime measurements of linear poly(α-olefin)s. The two shortest lifetimes, τ_1 and τ_2, arise from p-Ps self annihilation and

positron annihilation. These lifetimes are not affected by the sample structure. The longest lifetimes observed, τ_3 and τ_4, are attributed to o-Ps pick-off annihilation from free volume holes resulting from defects in the crystalline domains, and also from the free volume holes in the amorphous phase of the polymers respectively. The longest lifetime was used to estimate the mean volume of these holes. It was noted that the size of the free volume holes increased as the T_g decreased and the temperature difference between the measuring temperature and T_g increased.

Cerrada *et al*. [150] have also demonstrated a dependence of the temperature of the α-relaxation (associated with large scale motions in the amorphous regions) on the free volume fraction of PEs and ethylene copolymers. Higher relaxation temperatures were found to be related to lower free volumes. The molar fraction of comonomer was also found to influence the free volume, and two different regimes were discovered: one for relatively low comonomer contents and another for higher comonomer content, indicating different morphology types depending on the comonomer content.

Wang *et al.* [166] have also demonstrated the use of PALS to determine the temperature dependence of the free volume holes in propylene/ethylene copolymers. They demonstrated that the free volume hole size and amorphous density are strongly dependent on the crystallinity of the samples. Differences in the values obtained for crystallinity, as measuremed by DSC and density measurements, were attributed to the crystallinity dependence of the amorphous phase density.

In 2008, the microstructure of composites been studied by PALS. Hongmei *et al.* [167] studied different types of composites. (HDPE)/Bentonite (BT) and HDPE grafted with acrylic acid (HDPE-g-AA)/(BT). He reported that the mean free volume size is nearly the same in composites and HDPE matrices with different BT concentration. The o-Ps intensity decreased for HDPE-g-AA and its lifetime distribution was narrower than that for pure HDPE. Furthermore, carboxyl groups have an inhibition effect on Ps formation.

2.9 References

1. Charles, P. and Poole, F. Introduction to Nanotechnology; John Wiley & Sons: New Jersey, 2003.
2. Peacock, A. Handbook of Polyethylene; Marcel Dekker: USA, 2000.
3. Nicholas, P. and Cheremisinoff, P. Handbook of Applied Polymer Processing Technology; Marcel Dekker: New York, 1996.
4. Bruce, C., Gates, A. and Helmut, C. Advances in Catalysis; Academic press: USA, 2002.
5. Vasile, C. Handbook of Polyolefins; Dekker: New York, 2000.
6. Ebewele, R. Polymer Science and Technology; Chapman and Hall CRC: USA, 2000.
7. Smith, J. and Yiu, H. Food Processing: Principles and Applications; Blackwell: USA, 2004.
8. Matja, A., Zcaron, C., Denac, A., Vojko, M., Franjo, R. and Ivan, S. Macromolecular Symposia 2004, 217, 401-412.
9. Kocsis, K. Polypropylene: Copolymers and Blends; Chapman & Hall: UK, 1995.
10. Campo, A. Selection of Polymeric Materials; William Andrew Inc: USA, 2008.
11. Günter, D., Jürgen, P., Yang, Y., Stefan, T., Mohamed, E., Emad, B. and Reinhard, K R. Macromolecular Chemistry and Physics 2008, 209, 1920-1930.
12. Karian, H. Handbook of Polypropylene and Polypropylene Composites; Marcel Dekker: USA, 2003.
13. George, A., Alain, G. and Prakash, K. Beyond Oil and Gas: The Methanol Economy; Wiley-VCH: Germany, 2009.
14. Benedikt, G. and Brian, G. Metallocene-catalyzed Polymers; Plastics Desing Library: New York, 1998.
15. Hamielec, A. and Tony, S. Macromolecular Symposia 2000, 152, 9-14.
16. Albertsson, A. Long-term Properties of Polyolefins; Springer: USA, 2004.

17. Dealy, J. and Larson, R. Structure and Rheology of Molten Polymers; Hanser Verlag: USA, 2006.
18. James, W. and David, C. Polyolefins: Processing, Structure Development and Properties; Hanser Gardner: USA, 2004.
19. Clive, M. and Teresa, C. Polypropylene: The Definitive User's Guide and Databook; William Andrew: USA, 1998.
20. Selke, S. Understanding Plastics Packaging Technology; Carl Hanser Verlag: Munich, 1997.
21. Vasile, C. and Mihaela, P. Practical Guide to Polyethylene; Rapra Publishing: UK, 2005.
22. Peacock, A. and Calhoun, A. Polymer Chemistry: Properties and Applications; Hanser Verlag: Munich, 2006.
23. Ghosh, P. Polymer Science and Technology; Tata McGraw-Hill: New Delhi, 2002.
24. Shipman, J., Jerry, D. and Todd, W. An Introduction to Physical Science; Houghton Mifflin: USA, 2009.
25. Sinha, R. Outlines of Polymer Technology; Prentice-Hall: India, 2000.
26. Ramsden, E. A-level Chemistry; Nelson Thornes: UK, 2000.
27. Andrady, A. Plastics and the Environment; John Wiley & Sons: Canada, 2003.
28. Williams, T. and Thomas, K. A Short History of Twentieth-century Technology; Oxford University Press: New York, 1982.
29. Chung, T. Functionalization of Polyolefins; Academic Press: UK, 2002.
30. Alberto, B. and Gerhard, V. High Pressure Process Technology: Fundamentals and Applications; Elsevier: Amsterdam, 2001.
31. Amstock, J. Handbook of Adhesives and Sealants in Construction; McGraw-Hill Professional: USA, 2001.
32. Schweitzer, P. Mechanical and Corrosion-resistant Properties of Plastics and Elastomers; CRC Press: UK, 2000.
33. Tripathi, D. Practical Guide to Polypropylene; Rapra Technology Limited: UK, 2002.

34. George M. Benedikt, B L G. Metallocene-catalyzed polymers; William Andrew: New York, 1998.
35. Lewin, M. Handbook of Fiber Chemistry; CRC Press: USA, 2007.
36. Ebnesajjad, S. Melt Processible Fluoropolymers: The Definitive User's Guide and Databook Plastics Design: USA, 2003.
37. Hudson, R. Commodity Plastics-as Engineering Materials; Rapra Technology: UK, 1994.
38. Salamone, J. Concise Polymeric Materials Encyclopedia; CRC Press: USA, 1999.
39. Francisco, J., Baltá, C. and Rosłaniec, Z. Block Copolymers; Marcel Dekker: USA, 2000.
40. Hannay, F. Rigid Plastics Packaging-materials, Processes and Applications; Rapra Publishing: UK, 2002.
41. Stuart, B. Polymer Analysis; John Wiley & Sons: UK, 2003.
42. Sawyer, L. and Grubb, D. Polymer Microscopy; Chapman & Hall: UK, 1996.
43. Psaras, P. and Langford, D. Advancing Materials Research; National Academy of Sciences: USA, 1987.
44. Beswick, R. and Dunn, D. Plastics in Packaging; Rapra Publishing: UK, 2002.
45. Bruce C. Gates, H K. Advances in Catalysis Academic Press: UK, 2002.
46. Guan, Z. Metal Catalysts in Olefin Polymerisation; Springer-Verlag: German, 2009.
47. Kuran, W. Principles of Coordination Polymerisation; John Wiley & Sons: UK, 2001.
48. Joseph, R. and Lee, V. Controlled Drug Delivery; Marcel Dekker: New York, 1987.
49. Odian, G. Principles of Polymerization; John Wiley & Sons: Canada, 2004.
50. Olabisi, O. Handbook of Thermoplastics; CRC Press: New York, 1997.
51. Kuhlke, W. Volume Polymers in North America and Western Europe; Rapra Publishing: UK, 2001.
52. Shakhashiri, B. Chemical Demonstrations: a Handbook for Teachers of Chemistry; University of Wisconsin Press: UK, 1983.

53. Hongsheng, Z., Weihong, G., Yingbo, Y., Binyao, L. and Chifei, W. European Polymer Journal 2007, 43, 3662-3670.
54. James, C S. Polymer Composites 1986, 7, 158-169.
55. Drozdov, A. and Christiansen, C. Computational Materials Science 2007, 39, 729-751.
56. Michler, G H. Physica Status Solidi (a) 1995, 150, 185-200.
57. Soccio, M., Lotti, N., Finelli, L., Gazzano, M. and Munari, A. Journal of Polymer Science Part B: Polymer Physics 2008, 46, 170-181.
58. Rajen, M P., Thomas, I B., Kim, L W. and Knight, G W. Polymer Engineering & Science 1994, 34, 1506-1514.
59. Kalfoglou, N K. and Williams, H L. Polymer Engineering & Science 1972, 12, 224-235.
60. Fatemi, M H. and Haghdadi, M. Journal of Molecular Structure 2008, 886, 43-50.
61. Wang, M. and Bonfield, W. Biomaterials 2001, 22, 1311-1320.
62. Raj, B., Annadurai, V., Somashekar, R., Raj, M. and Siddaramaiah, S. European Polymer Journal 2001, 37, 943-948.
63. Janimak, J J. and Stevens, G C. Thermochimica Acta 1999, 332, 125-142.
64. Cheng, M L., Sun, Y M., Chen, H. and Jean, Y C. Polymer 2009, 50, 1957-1964.
65. Bubeck, R A. Materials Science and Engineering: R: Reports 2002, 39, 1-28.
66. Todo, A N K. Macromolecular Symposium 1996, 110, 301-308.
67. Paukkeri, R. and Lehtinen, A. Polymer 1993, 34, 4075-4082.
68. Kim, Y., Chung, C., Lai, S. and Hyun, K. Korean Journal chemical Engineering 1996, 13, 294-303.
69. Kale, L., Plumley, T., Patel, R., Redwine, O. and Jain, P. Journal of Plastic Film and Sheeting 1996, 12, 27-40.
70. Tim, O., Sheng, T. and Paul, G. Injection Molding Handbook; Hanser Verlag: Munich, 2007.
71. Osswald, T. Polymer Processing Fundamentals; Hanser Verlag: Munich, 1998.
72. Calhoun, A. and Peacock, A J. Polymer Chemistry; Hanser Munich, 2006.

73. Eichhorn, K. and Fischer, D. Polymer Spectroscopy; Wiley-VCH: Germany, 2002.
74. Bower, D. An Introduction to Polymer Physics; Cambridge University Press: UK, 2002.
75. Karger-Kocsis, J. Polypropylene; Chapman & Hall: UK 1995.
76. Mezghani, K. and Phillips, P J. Polymer 1998, 39, 3735-3744.
77. Mezghani, K. and Phillips, P J. Polymer 1997, 38, 5725-5733.
78. Mills, N J. Plastics: microstructure and applications; Nigel Mills: UK, 2005.
79. Wang, S W., Yang, W., Xu, Y J., Xie, B H., Yang, M B. and Peng, X F. Polymer Testing 2008, 27, 638-644.
80. Arranz, J., Peña, B., Benavente, R., Pérez, E. and Cerrada, M L. European Polymer Journal 2007, 43, 2357-2370.
81. Cermák, R., Obadal, M., Ponízil, P., Polásková, M., Stoklasa, K. and Lengálová, A. European Polymer Journal 2005, 41, 1838-1845.
82. Wang, Z-G., Hsiao, B S., Srinivas, S., Brown, G M., Tsou, A H., Cheng, S Z D. and Stein, R S. Polymer 2001, 42, 7561-7566.
83. Assouline, E., Pohl, S., Fulchiron, R., Gérard, J F., Lustiger, A., Wagner, H D. and Marom, G. Polymer 2000, 41, 7843-7854.
84. Bassett, D C. and Olley, R H. Polymer 1984, 25, 935-943.
85. Nakafuku, C. Polymer 1981, 22, 1673-1676.
86. Reiter, G. and Sommer, J-U. Polymer Crystallization: Observations, Concepts, and Interpretations; Springer: Germany, 2003.
87. Reiter, G. and Strobl, G. Progress in Understanding of Polymer Crystallization; Springer: USA, 2007.
88. Androsch, R. and Wunderlich, B. Polymer 2005, 46, 12556-12566.
89. Gautam, S., Balijepalli, S. and Rutledge, G C. Macromolecules 2000, 33, 9136-9145.
90. Wunderlich, B. Thermal Analysis of Polymeric Materials; Springer-Verlag: Berlin, 2005.
91. Reneker, D H. and Mazur, J. Polymer 1988, 29, 3-13.

92. Reneker, D H. Journal of Polymer Science 1962, 59, S39-S42.
93. Predecki, P. and Statton, W. Journal of Applied Physics 1966, 37, 4053.
94. Lubin, G. and Peters, S. Handbook of Composites; Springer: UK, 1998.
95. Lipatov, Y. Polymer Reinforcement; Academy of Sciences: Ukraine, 1995.
96. Shonaike, G. and Simon, G. Polymer Blends and Alloys; Marcel Dekker: USA, 1999.
97. Meister, J. Polymer Modification; CRC Press: New York, 2000.
98. Flores, A., Baltá, C., Attenburrow, G E. and Bassett, D C. Polymer 2000, 41, 5431-5435.
99. Sobieraj, M C. and Rimnac, C M. Journal of the Mechanical Behavior of Biomedical Materials 2009, 2, 433-443.
100. Fakirov, S., Krumova, M. and Rueda, D R. Polymer 2001, 42, 1293-1293.
101. Fakirov, S., Krumova, M. and Rueda, D R. Polymer 2000, 41, 3047-3056.
102. Henderson, P J. and Wallace, A J. Polymer 1989, 30, 2209-2214.
103. La Mantia, F P., Valenza, A. and Acierno, D. European Polymer Journal 1986, 22, 647-652.
104. Rakesh, P. and Leo, M. Journal of Polymer Science Part B: Polymer Physics 1987, 25, 441-483.
105. Balta-Calleja, J. and Fakirov, S. Microhardness of Polymers; Cambridge University Press: UK, 2000.
106. Martinez, S. and Balta-Calleja, B. Journal of Materials Science 1983, 18, 1077.
107. Balta-Calleja, B., Rueda, D., Pena, J., Wolf, F. and Karl, V. Journal of Materials Science 1986, 21, 1139.
108. Salazar, M., Garcia, T. and Balta-Calleja, B. Journal of Materials Science 1988, 23, 862.
109. Brinson, H. and Brinson, C. Polymer Engineering Science and Viscoelasticity; Springer: Hoston, 2007.
110. Dupasquier, A. and Mills, A. Positron Spectroscopy of Solids; IOS Press: Amsterdam, 1995.
111. Lvovich, K. Molecular Dynamics of Additives in Polymers; VSP: Tokyo, 1997.

112. Macmillan, W. and John, S. An Introduction to the Mechanical Properties of Solid Polymers; John Wiley and Sons: UK, 2004.
113. Joseph, Y. and Peter, L. Introduction to Polymers; Chapman &Hall: USA, 1981.
114. James E. Mark, W W G. Physical properties of polymers; Cambridge University Press: UK, 2004.
115. Wypych, G. Handbook of Plasticizers; ChemTec: Canada, 2004.
116. Nobbs, H. and Young, J. The Physics of Glassy Polymers; Springer: UK, 1997.
117. Gilbert, C., Davies, J. and Murphy, M. Electron Paramagnetic Resonance; Royal Society of Chemistry: UK, 2006.
118. Roe, R J. and Curro, J J. Macromolecules 1983, 16, 428-434.
119. Roe, R J. and Song, H H. Macromolecules 1985, 18, 1603-1609.
120. Jean, Y C., Mallon, P E. and Schrader, D M. Principles and Applications of Positron & Positronium Chemistry; World Scientific: New Jersey, 2003.
121. Sperling, L. Introduction to Physical Polymer Science; John Wiley & Sons: Canada, 2006.
122. Van Prooijen, M., Jorch, H H., Stevens, J R. and Rudin, A. Polymer 1999, 40, 5111-5117.
123. Nakanishi, H., Jean, Y C., Smith, E G. and Sandreczki, T C. Journal of Polymer Science Part B: Polymer Physics 1989, 27, 1419-1424.
124. Reiter, G. and Kindl, P. Physica Status Solidi (a) 1990, 118, 161-168.
125. Misheva, M., Mihaylova, M., Djourelov, N., Kresteva, M., Krestev, V. and Nedkov, E. Radiation Physics and Chemistry 2000, 58, 39-47.
126. Sudarshan, K., Rath, S K., Patri, M., Sachdeva, A. and Pujari, P K. Polymer 2007, 48, 6434-6438.
127. Fraser, G. The Particle Century; Institute of Physics Publishing: UK, 1998.
128. Hubbell, J H. Radiation Physics and Chemistry 2006, 75, 614-623.
129. Pethrick, R A. Progress in Polymer Science 1997, 22, 1-47.
130. Jean, Y C., Zhang, J., Chen, H., Li, Y. and Liu, G. Spectrochimica Acta Part A: Molecular and Biomolecular Spectroscopy 2005, 61, 1683-1691.

131. Eman, Y. and Kirsh, Y. The Particle Hunters; Cambridge University Press: UK, 1996.
132. Falkenburg, B. Particle Metaphysics; Springer: New York, 2007.
133. Rehberg, K. and Leipner, H. Positron Annihilation in Semiconductors; Springer: New York, 1999.
134. Attila, V., Nagy, S., Klencsár, Z., Lovas, G. and Rösch, F. Handbook of Nuclear Chemistry; Springer: USA, 2003.
135. Charlton, M. and John, H. Positron Physics; Cambridge University Press: UK, 2001.
136. Coleman, P. Positron Beams and their Applications; World Scientific: USA, 2000.
137. Jouffrey, B. and Svejcar, J. Microstructural Investigation and Analysis; Sterling Publishing: USA, 2000.
138. Weinberg, S. The Discovery of Subatomic Particles Cambridge University Press: UK, 2003.
139. Tsoulfanidis, N. Measurement and Detection of Radiation; Taylor & Francis: USA, 1995.
140. Marton, L., Ronald, A., Fava, J. and Stevens, R. Methods of Experimental Physics; Academic Press: USA, 1980.
141. Claverie, J. and Pichot, C. Polymers in Dispersed Media: Polymerization in Dispersed Media; Wiley-VCH: France, 2000.
142. Peter E. Valk, D L B. Positron emission tomography: basic science and clinical practice; Springer: London, 2003.
143. Kurt, G. and Frederick, W. Concepts of Particle Physics; Oxford University: USA, 1986.
144. Lightbody, D., Sherwood, J. and Eldrup, N. Chemical Physics 1985, 93, 475-484.
145. Danch, A. and Osoba, W. Radiation Physics and Chemistry, 68, 445-447.
146. Kumar, R., Ali, S A., De, U., Naqvi, A H., Chaudhary, S K., Das, D. and Prasad, R. Radiation Measurements 2008, 43, S578-S582.

147. Abdel-Hady, E E., Mohamed, H F M. and Fareed, S S. Radiation Physics and Chemistry 2007, 76, 138-141.
148. Kobayashi, Y., Zheng, W., Hirata, K. and Suzuki, T. Radiation Physics and Chemistry 1997, 50, 589-593.
149. Zheng, W., Kobayashi, Y., Hirata, K. and Suzuki, T. Radiation Physics and Chemistry 1998, 51, 269-272.
150. Cerrada, M L., Perez, E., Perena, J M., Benavente, R., Misheva, M. and Grigorov, T. Macromolecules 2005, 38, 8430-8439.
151. Stevens, J R. and Lichtenberger, P C. Physical Review Letters 1972, 29, 166.
152. Suzuki, T., Miura, T., Oki, Y., Numajiri, M., Kondo, K. and Ito, Y. Radiation Physics and Chemistry 1995, 45, 657-663.
153. Suzuki, T., Oki, Y M., Numajiri, T., Miura, K. and Kondo, Y. Journal of Polymer Science Part B: Polymer Physics 1992, 30, 517-525.
154. Nakanishi, H. and Jean, Y C. Macromolecules 1991, 24, 6618-6621.
155. Lung, C W. and March, N. Mechanical Properties of Metals/Atomistic and Fractal Continuum Approaches; World Scientific: USA, 1999.
156. Brusa, R S., Naia, M D., Margoni, D. and Zecca, A. Applied Physics A: Materials Science & Processing 1995 60.
157. Hans, A. Positronium and Muonium Chemistry; American Chemical Society: Washington, 1979.
158. Zaydouri, A. and Grivet, M. Radiation Physics and Chemistry 2009, 78, 770-775.
159. Matsuo, M., Bin, Y., Xu, C., Ma, L., Nakaoki, T. and Suzuki, T. Polymer 2003, 44, 4325-4340.
160. Mei-Ling, C. and Yi-Ming, S. Physica Status Solidi (c) 2007, 4, 3916-3919.
161. Kindl, P. and Sormann, H. Physica Status Solidi (a) 1981, 66, 627-633.
162. Mei-Ling, C. and Yi-Ming, S. Journal of Polymer Science Part B: Polymer Physics 2009, 47, 855-865.
163. Matsuo, M., Ma, L., Azuma, M., He, C. and Suzuki, T. Macromolecules 2002, 35, 3059-3065.

164. Ma, L., He, C., Suzuki, T., Azuma, M., Bin, Y., Kurosu, H. and Matsuo, M. Macromolecules 2003, 36, 8056-8065.

165. Dlubek, G., Bamford, D., Henschke, O., Knorr, J., Alam, M A., Arnold, M. and Lüpke, T. Polymer 2001, 42, 5381-5388.

166. Wang, C L., Kobayashi, Y., Zheng, W. and Zhang, C. Polymer 2001, 42, 2359-2364.

167. Hongmei, W., Zhe, C., Pengfei, F., Shaojie, W., Yuzhen, X. and Zhengping, F. Journal of Applied Polymer Science 2008, 108, 1557-1561.

Chapter 3
Experimental

3.1 Introduction

Details of the material, fractionation and characterization techniques used in this study are described. The latter include differential scanning calorimetry (DSC), high temperature size exclusion chromatography (HT-SEC), nuclear magnetic resonance (NMR), and positron annihilation spectroscopy (PAS).

The procedures used in certain techniques are described in cases where they are not standard techniques used in routine analyses.

3.2 Materials

3.2.1 Polypropylene homopolymer

The polypropylene homopolymer (PP) was obtained from Himont, (Italy), its properties are included in Table 3.1.

3.2.2 Polypropylene copolymers

Two commercial random propylene copolymers with different pentene contents were used. These unfractionated copolymers were provided by Sasol Polymers (South Africa). There properties are tabulated in Table 3.1.

Table 3.1 Properties of PP and two PP copolymers used in this study.

Sample	MFI (g/10ml)	Mn (g/mol)	Mw (g/mol)	PD	Crystallinity $(\%)_{Density}$	1-pentene content (%)	mmmm (%)
PPC	-	1.3E+05	6.9E+05	5.2	62.47	-	90.49
PPA	1.25	8.0E+04	5.5E+05	6.94	58.75	4.62	88.32
PPB	1.40	8.4E+04	5.6E+05	6.69	54.75	5.84	86.15

3.2.3 Plastomers

Two different plastomers (LLDPE) were used in this study. The first plastomer (PE1) was from the Affinity range of DOW Chemicals PL1881. The plastomer consisted of ethylene and octane, as comonomer. The percentage comonomer content was 4.8 % as determined by ^{13}C NMR. It's physical properties are tabulated in Table 3.2.

The second plastomer (PE2) used was Exceed 1327CA produced by ExxonMobil Chemicals. The plastomer consisted of ethylene and hexene, as comonomer. The percentage comonomer content was 3.2 % as determined from the ^{13}C NMR.

Table 3.2. Physical properties of the two plastomers

Sample	MFI (g/10ml)	Density (g/cc)	T_m [a] (°C)	T_c [a]	Crystallinity [b] (%)
PE1	1	0.9035	100	82	26
PE2	1.3	0.927	120	110	35

a) Melting and crystallization temperature from DSC.
b) Crystallinity according to density.

3.2.4 Solvents

Xylene (Aldrich, 99% purity) was used as the solvent in all TREF procedures. It was recycled (by distillation) and re-used.

3.2.5 Stabilizers

Irganox 1010 and Irgafos stabilizer mix (Sasol) were used in the TREF procedures to inhibit thermal degradation. They are required because high temperatures are used in the crystallization step.

3.3 Fractionation techniques

The distribution of crystallizable fractions of polyolefins is usually measured by either crystallization analysis fractionation (CRYSTAF) or temperature rising elution fractionation (TREF). Both techniques are based on the fact that semicrystalline polymers in solution at high temperatures will crystallize and precipitate as the solution temperature is reduced. The chains with fewer comonomer molecules will precipitate at higher temperatures, whereas the chains with more comonomer molecules will precipitate at lower temperatures. The main difference between these two techniques is that CRYSTAF monitors the concentration of

polymer in solution during the crystallization process, whereas TREF measures the concentration of polymer in solution during the dissolution step that takes place after all the polymer has been crystallized from solution. Consequently, the CRYSTAF analysis time is significantly shorter than that time required for TREF analysis.

3.3.1 CRYSTAF

The CRYSTAF apparatus had five, stirred stainless steel crystallization vessels placed inside a temperature-programmable oven, which means that up to five samples could be analyzed simultaneously. Figure 3.1 shows the CRYSTAF setup. The crystallization vessels are connected to a nitrogen line, a waste line, and a sampling line attached to an in-line filter. The sampling line is connected to an on-line detector cell used to measure the polymer solution concentration as a function of the crystallization temperature.

In this study, CRYSTAF was carried out using a CRYSTAF commercial apparatus, model 200, manufactured by Polymer Char S.A. (Valencia, Spain). Before the fractionation, about 20 mg of sample is dissolved in a good solvent at 130 ºC inside a crystallization vessel (volume 60 ml). 1,2,4-Tricholobenzene was generally used as solvent in this study.

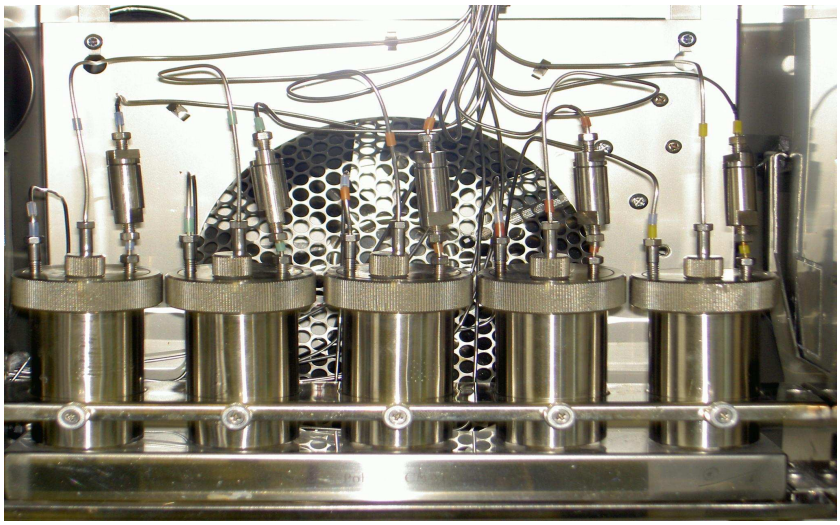

Figure 3.1 CRYSTAF setup showing stainless steel crystallization vessels inside a temperature-programmable oven.

The dissolution step is followed by the stabilization period, during which the temperature of the polymer solution is kept a few degrees above the initial crystallization temperature. During the crystallization step the temperature of the solution is decreased at a

constant cooling rate, typically in the range of 0.1–0.2 ºC/min. This allows the polymer chains with the highest crystallizabilities to precipitate first at high temperatures, followed by the chains with lower crystallizabilities. A slow cooling rate is essential to minimize undesirable crystallization kinetics and co-crystallization effects. The concentration of the polymer in the solution as a function of the crystallization temperature is monitored through the on-line infrared detector and recorded by the data acquisition software.

3.3.2 TREF

Temperature rising elution fractionation, which separates semi-crystalline polymer chains is based on the relative crystallizability of molecules.

The polymer is dissolved in a solvent (xylene) at high temperature (135^{o}C). A heated inert support is added, and the mixture then slowly cooled, allowing polymer molecules to crystallize on the support according to their respective crystallizabilities. Decreased crystallinty is reflected in a lower crystallization temperature. After crystallization the temperature is raised continuously, with solvent flowing through the column. As a result, at the lower temperatures the fractions with less crystallinity dissolve. With increasing elution temperature the fractions of higher crystallinity dissolve. Figure 3.2 illustrates the TREF process.

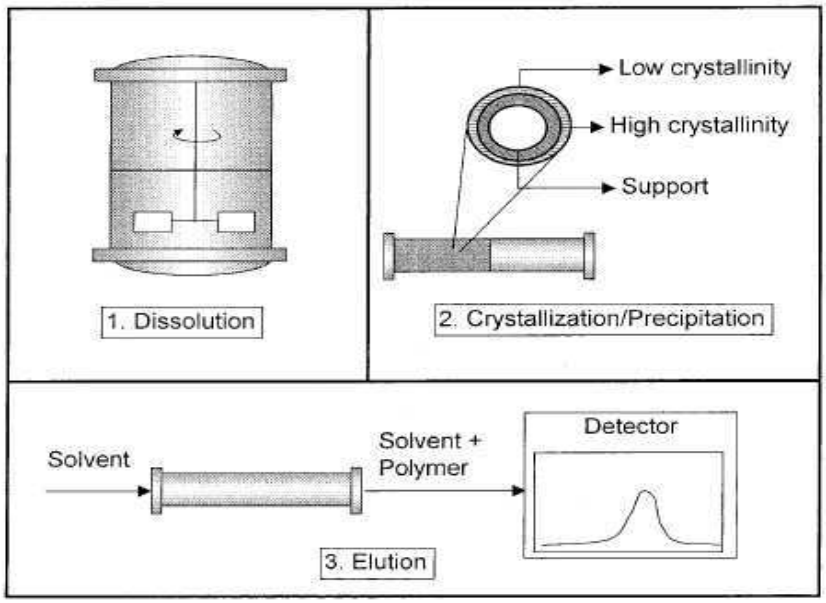

Figure 3.2 Schematic representation of the TREF process [1].

3.3.2.1 Prep-TREF

In this study preparative TREF was used to fractionate the polymers and the blends. The general procedure is described below. The operation of prep-TREF is divided into two steps.

1. About 2 g of polymer is dissolved in 200 ml of xylene, followed by the addition of 3 mg of an anti-oxidant. The solution is heated to 135 ºC to ensure that all the sample is dissolved. This solution is then placed in a 1-L round bottom flask and placed into a preheated oil bath with attached temperature profiler. A dilute solution of polymer is mixed with an inert support (sea sand). The amount of the support will depend on the initial amount of polymer and xylene used (2–3 kg of support). This mixture is slowly cooled to room temperature. As the temperature gradually decreases, the polymer fractions precipitate from the solution and coat the support in layers of different crystallinity. The most crystallizable fraction precipitates first, as is shown in Figure 3.2. On the other hand, the fraction with the least crystallinity precipitates last and deposits on the outermost layer. This step can be performed in a stirred vessel or directly in the TREF column.

2. In the second step the precipitated polymer is eluted with a solvent using increasing or stepwise temperatures. As a result, chains that crystallize with difficulty are eluted first (at lower temperatures). As the temperature rises, less defective and more perfect chains are eluted. Since physically separate fractions are obtained, they can be analyzed by standard polymer characterization techniques like DSC, NMR and HT-SEC. A thorough quantitative characterization of each fraction can be obtained. TREF was also used in other profiles which will be discussed in chapter 4 and 5 in details. The bulk sample has been treated to the same temperature profile used for TREF fractionation.

3.4 Analyses

3.4.1 DSC measurements

The melting and crystallization properties of samples were determined on a DSC instrument, in a nitrogen atmosphere, using the following method. Approximately 4-5 mg of each sample was used for analysis. All the experiments were performed after heating the samples to 200 °C at a rate of 10°C/min to eliminate the thermal history. The crystallization

curves were obtained by cooling the sample from the melt to -40 °C at a rate of 10 °C/min. The melting curves were obtained on reheating the sample to 200 °C at the same scanning rate. The data were only stored on the second run. The instrument used was a TA Instruments Thermal Analysis DSC standard cell.

3.4.2 NMR measurements

^{13}C NMR spectra of the polymers were recorded at 100 ^{0}C on a Varian VXR 300 instrument, in a 9:1 mixture of 1,2,4-trichlorobenzene/C_6D_6 as solvent, using C_6D_6 at 127.9 ppm as internal secondary reference. The pulse angle was 45 degrees and the repetition time 0.82 s.

3.4.3 HT-SEC measurements

Molecular weights were determined using size exclusion chromatography (SEC). The measurements were performed at a flow rate of 1 ml/min in 1,2,4 trichlorobenzene at 160 °C, using a Waters 1500C high-temperature SEC system. A polystyrene calibration curve was used for all molecular weights determinations. The detector used was a differential refractive index detector.

3.4.4 Positron annihilation spectroscopy (PAS)

The positron annihilation lifetime measurements were carried out using a standard fast-fast coincidence system with timing resolution of 240.34 ps full width of half-maximum (FWHM) and total of 1024 channel. The positron source used was $^{22}NaCl$ deposited and the sandwiched between two thin aluminum foils. This source is placed between two pieces of sample. The duration of each measurement was about 80 min maximum, during which time a total of 1×10^6 where collected. All measurements were made in air at room temperature unless otherwise stated.

3.4.5 Temperature dependent positron annihilation studies

A new temperature control unit was designed and developed in this study. The unit was designed to allow for effective heating of the sample, while at the same time still allowing for a relatively high annihilation count rate. The unit consisted of an aluminum disk mold with a diameter of 8 cm, the outside heating ring had a thickness of 1 cm and the inside

heating plate a thickness of 0.3 cm. The outside heating ring of the molded disk contained an inset rim in which was coiled a copper wire which was in turn connected to an electrical source and a temperature control unit. A small hole was pitted in the center of this aluminum disk to accommodate the positron sample and source without blocking the detectors. The positron source with the sandwiched sample was placed in this hole and covered from both sides with a thin foil to ensure effective heating of the sample. This is shown in the inset in the Figure 3.3. A temperature probe was connected to the mold from one side at a point very near the sample and a temperature control unit from the other side to control and measure the temperature. The temperature range used in this study is between 40 °C to 150 °C, and the duration of each measurement was about 90 min maximum, during which time 1×10^6 counts were collected. This is an indication that this unique heating design allows for heating studies without the normal dramatic decrease in the count rates that occur due to the configuration of the heating devices.

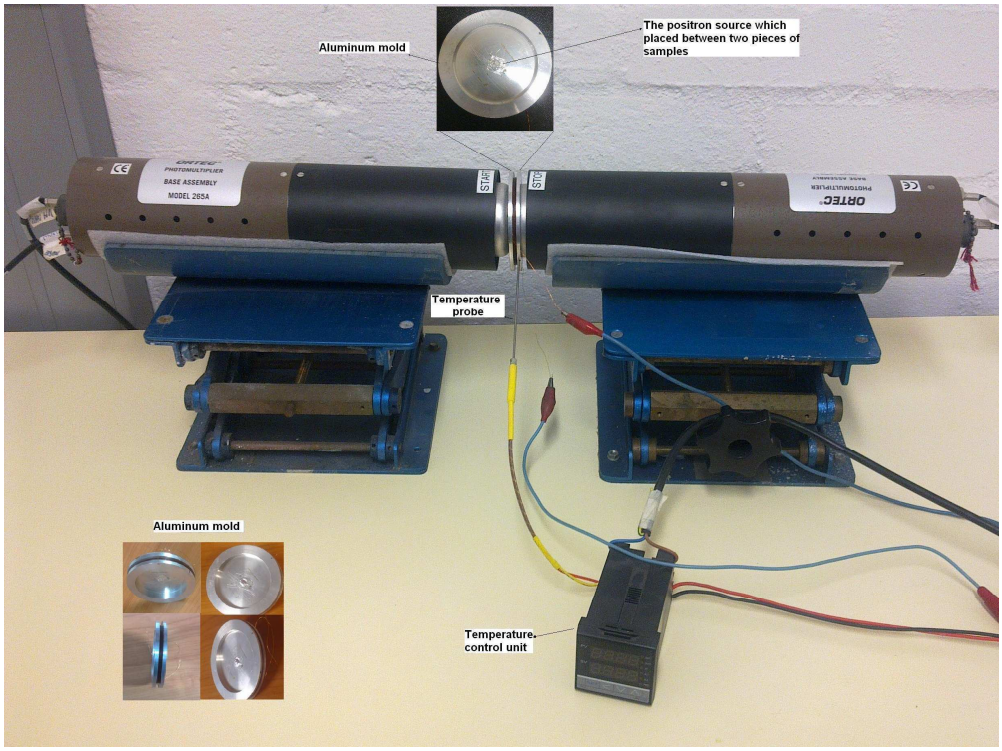

Figure 3.3 Temperature control unit designed for the measurement of positron parameters at different temperature.

3.4.6 Microhardness testing

The microhardness is usually defined as its resistance to local plastic deformation [2, 3]. Microhardness measurements were carried out using a Vickers's hardness tester equipped with diamond indentor and a load of 10 gf was applied to obtain the deformation pattern. All the measurements recorded were averages of at least five measurements.

3.5 References:

1. Anantawaraskul, S., Soares, J B P., Wood-Adams, P M. and Monrabal, B. Polymer 2003, 44, 2393-2401.
2. Lopez, J. Polymer Testing 1993, 12, 437-458.
3. Crawford, R. Polymer Testing 1982, 3, 37-54.

Chapter 4
The effect of short–chain branching and distribution on the free volume properties of polyethylene as determine by PALS

4.1 Introduction

The physical properties of polyethylenes (PEs) can be widely varied by manipulating their microstructural parameters, in particular, the amount, length and placement of the alkyl branches along the chain. The comonomer content constitutes the most important factor affecting both structure and properties of the PEs, although the length of the comonomer may also be important. A considerable decrease in crystallinity and increase in the free volume as the comonomer content increases is expected. The incorporation of another comonomer into an otherwise crystalline copolymer will generally reduce the crystallinity and reduce the melting point in a continuous manner. This is due to incorporation of the comonomer as defects, and these defects decrease the melting point and heat of fusion by disrupting the intermolecular bonding within the crystalline lattice [1].

As discussed earlier the use of metallocene catalysts has allowed for the synthesis of linear low density polyethylene (LLDPE) by inclusion of comonomers. In this study m-LLDPE was selected because all metallocene sites produce polymer chains with virtually the same architectures compared to using Ziegler-Natta catalyst.

The material is expected to produce homogeneous fractions. The degree of chain branching plays a significant role in preventing the copolymer chains from packing together in a regularly and closely packed structure, which will affect the density and crystallinity as well as the free volume properties, and hence the final properties of the copolymer. Studies were carried out to determine the influence of the comonomer length on the free volume properties of LLDPE. Two different types of LLDPE, with different comonomer lengths, were first fractionated by temperature rising elution fractionation (TREF), and each fraction was characterized by CRYSTAF, DSC, NMR, HT-GPC and PALS. Several authors have

reported on the effect of short-chain branch distribution on melting and crystallization behaviur of m-LLDPEs [2-5].

The measurement of parameters relating to free volume within polymeric systems is an important aspect of their characterization. Free volume can be correlated to many properties, such as crystallinity, comonomer content, and comonomer length. Therefore, the behaviour of the copolymer will depend largely on the microstructure free volume.

Positron lifetime spectroscopy (PALS) has been used to determine the free volume properties of PE polymers [6-9]. Cerrada *et al*. [7] reported PALS measurements for a LDPE and several ethylene-1-hexene copolymers synthesized with metallocene catalysts. They found a linear relationship between the location of the β relaxation and the free volume fraction: the higher the relaxation temperature is the lower the free volume value will be.

4.2 Experimental

4.2.1 Materials

Two different types of LLDPE, with different comonomer length (hexene and octene), were used in this study. These materials are compared in order to understand the subtle effects of sparse degrees of short-chain branching on the copolymer structure including the free volume properties. The properties of both copolymers were described in Section 3.2.3.

4.2.2 Calculation of crystallinity

The crystallinity of PE1 and PE2 were determined by two different methods. The first method used the melting endotherm area of DSC peak, where the percentage crystallinity in each fraction was calculated using the heat of fusion for 100 % crystallinity for PE and observed heats of fusion in DSC.

The second method involved calculating the crystallinity according to density by assuming a two-phase system with constant amorphous and crystalline phase densities. The second method is based on two simple assumptions: that PE samples consist of a two-phase morphology and that the density of each phase is uniform within the sample and consistent from one sample to another. The following equation was used:

$$X = \frac{(\rho - \rho_a)}{(\rho_c - \rho_a)} \qquad 4.1$$

where X is the crystallinity present, ρ_a and ρ_c are the fully crystalline and amorphous density, respectively. The following density values were used: 0.855 g/cm^3 for fully amorphous PE and 1.0g/cm^3 for fully crystalline PE [10].

4.2.3. Calculation of the comonomer content

The percentage comonomer was calculated according to the following equation:

$$\text{Comonomer content} = \frac{(\alpha \text{ Br carbon}/2) + \text{Br carbon}}{\text{Total number of backbone carbons}} \qquad 4.2$$

The comonomer content was determined by using the integration of the peaks associated with the backbone carbons and relating this to the peaks associated with backbone carbons at the branch points, and then using equation 4.2 to determine the comonomer content. The percentage of the carbons α to branching was divided by two; because there are two carbons α to the branching and the percentage of the branching carbons are added together.

4.2.4 Free volume measurements

PALS measurements were used to determine the free volume properties in both copolymers and their fractions. The measured lifetime spectra were resolved into four lifetime components with the help of the computer program PATFIT-88.

4.3 Results and discussion

The aim of this part of the study is to study the measured positron annihilation parameters as a function of the nature and degree of short chain branching in semi-crystalline polymers. Two LLDPEs of different branch length were selected. The PE1 copolymer is an ethylene 1-octene copolymer and the PE2 copolymer is an ethylene 1-hexene copolymer. These two copolymers were fractionated by TREF to produce two systematic series of

copolymers with different degrees of branching and branch length. This approach has the advantage over other studies in which commercial PE samples with different branching content (comonomer content) were studied. Here, using the approach described will produce more homogenous fractions which allow for better control and understanding of the molecular structure, and resulting morphology, thus making the interpretation of PALS results more reliable. Critical to this process is that each of the homogenous fractions is fully characterised in terms of molecular structure and morphology.

The first part of this section summarizes the results of fractionation and subsequent characterization of the two LLDPEs. The free volume of the fractions was determined by PALS. Results of the measured positron annihilation parameters and microhardness analysis were used to study the relationship between the measured free volume properties and bulk physical properties. The last part of this section describes the extension of this investigation that involved further manipulation of the copolymer microstructure by the removal of certain fractions from the bulk material.

In order to obtain a good insight into the main parameters that influence the structure in copolymers, a full characterization of the copolymer microstructure and copolymer morphology is indispensable. Many studies dealing with the polymer structure lack such a detailed and complete characterization of the polymer chain microstructure. In this study a full characterization of the copolymer microstructure was done by fractionation of each copolymer by TREF, and analysis of each fraction using different techniques.

4.3.1 Fractionation

It is well known that in LLDPE it is not only the average molecular mass and the number of short-chain branches, but also their distributions, that have a significant effect on the end-use properties of the material. There are many ways to characterize LLDPE including the use of cross fractionation. In this study LLDPE is fractionated by crystallizability (comonomer composition and degree of branching).

In this study, preparative TREF is used as a primary technique for fractionation of the copolymers. This technique separates semi-crystalline macromolecules according to their

crystallizability due to the chemical compositions of the polymeric chains (molecules). Increasing comonomer content or greater amounts of SCB results in an almost linear depression of the melting or elution temperature [11]. In this study both of the copolymers were fractionated by TREF into eleven fractions.

Compared to TREF, CRYSTAF is a much more feasible technique for the analysis of large numbers of samples. This powerful method, which has been developed by Monrabal [12], is based on the monitoring of the concentration of a polyolefin solution during the crystallization. CRYSTAF relies on the measurement of the concentration of dissolved polymer during crystallization following dissolution at high temperature. The temperature is decreased at a controlled rate. During the crystallization process, aliquots of sample are filtered and the concentration of polymer in solution is determined. The main difference between CRYSTAF and TREF is that CRYSTAF analysis is done by monitoring the decrease in concentration of the polymer as it crystallize (out of solution) while in TREF the polymer is eluted by a melt dissolution process after being crystallized onto a support.

Figure 4.1 shows the CRYSTAF profiles for both bulk copolymers PE1 and PE2. The bulk copolymer trace indicates two crystallization peaks for PE1 at 32ºC and 55ºC. The low temperature crystallization peak represents the highly branched polymer chains and the higher temperature crystallization peak is attributed to lower branched polymers chains. Similar results were later obtained from TREF analysis.

The bulk copolymers trace indicates two crystallization peaks for PE2 at 80ºC and 88ºC. This is due to broad and bimodal short-chain branch distributions, which occur due to either non-homogeneous active sites in the metallocene catalysts or the presence of more than one type of active site. Soga *et al.* [13] observed a similar profile for m-LLDPE. This bimodality was ascribed to the types of active sites present in the metallocene catalysts.

The higher crystallization temperature of PE2 compared to PE1 is due to a lesser degree of branching in PE2, as a result of its lower comonomer content (4.8% for PE1 and 3.2% for PE2).

The CRYSTAF profiles and the presence of the two distinct peaks are illustrative of the complexity of the molecular structure of the commercial samples and resulting limitation of previous PALS studies on these types of commercial samples.

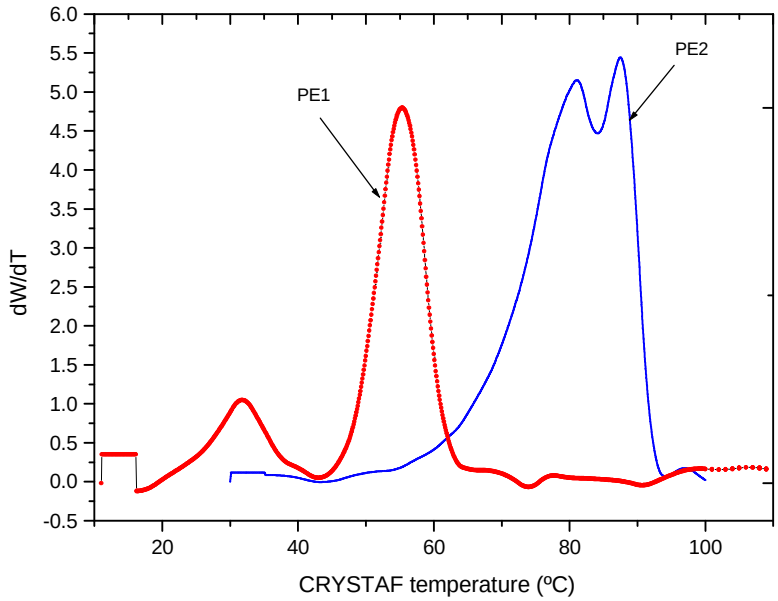

Figure 4.1 CRYSTAF traces for bulk copolymers PE1and PE2.

Figure 4.2 shows the distributions of eluted material of the TREF fractionation of PE1 and PE2. The elution profiles are relatively broad for both copolymers, but it is much broader for PE2. This indicates a much broader distribution in the chemical composition of the chains in the hexene copolymer (PE2) compared to the octene copolymer (PE1).

The ethylene/1-octene copolymer (PE1) showed an elution distribution in the temperature range 50-100°C, while the ethylene/1-hexene copolymer (PE2) showed a relatively broad elution distribution in the range 60-120°C. As was the case on the CRYSTAF profiles, this difference is due to the difference in the comonomer content: 4.8% in 1-octene compared to 3.2% for the 1-hexene copolymer.

PE1 showed a broad crystallization peak with a maximum at 70 ºC and a smaller peak at 30 ºC. This is consistent with the bimodal peak observed in the CRYSTAF analysis. PE2 showed only one peak at a higher temperature (87 ºC), which suggests that PE2 has less chain heterogeneity than PE1 [14]. It is also noted from the figure that the TREF elution

temperatures of PE1 shift to lower values, compared to PE2 as was the case in the CRYSTAF analysis. This may be explained by the difference in the short chain branch distributions, but also may be due to the fact that as the length of the branches increases, the branches become more effective at disruption of regular packing and thus decrease the melting point of the crystalline regions [15].

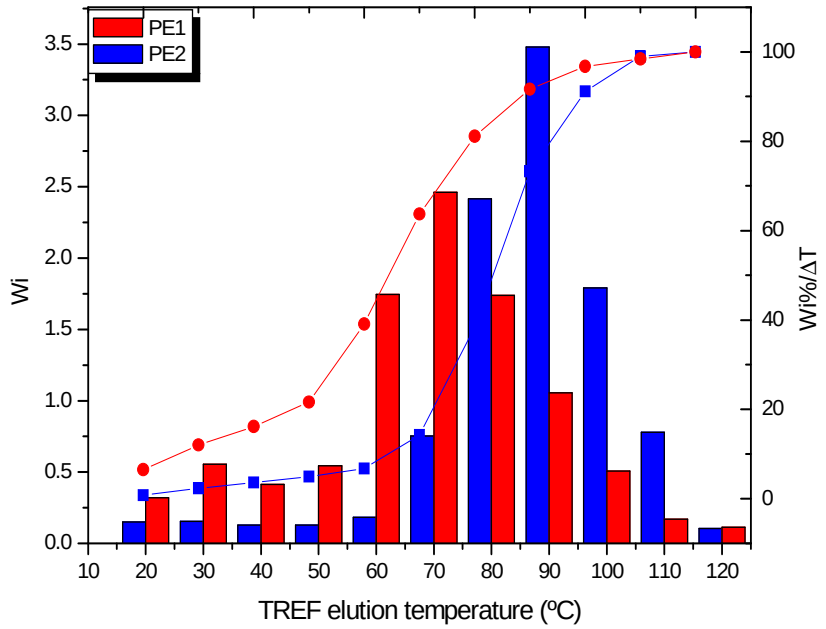

Figure 4.2 TREF profiles of PE1 and PE2. (Tabulated data can be found in Appendix A)

There is a significant difference in terms of the peak maxima for CRYSTAF and TREF for the higher temperature peaks. It is much higher in the case of prep-TREF (70 ºC), compared to CRYSTAF (60 ºC). This shift is a result of the under-cooling effect. A similar result was reported by Britto *et al.* [16] and Gabriel and Lilge [17]. They pointed out that the shift between CRYSTAF and TREF profiles is due to the "super cooling effect" because CRYSTAF profiles are measured during crystallization, while TREF data is measured during the melting/dissolution process [18].

4.3.2 Characterization of copolymer fractions

Table 4.1 summarises the properties of each of the fractions of PE1 and PE2, after fractionation by TREF. Because of the limited amount of material in the soluble fractions in each experiment, it was decided to combine all the fractions below 50 ºC into one fraction, which is designated as the soluble fraction (SF). The soluble fraction plays a critical part in the ultimate properties of the copolymer. Table 4.1 shows the DSC crystallization (T_c) and melting temperatures (T_m) of the fractions as well as the peak maximum temperature of the CRYSTAF analysis of each fraction ($T_{CRYSTAF}$). As is expected, the T_c, T_m and $T_{CRYSTAF}$ all increase with an increase in the TREF elution temperature. The T_m temperature increases from 26 ºC to 60 ºC for PE1 and from 64 ºC to 88 ºC for PE2. CRYSTAF traces of the TREF fractions are shown in Appendix B. All the CRYSTAF traces of the fractions show a single narrow peak, indicating that all of the TREF fractions are relatively homogenous at least with regards to crystallizability.

Table 4.1 Properties of TREF fractions of PE1 and PE2.

Fraction temperature (ºC)	T_m [a] (ºC)		T_c [a] (ºC)		$T_{CRYSTAF}$ [b] (ºC)		Comonomer content (%) [c]	
	PE1	**PE2**	**PE1**	**PE2**	**PE1**	**PE2**	**PE1**	**PE2**
SF	72.4	93.2	62.9	85.7	-	-	5.60	3.50
60	76.2	96.1	65.4	89.1	26.3	62.8	3.52	3.46
70	81.5	102.7	68.2	90.4	34.4	64.0	2.64	2.60
80	96.1	109.8	77.6	97.3	45.1	75.1	2.77	2.55
90	98.4	118.4	81.8	106.4	54.8	82.5	2.61	1.91
100	101.4	118.6	85.4	110.4	58.1	88.4	1.61	1.20
110	103.3	122.7	86.9	111.6	58.6	87.6	1.20	1.15
120	103.4	124.9	87.7	107.4	60.4	87.7	0.90	0.62

a) Melting and crystallization temperature from DSC
b) CRYSTAF peak maximum temperature
c) Comonomer content as calculated from ^{13}C NMR and equation 4.2

Figure 4.2 shows that both TREF profiles have relatively broad distributions. This indicates that there is a broad distribution in the chemical composition of the chains. This broadness is due to chain defects, or comonomers, which prevent the crystallization of the polymer chain, and generally lead to a broadening and lowering of the melting range. The effect of chain defects can be clearly seen in the crystallization and melting temperatures shown in Table 4.1. The exact melting point depression depends on the number, kind, and distribution of defects, and on the crystallization conditions [19].

DSC can give complementary information about the molecular structure of LLDPEs. This is primarily because the segregation of polymers by DSC is governed by a different mechanism than that in TREF. As mentioned above, TREF fractionates macromolecules based on the crystallizability difference between molecules; in other words, TREF physically separates polymeric molecules. However, DSC does not physically separate molecules; rather, it segregates molecular segments according to lamellar thickness or methylene sequence length. Hence, the difference in lamellar thickness between molecules and within individual molecules can be evaluated.

Figure 4.3 shows the DSC thermograms of the bulk copolymers PE1 and PE2. The crystallization exotherms of both copolymers are fairly similar in shape, but PE2 shows a higher crystallization temperature exotherm. Both copolymers show distinct high temperature peaks, followed by a minor broad peak to a long tail. This behavior, particularly in the PE2, is attributed to the non-uniformity in the branch distribution due to intramolecular compositional heterogeneity. There is also a significant difference in the melting temperatures of both copolymers. The PE1 copolymer shows a lower melting temperature peak (98 ºC), compared to PE2 (123 ºC). These differences can be attributed to morphological influences, particularly the perfection in lamellae structure. These DSC results are consistent with the CRYSTAF and TREF results.

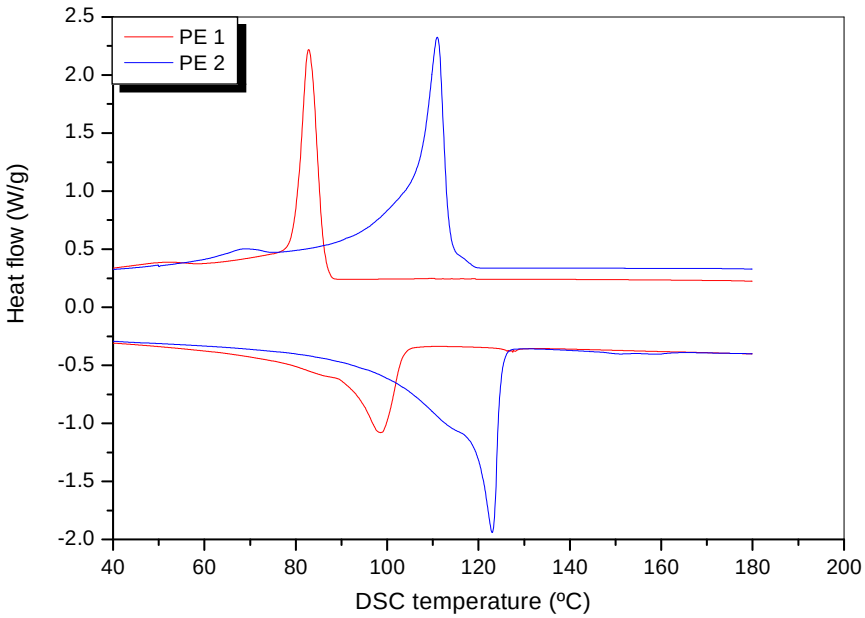

Figure 4.3 DSC crystallization and melting endotherms of PE1and PE2.

The DSC thermograms of the preparative TREF fractions are shown in Appendix C. The low-temperature fractions crystallized at lower temperatures with a relatively broad crystallization peak, which is associated with the high SCB contents. As the elution temperature increases the crystallization temperature increases and the crystallization peak becomes sharper. This is as a result of the lower SCB contents and lower comonomer content in these fractions. A single peak was observed for each fraction. Again this confirms the greater molecular homogeneity in the fractions than in the bulk material.

Table 4.1 shows a change in the melting temperature with increasing elution temperature. This is well documented and is a result of the effect that a decrease in the SCB content has on the melting temperature of both copolymers. Zhang *et al.* [3] also observed changes in the melting temperature of ethylene-butene copolymer as the elution temperature increased. It is also noted that as the elution temperature increases the melting peak become much narrower. This may be due to a number of factors, as reported by Simanke *et al.* [20]. They attributed possible broadening of the DSC endotherms to different thermal histories of the polymers, broader molecular weight distributions and different crystal sizes being present in the fractions. Because in this study DSC analysis of both copolymers were performed

under identical conditions, the effect of thermal history and crystallization method can be eliminated as a factor leading to broadening. The broadening of the endotherms is rather due to differences in the crystal sizes and the degree of their perfection, which is directly affected by the introduction of increasing amounts of the comonomer in the PE chain [20, 21]. Specifically, increasing comonomer content decreases the sequence length between comonomer points and results in thinner lamellae, which will lower the crystallization temperature.

A similar behavior was observed for both copolymers; all the fractions show a single melting peak (see appendix C). The peak temperature increases as the fractionation temperature increases. However, the melting temperature was much higher in the case of PE2 compared to PE1 for all fractions. This is in accordance with TREF and CRYSTAF results.

4.3.2.1 Lamellar thickness

The lamellar thickness plays an important role in crystallization and it can be an important parameter in determining the mechanical properties of a material. In the present study, the lamellar thickness is an important parameter in the PALS analysis because it can potentially give an indication of the degree or extent of the crystal/amorphous interfacial area. As will be discussed later the third lifetime component (τ_3) is attributed to annihilation within this interfacial region. It is, therefore, important to determine the lamellar thickness when characterizing the morphology of the copolymers.

The amount and type of comonomer and the short-chain branch distribution are the dominant factors affecting the spherulitic texture and the lamellar morphology, and hence the melting behaviur of LLDPE [22]. It is also known that the main factor determining the melting temperature of a polymer is the lamellar thickness of the crystallites and the breadth of the DSC curves reflect the lamellar thickness distribution. The crystal thickness (L) can be related to the melting temperature (T_m) by rearranging the Gibbs-Thomson equation as follows:

$$\frac{L}{\sigma_e} = \frac{2}{\left(\Delta H_m^0 . \rho_c\right)}\left[1 - \frac{T_m}{T_m^0}\right]^{-1} \qquad 4.3$$

where T_m^0 is the melting temperature of a PE crystal of infinite thickness, which is 414.6 K [23] , ΔH_m^0 is the heat of melting of the perfect crystal (290 J/g) [23] σ_e is the surface energy which is of the order of 100 erg/cm^2 for regular folding [5], T_m is the peak melting temperature of the fraction and ρ_c is the fully crystalline density.

Figure 4.4 shows the results of this analysis using equation 4.3 and the DSC curves for each of the fractions for the PE1 and PE2 copolymers. It can be seen that the PE2 copolymer has a higher lamellar thickness compared to PE1 for each of the temperature fractions which is reflected by the higher relative melting temperature for this copolymer. This difference is most probably due to the difference in the distribution of the short branches of each of the copolymers. It is known that short branches reduce the regularity of the polymer chains and decrease the lamellar thickness of the formed crystallites. The more short-chain branches in the copolymer the lower the lamellar thickness. In other words, a thicker lamella is formed from the longer ethylene sequence lengths in the intrachain sequence length distribution, whereas a thinner lamella is formed from the shorter ethylene sequence lengths. The longer ethylene sequence crystallizes first because they can overcome the nucleation barrier at lower undercoolings than the shorter sequences. The crystals are therefore formed from sequences of different lengths that are in the same polymer sample.

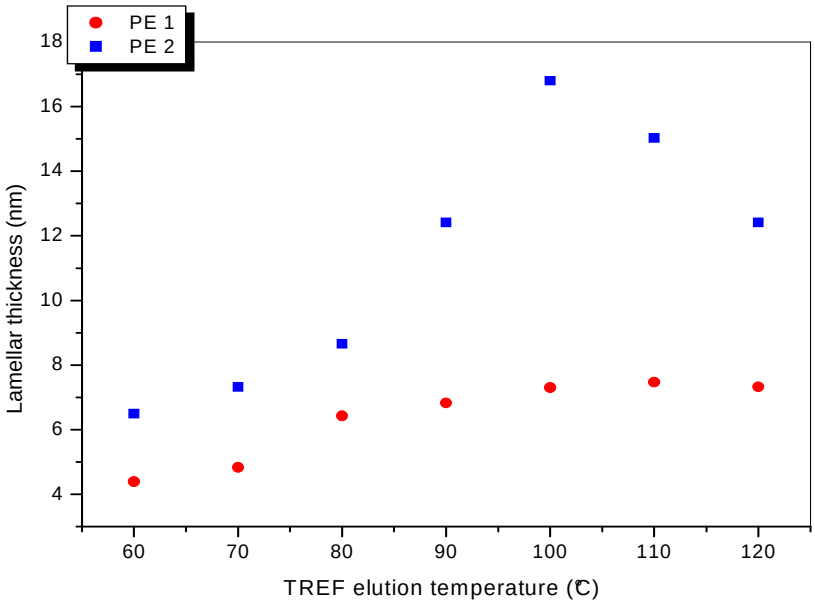

Figure 4.4 Calculated lamellar thickness of TREF fractions of PE1 and PE2.

4.3.2.2 Chain microstructure

The heterogeneity of the comonomer or short-chain branch distribution is an important characteristic in describing the molecular structure of LLDPE. The effect of short-chain branching has been the topic of many studies [20, 24, 25]. Some studies revealed that the melting point depression in semi-crystalline polymers is linear with the number of defects and often independent of the chemical nature of the defect [26, 27].

Using ^{13}C-NMR, it is possible to observe that the lower temperature TREF fractions have higher comonomer contents and, as the temperature increases, the percentage of the comonomer decreases, as expected. The comonomer content analysis of the TREF fraction is shown in Figure 4.5. The decrease in the comonomer content at higher temperatures can be explained by the fact that at low temperature the comonomer units are isolated between the ethylene units which will reduce the crystallization temperature, and consequently the crystallinity present will decrease. At high temperature the ethylene units will easily crystallize because of the absence of the comonomer units, and disruption of crystallization. It was also observed that the comonomer content is slightly higher in PE1 fractions compared to

PE2 fractions, which reflects the low crystallization temperatures of PE1 fractions. (The NMR spectra of both copolymers are shown in the Appendix D).

The comonomer content of each TREF fraction is very similar at any given temperature for both copolymers. The exception is the soluble fraction (SF) where the PE1 (octane copolymer) has a much higher comonomer content than the PE2 copolymer. It is interesting to note that despite the relatively similar comonomer contents, there is a significant difference observed in lamellar thickness (melting temperatures) of each fraction. . This may be due to distribution of the SCB in both copolymers.

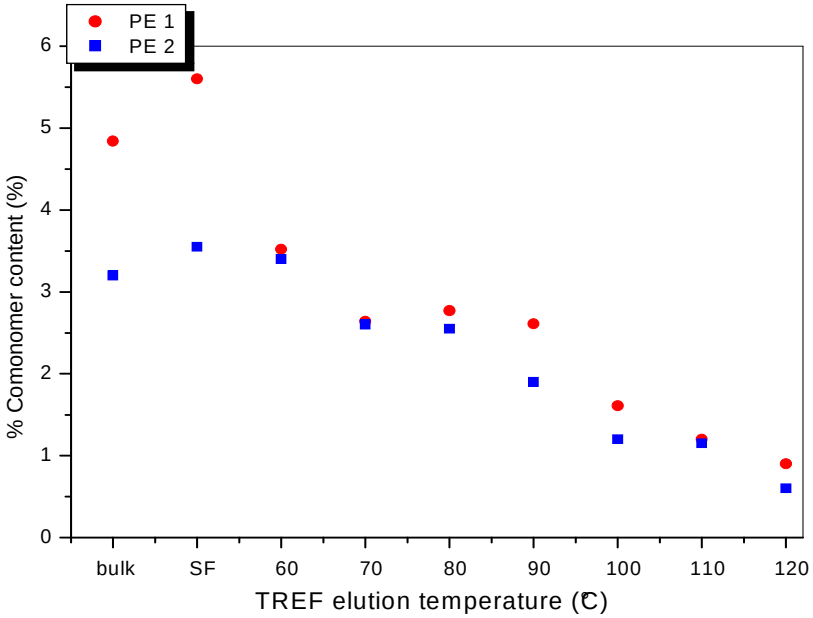

Figure 4.5 Comonomer content of bulk copolymers and TREF fractions of PE1 and PE2.

In the case of LLDPE copolymers, the amount and type of comonomer and the short-chain branching distribution are the dominant factors affecting the spherulitic and the lamellar morphology, and hence the melting behavior [28]. The characterization of the heterogeneity of SCB distribution is, therefore, important because not only does it affect the melting and thermodynamic properties of LLDPE, but it also provides useful information on the heterogeneity of LLDPE.

Two types of heterogeneity exist for LLDPE. The first is intramolecular heterogeneity, where the SCB distribution of individual macromolecules in the system is not uniform along the chain backbone, but all the molecules possess the same SCB distribution. The second is intermolecular heterogeneity where the SCB distribution differs from one molecule to another [29]. See Figure 4.6.

Intramolecular heterogeneity Intermolecular heterogeneity

Figure 4.6 Types of SCB heterogeneity in LLDPE.

Hosoda [30] developed equations for the estimation of the SCB in LLDPE copolymers based on the copolymers melting point. These equations were used to estimate the extent of the short-chain branching in the present study and are shown in equation 4.4 and 4.5 below (only the equations relevant to the copolymers in this study are given below). These equations have been used by several authors [31]. Hosoda investigated both the molecular structure and crystalline structure of different LLDPE's using various techniques and proposed the following relationships to determine the short-chain branching distribution.

$$\text{For 1-hexene copolymers, } T_m = -1.69SCB + 133 \quad (4.4)$$

$$\text{And for 1-octene copolymers, } T_m = -2.18SCB + 134 \quad (4.5)$$

where T_m is the observed melting temperature and SCB is the short-chain branching in branches per 1000 backbone carbon atoms.

Table 4.2 gives the percentage crystallinity and short-chain branching per 1000 backbone carbon atoms (calculated from the above equations) for each fraction in both copolymers. It is clear especially in PE2 that an increase in the SCB leads to a reduction in crystallinity by up to a half. It has been suggested that as the comonomer content in LLDPE copolymers increases and the average number of consecutive ethylene units decreases, the

branch points (due to the comonomer) prevent the formation of long ethylene segments that facilitate chain folds, thereby reducing the crystallisable part of the copolymer with the associated decrease in crystallinity [20, 32].

Tables 4.1 and 4.2 show that as the comonomer increases, the T_m and crystallinity percentage decreases. As has been mentioned previously, this is explained by the fact that as the comonomer content increases, the average number of consecutive ethylene units decreases and the crystallisable part of the copolymer becomes smaller. As a consequence, the crystallinity decreases and the amorphous and interfacial contents increase. Raul *et al.* [33, 34] observed similar results for ethylene with 1-hexene and 1-octene as a comonomer. It has also previously been mentioned that the melting temperatures of the PE2 fractions are systematically slightly higher than those of PE1 and this is reflected in the calculated SCB values for the two copolymer series where the PE2 series has a lower degree of SCB for each of the respective fractions. This is due to a difference in sequence length distribution in both copolymers, since they have relatively similar branching content for a given fraction. This also highlights the fact that the calculated SCB values (based on T_m) are single values and the calculations assume a completely uniform distribution of the SCB in the materials.

Table 4.2 Percentage crystallinity and calculated SCB in each TREF fraction for PE1 and PE2

Fraction temperature (°C)	Crystallinity % (DSC)[a]		Crystallinity % (Density)[b]		SCB CH_3/1000C	
	PE1	PE2	PE1	PE2	PE1[c]	PE2[d]
SF	12.06	16.56	13.4	18.4	28.2	17.92
60	13.95	17.19	15.5	19.1	26.6	17.0
70	25.10	23.67	27.9	26.3	23.9	14.6
80	25.72	30.33	28.5	33.7	17.2	11.2
90	27.86	41.22	30.9	45.8	16.0	6.9
100	29.38	44.55	32.6	49.5	14.7	4.3
110	30.91	45.72	34.3	50.8	14.3	5.3
120	29.43	34.47	32.7	38.3	14.6	7.2

a) Where: $\Delta H^o_{f,c}$ % 100 crystallinity for PE is 293.6 J/g [35]
b) Crystallinity from equation 4.1
c) Short-chain branching as calculated from equation 4.5
d) Short-chain branching as calculated from equation 4.4

It is also noted that as the elution fractionation temperature increases, the crystallinity, melting temperature, and SCB content decrease. These results are in accordance with those of Hosoda [30] and Mirabella [14]. Furthermore, molecules that elute at each temperature

interval have different methylene sequence length (calculated from the T_m values) despite eluting at the same temperature interval and have similar average comonomer contents.

Crystal populations are formed from sequences of different lengths that are in the same polymer chains (i.e., intrachain heterogeneity). The SCB values calculated above can be translated into methylene sequence length (MSL) via the following equation:

$$MSL = (998 - SCB)/ (SCB + 1) \qquad 4.6 \quad [36]$$

It is claimed that during the crystallization process the sequences of the polymer chain crystallize independently, and subsequently melt at a temperature corresponding to their crystallite size. In other words, the branches are excluded from the crystals and the methylene sequence length will limit the lamellar thickness. Therefore, each point on the DSC curve can, theoretically be considered to represent a group of methylene sequences of equal or similar length. The MSL distributions of PE1 and PE2 are shown in Table 4.3.

Table 4.3 presents a summary of the calculated parameters for the T_m values of the copolymer fractions. It should be noted that all the data presented in Table 4.3 is simply manipulation of one single parameter determined from the T_m in the DSC melt endotherm. Nerveless, it can be useful to consider the variation in terms of the values presented.

The table shows that as the fraction of non-crystallizable units increases, a significant drop of the lamellar thickness is observed. The thickness and lateral size of the lamellae decrease, as well as the degree of crystallinity as mentioned above. These changes in morphology can affect both the mechanical and thermal properties, like the melting point of the copolymer. This results are in agreement with others [37, 38].

Table 4.3 Methylene sequence length distribution for fractionated copolymers PE1 and PE2

Fraction temperature (°C)	MSL[a]		SCB[b]		Lamellar thickness [c]	
	PE1	PE2	PE1	PE2	PE1	PE2
SF	33.21	51.80	28.2	17.92	4.1	5.97
60	35.19	54.31	26.6	17.06	4.3	6.48
70	39.12	62.75	23.9	14.67	4.8	7.32
80	53.89	80.68	17.2	11.23	6.4	8.65
90	57.76	124.34	16.0	6.97	6.8	12.41
100	62.63	185.72	14.7	4.35	7.3	16.79
110	64.29	156.07	14.3	5.36	7.4	15.02
120	63.03	120.82	14.6	7.20	7.3	12.41

a) Determined from equation 4.6
b) Determined from equations 4.4 and 4.5
c) Determined from equations 4.3

The result suggests that the crystal thicknesses of these copolymers are predominantly controlled by MSL rather than by chain folding [3]. The table also shows that the lamellar thickness increases almost linearly with increasing methylene sequence length. These results are in agreement with those obtained by Defoor [39].

DSC is one of the most widely used techniques to calculate the degrees of crystallinity in polyolefin sample. There are, however, several difficulties with respect to the calculation of the crystallinity from the melting endotherm area of DSC. A major problem is the fact that due to the broad melting range, the drawing of a baseline, according to the peak area determination method to integrate the endotherm is often ambiguous and may introduce considerable error in the determined crystallinity values. It is also known that in many cases the peak consists of a combination of melt-recrystallization [40]. In the present study it was decided to use crystallinity values determined via density measurements to overcome these difficulties in addition to the fact that the positron measurements are largely done at room temperature (the same temperature at which the density measurements are done). The crystallinity is determined according to density by assuming a two-phase system with constant amorphous and crystalline phase densities at the measurement temperature.

The calculation of the degree of crystallinity from density is advantageous in that it is simple, precise, and applicable to samples of virtually any configuration.

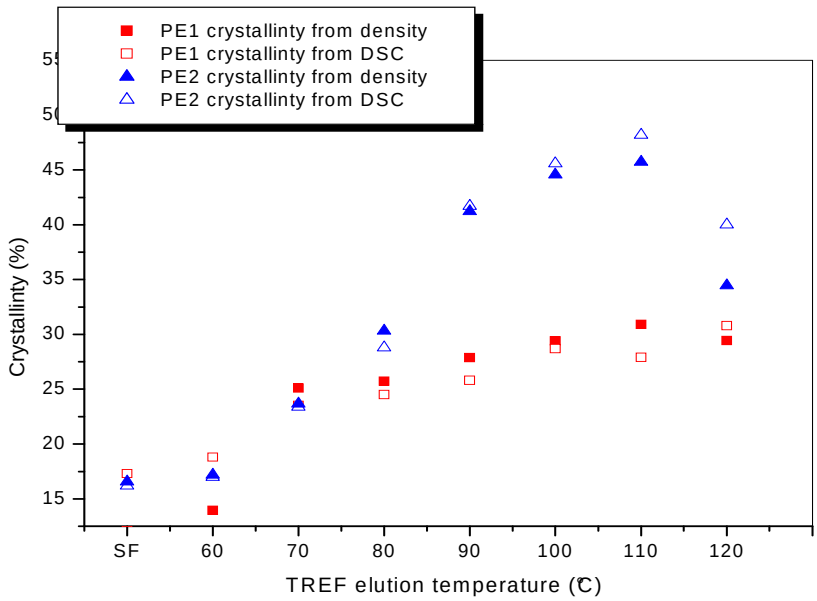

Figure 4.7. Crystallinity of PE1 and PE2, from DSC and density measurement.

Figure 4.7 shows the crystallinity of each of the TREF fractions based on the two different crystallinity measurements. Similar values were observed from both measurements. However, the density based measurement gives slightly higher values. All the crystallinity results reported in the rest of this study are based on density measurements. As mentioned above this not only has the advantage that potential problems with DSC measurements are avoided, but also the PALS measurements are preformed at room temperature.

The variations in crystalline structure significantly influence the mechanical behaviour of the copolymers. The effect of the comonomer type on mechanical properties is confirmed by microhardness, as is described in the following.

4.3.3 Microhardness

The mechanical properties are of relevance for all applications of polymers in industry. In addition there is a strong correlation between molecular structure, morphology and mechanical properties of polymers. It is also useful to correlate the mechanical property to the measured PALS parameters which are presented in the next section.

Microhardness is an extremely sensitive tool to detect structural changes occurring in polymer microstructure [41-43]. In this section the results of microhardness analysis of the copolymer fractions are discussed. Determination of the microhardness is often a useful and sensitive technique to probe small differences in materials not detectable by other large scale tests. An advantage of this test in the present study is that relatively small sample sizes are required to do the analysis.

Microhardness can be defined as the resistance of a material to deformation, particularly permanent deformation, indentation or scratching [44]. The microhardness values of the fractions for both copolymers correlated well with percentage crystallinity values as is shown in Figure 4.8. The microhardness values increased with an increase in the percentage crystallinity. It is probable that at low crystallinity the steric hindrance and compression of the disordered molecular region are responsible for plastic deformation, whereas at higher levels of crystallinity the deformation modes of the microcrystals predominate [45]. The microhardness depends on the distribution and the amount of crystalline and amorphous phases present in the polymer [45, 46].

The higher values of microhardness for the higher TREF temperature fractions can be attributed to higher crystallinity compared to the lower TREF temperature fractions. This increase in microhardness can be correlated with an increase in lamellae thickness; as can be clearly seen in the Figures 4.9 and 4.10.

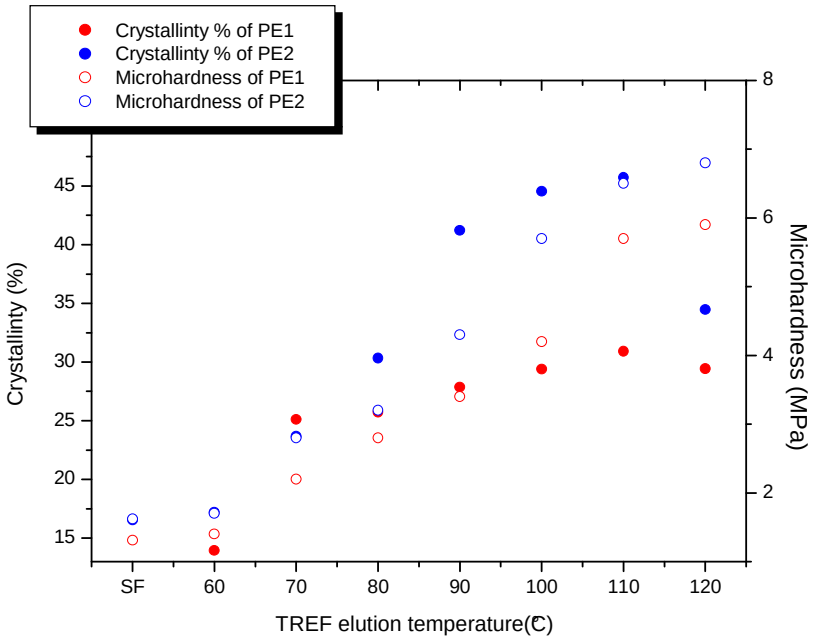

Figure 4.8 Microhardness (open symbols) and crystallinity (closed symbols) of PE1 and PE2.

Figures 4.9 and 4.10 shows the relationship between the crystallinity percentage (by density), microhardness and lamella thickness for each of the copolymers. The microhardness increases as the lamellae thickness increases in both cases. This result is in agreement with reports by others [41, 44, 47].

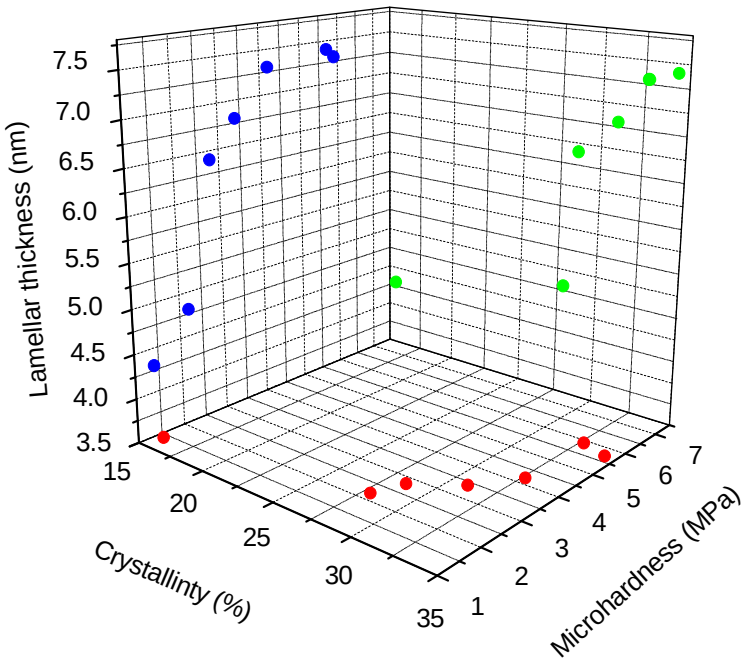

Figure 4.9 The relationship between crystallinity (from density), lamellar thickness and microhardness of PE1.

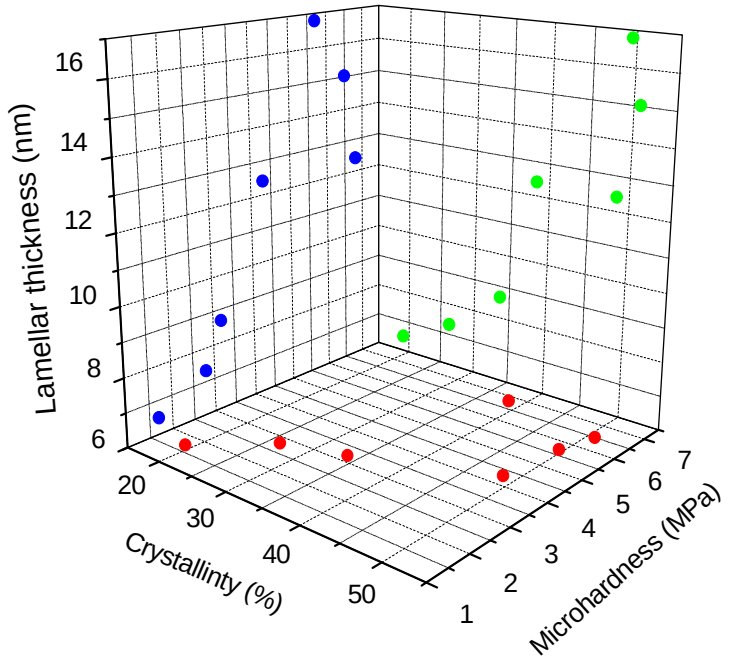

Figure 4.10 The relationship between crystallinity (from density), lamellar thickness and microhardness of PE2.

The above results show that the crystallinity and microstructure have a considerable direct influence on the microhardness of the copolymer and that the determination of microhardness is a simple technique for detecting and studying morphological changes. The overall increase in microhardness observed with crystallinity can be partly explained by the combined effect of the presence of a greater number of thicker lamellar crystals, due to a higher crystallinity.

The results presented in the preceding sections show the analysis in detail of the chemical and morphological variation of the fractionated copolymers. It is clear that these fractionated copolymers represent two systematic series of sample where there are varying degrees of SCB and resultant differences in crystal morphology. The following section presents the measurement of the positron annihilation parameters of each of these fractionated series

4.3.4 Measurement of positron annihilation parameters.

The primary objective of this part of the study is to determine how the measured positron annihilation parameters change as a result of differences in the comonomer length and content. Positron Annihilation Lifetime Spectroscopy (PALS) analysis is used for both the bulk and fractionated copolymers.

In all cases it was found that a four lifetime component fit gave the best fitting to the raw positron lifetime data. The shortest lived component, τ_1, is usually attributed to p-Ps annihilation. The intermediate component, τ_2, describes the annihilation of the free positrons. The two longest lifetime components designated as τ_3 and τ_4 represent the annihilation of the longer lived o-Ps localized within the open spaces in the polymer. In a typical amorphous material, only one o-Ps lifetime is detected. The fact that in the copolymer samples studied here an additional lifetime is detected is reflective of the complex morphology of the semi-crystalline sample. In previously reported studies, the third component, τ_3, has been attributed to the “pick-off” annihilation of the o-Ps in the crystalline regions (interface and/or defects) of the polymer. The longest lived component, τ_4, has been attributed to the pick-off annihilation of o-Ps in the amorphous regions of the polymer [48]. The results of the analysis of the raw

positron data for the two longest lifetime components (lifetimes τ_i and intensities I_i) of the fractions are tabulated in Table 4.4..

Table 4.4: Value of o-Ps lifetimes τ_i, and intensities I_i obtained for the bulk and fractionated copolymers PE1 and PE2

Fraction temperature	τ_3 (ns)		I_3 (%)		τ_4 (ns)		I_4 (%)	
(°C)	PE1	PE2	PE1	PE2	PE1	PE2	PE1	PE2
bulk	0.68±0.04	0.61±0.01	6.45±1.80	9.88±0.52	2.77±0.01	2.72±0.01	27.27±0.2	19.32±0.10
SF	0.49±0.02	0.51±0.02	5.84±1.15	7.87±1.81	2.79±0.01	2.78±0.01	28.38±0.2	23.67±0.10
60	0.53±0.03	0.56±0.03	9.51±2.53	9.93±1.61	2.76±0.01	2.70±0.01	27.26±0.2	22.95±0.20
70	0.54±0.03	0.59±0.03	6.72±0.87	11.09±2.14	2.73±0.02	2.67±0.01	27.23±0.2	22.45±0.20
80	0.55±0.03	0.59±0.03	9.56±2.47	6.80±0.73	2.71±0.02	2.68±0.01	27.39±0.2	21.39±0.20
90	0.57±0.04	0.62±0.03	9.69±1.16	9.87±1.69	2.68±0.02	2.66±0.01	24.95±0.2	21.21±0.30
100	0.65±0.05	0.72±0.05	9.89±0.90	9.08±1.31	2.65±0.02	2.63±0.01	24.22±0.3	19.14±0.30
110	0.67±0.01	0.76±0.03	10.15±0.83	11.37±2.31	2.62±0.02	2.57±0.01	23.24±0.1	17.14±0.20
120	0.68±0.04	0.77±0.11	10.19±1.35	11.80±2.23	2.63±0.05	2.54±0.02	21.11±0.2	15.70±0.60

Table 4.4 shows that the τ_4 values for both bulk and fractionated copolymers are in a range of 2.55–2.75 ns. This is in agreement with reports by others for the longest lifetime in polymers [49-51], and supports the conclusion that this component represents the o-Ps annihilation in the amorphous region of the polymer.

The shorter lifetime τ_3 component (considered to be o-Ps annihilation in the crystalline or interfacial regions of the polymer) has a lifetime in the range of 0.5–1.0 ns. This lifetime reflects the more dense molecular packing in the crystalline structure or the denser packing of the molecules at the interfacial crystalline area compared with the holes (2.7 ns) in the amorphous phase. Similar interpretation of this shorter o-Ps lifetime have been suggested in other studies [52].

Figure 4.11 shows a graphical representation of the τ_3 and τ_4 lifetimes as a function of the TREF elution temperature. The value of τ_4 (which is attributed to the pick-off annihilation of o-Ps in the amorphous regions of the polymer) shows a slight decrease as the fractionation temperature increases while the τ_3 values show the opposite trend where the value increases at higher elution temperature.

The decrease in the τ_4 value (and corresponding decrease in the mean free volume hole size in the amorphous parts of the polymer) can be explained by the fact that in the

higher temperature fractions, the chains in the amorphous areas of the copolymer have fewer short chain branches than the lower temperature fractions (as shown in the previous sections). This effectively leads to a slightly smaller average free volume hole size within these amorphous areas and a decrease in τ_4 lifetime due to a higher "packing density" of the chain in the amorphous region. The average hole size in the amorphous region may also be decreased due to the very high crystallinity of the sample. Since the amorphous areas are "connected" to the crystalline areas, the increase in crystallinity will affect the chains segmented mobility in the amorphous region to a small degree which may contribute to the overall decrease in the measured values.

In all cases the τ_4 value for all the fractions of PE1 compared to PE2 are slightly higher. This is explained by the difference in the nature of the comonomer. PE1 has an octene comonomer which has a longer carbon side chain than the hexene comonomer in PE2.

The results also suggest that there is a correlation between τ_3 and the TREF fractionation temperature. The τ_3 value increases as the fractionation temperature increases. The increase of τ_3 (which is attributed to the pick-off annihilation of o-Ps in the crystalline regions or crystalline interface) can be correlated to the increase in the crystalline region as the fractionation temperature increases. The increase is most likely reflective of the greater degree of crystalline defects as well as the increasing amount of interfacial area as the amount of crystallinity increases. It is also interesting to note that the PE2 copolymer with the hexene comonomer shows slightly higher values than the PE1 octene copolymer.

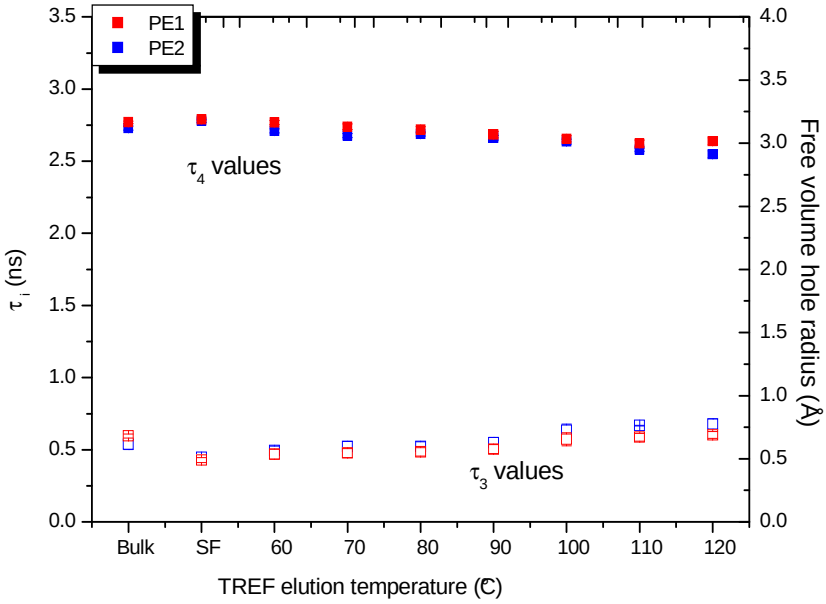

Figure 4.11 τ_3 (open symbols) and τ_4 (closed symbols) lifetimes for the bulk and TREF fractions of PE1 and PE2.

Figure 4.12 illustrates both intensities I_3, and I_4 for the bulk and fractionated copolymers. For clarity of purposes, the I_3 values are plotted on a shifted axis on the right-hand side of the figure. The I_3 and I_4 values represent the annihilation probability of o-Ps trapped by the open spaces in the crystalline and amorphous regions respectively. Although many factors can contribute to the relative yield of o-Ps in copolymer materials including inhibition by certain chemical species in the copolymer chains, the relative yields can be considered to generally give an indication of the relative amount (concentration) of each of the different regions. Thus, the observed decrease of I_4 could be attributed mainly to the decrease in the concentration of the open spaces due to the successive decrease in the mobility of molecules and decreased degree of chain branching.

It is clear from the plot that the PE1 (octene) copolymer has a considerably higher I_4 value than the PE2 copolymer for the same temperature TREF elution fraction. This would indicate that there are a considerably larger number of free volume holes in the amorphous regions of this copolymer.

There is an increase in the I_3 intensity (the component associated with annihilation at crystalline defects or interfaces) with an increase in the fractionation temperature although

this increase is very small. The values of I_3 are considerably smaller than the I_4 values and are indicative of the fact that the probability of o-Ps formation in or around the crystalline regions is much smaller than in the amorphous regions as a result of the closer packing of the polymer chains. The small increase in the I_3 values with an increase in the amount of crystallinity in PE samples agrees with reports in the literature on PE [50, 53] where higher crystallinity sample typically show higher I_3 values. It should also be pointed out that if we assume I_1 and I_2 remain constant then there must be a somewhat inverse relationship between I_3 and I_4 values since those values reflect the fraction of o-Ps in each state. This fact highlights the challenge of using a simple relationship of o-Ps intensity to determine the free volume hole content by the simple proportional relationship in complex copolymer morphologies [49].

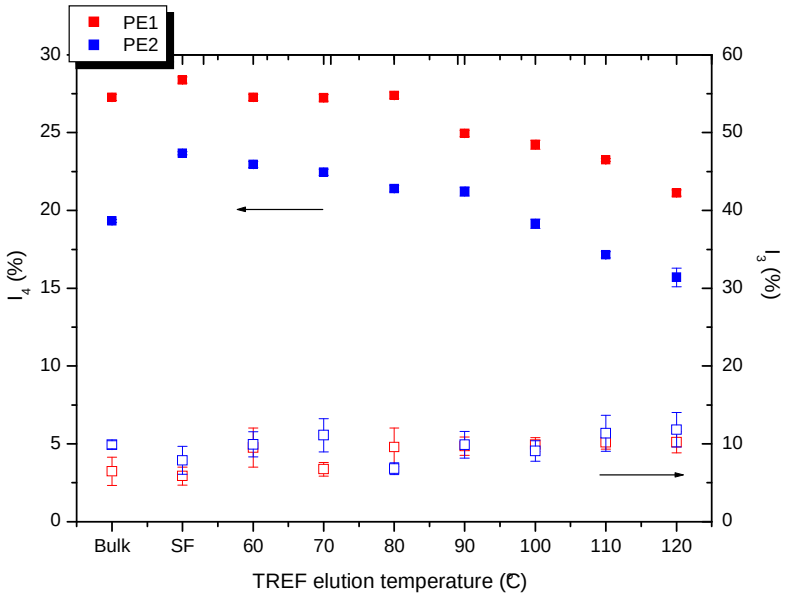

Figure 4.12 Intensities I_3 (open symbols) and I_4 (closed symbols) for the bulk and TREF fractions of PE1 and PE2.

In the preceding discussion, the variation of the positron annihilation parameters has been discussed in terms of the TREF elution temperatures. It will, however, be more instructive to consider the variation of these parameters not in terms of their elution temperatures, but rather in terms of the other factors related to the chain structure and morphology of the fractions. Figure 4.13 shows the relationship between τ_4, τ_3, and the

crystallinity of the fractions. It should be noted that in these figures, the points for the highest temperature fractions of both copolymers have been omitted since these produces anomalous points due to the relative decrease in the measured crystallinity in these samples. What is interesting is that this "anomaly" only occurs when the data points are plotted with regards to crystallinity but not with regards to TREF fractionation temperature or other factors such as comonomer content. The reason for the decrease in the measured crystallinity in the high temperature fraction is not immediately clear. Similar decreases have been reported in other studies using the same preparative TREF set [54, 55] Figure 4.13 illustrates the effects discussed above for the relationship between the crystallinity (by density) and the two o-Ps lifetimes.

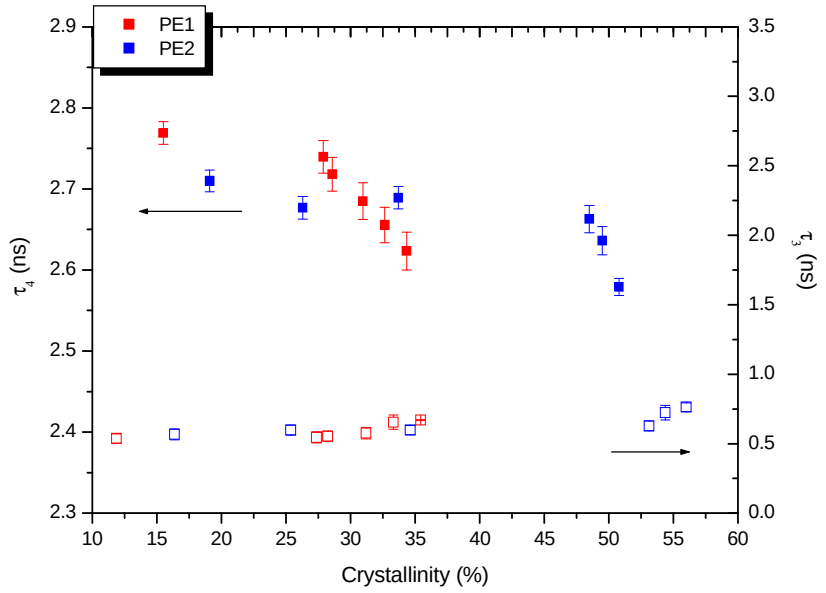

Figure 4.13 Crystallinity effect on τ_3 (open symbols) and τ_4 (closed symbols) lifetimes of PE1 and PE2.

Figure 4.14 shows the two o-Ps state intensities (formation probabilities) for the copolymer series plotted as a function of the copolymer crystallinity. As mentioned above there is a general decrease in the I_4 values with an increase in the crystallinity (again with the exception of the highest temperature fraction when plotted by crystallinity). A very slight increase in I_3 (which gives information about the relative fraction of o-Ps annihilation) was observed as the amount of crystallinity increased.

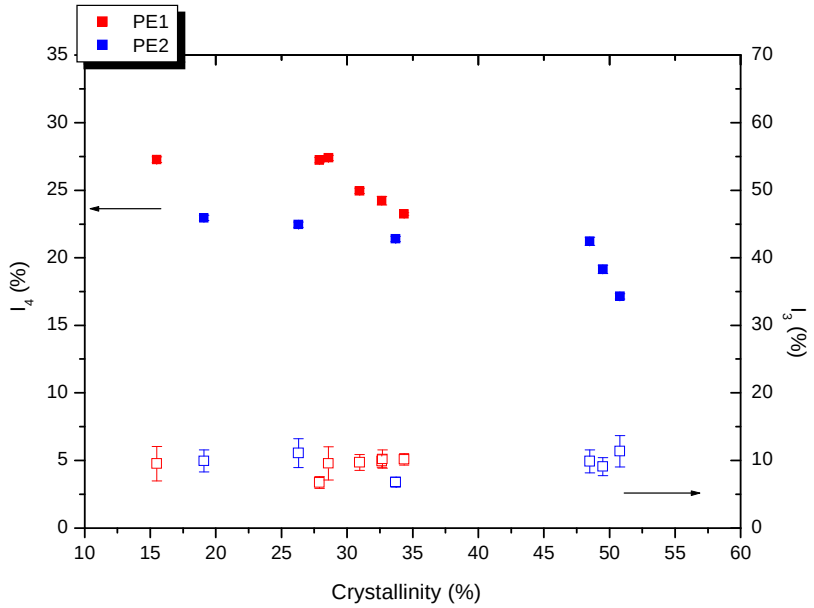

Figure 4.14 Crystallinity effects on I_3 (open symbols) and I_4 (closed symbols) of TREF fractions of PE1 and PE2.

Figure 4.15 shows the o-Ps lifetimes τ_3 and τ_4 as a function of comonomer content. The comonomer content is an important factor affecting chain crystallizability and, therefore, crystallization temperature. This is because comonomers act as chain defects, interrupting chain regularity and greatly lowering chain crystallizability. The behavior of τ_4 shows that the free volume increases in mean size in the amorphous phase with increasing branching, as mentioned previously. This indicates that the free volume holes within the copolymer become bigger with increasing comonomer content in the amorphous region. It is also interesting to note that there is no significant difference in the trend between the two copolymers with regards to the trend in the τ_4 values unlike when the data is plotted with regards to TREF elution temperature as in Figure 4.11.

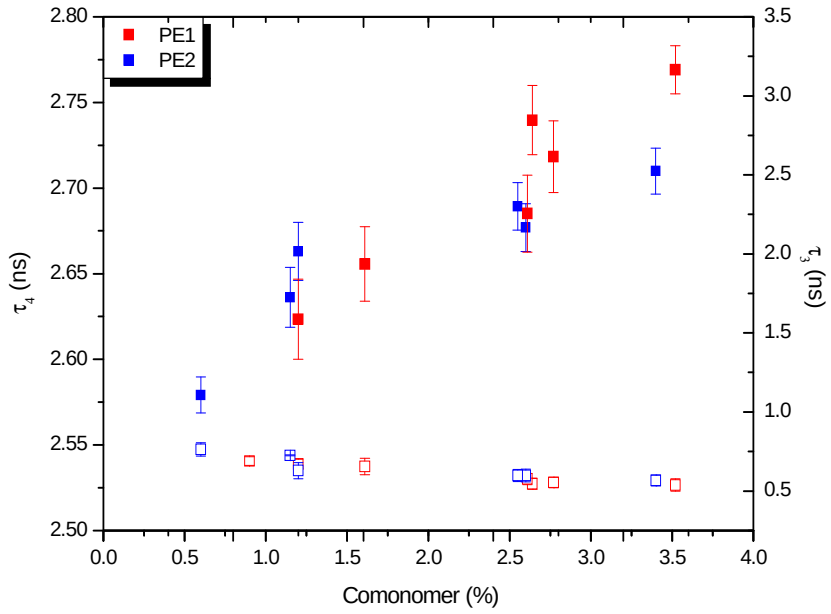

Figure 4.15 Comonomer content effects on τ_3 (open symbols) and τ_4 (closed symbols) lifetimes of TREF fractions of PE1 and PE2.

It has already been mentioned in Section 2.8.1.4 that it is common to calculate the fractional free volume *f* using equation 2.4. However this equation is not strictly valid for semi-crystalline polymers because the empirical scaling factor in the equation assumes a homogenous morphology, which is not the case in semi-crystalline polymers where there is more than one phase (crystalline, interface and amorphous) and consequently more than one o-Ps lifetime. It is, however still of interest to estimate the relative free volume of the amorphous material which can be calculated by simply taking the product of the o-Ps I_4 intensity (which is generally accepted as being proportional to the number of holes in the amorphous phase [49]) and the calculated "hole volume" in the amorphous areas based on the τ_4 value using the following equation:

$$\text{Relative free volume} = V_f I_4 \qquad 4.7$$

where V_f is the free volume cavity size (based on the τ_4 value) and I_4 is the annihilation probability of o-Ps in the amorphous phase

The relative free volume values are presented in Figure 4.16 where the relative fractional free volume of the amorphous phase is plotted against the τ_4 lifetime (hole size) of the amorphous phase. The results shows that at a given o-Ps lifetime (τ_4), the relative free

volume is larger for PE1 than the PE2 copolymer. This essentially means that for the same average amorphous hole size in the two samples, the free volume on the amorphous phase of the PE2 is lower than that of the PE1 copolymer. This is due to the fact that the I_4 value in the PE2 copolymer (hexene copolymer) is lower than the corresponding point in the PE1 copolymer (octene copolymer). It should also be noted that similar plots of relative free volume in the amorphous phase versus the TREF elution temperature, comonomer content or crystallinity would result in the PE1 copolymer having slightly higher relative free volume values due to the larger I_4 in all cases in this copolymer. Again this may be attributed to the larger (longer) octene comonomer in the PE1 sample and the difference of the SCBD in the amorphous phase.

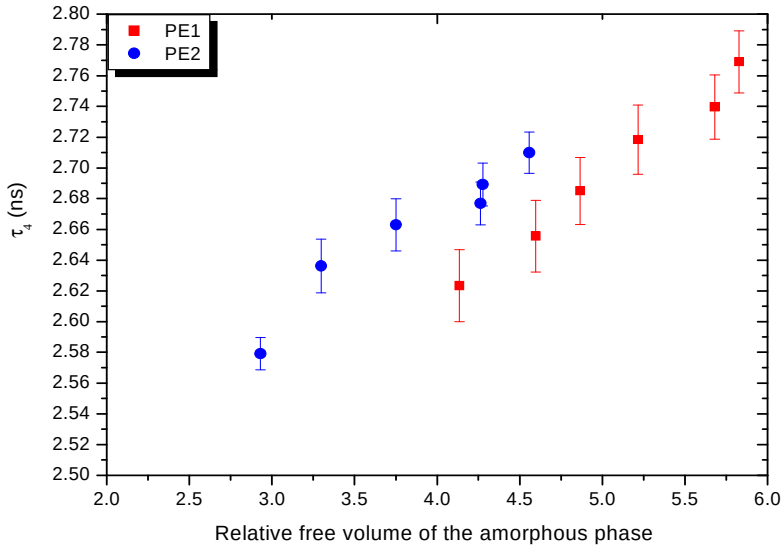

Figure 4.16 Change in the relative free volume with the o-Ps lifetime τ_4 for PE1 and PE2.

In order to get a full picture of the relationship between free volume and copolymer deformation; three dimensional (3-D) plots were produced to allow for the easy visual representation of variation of the free volume parameters with the measured bulk physical property of microhardness and the crystallinity of the samples. Section 4.3.3 has already established (as has been the case in previous studies) a relationship between the crystallinity and the microhardness of the samples. In the following plots we wish to see of there is any correlation between the microhardness and relative free volume of the amorphous parts of the materials. Figures 4.17 and 4.18 show the variation of the relative fractional free volume of

the amorphous phase as a function of crystallization percentage and microhardness for both copolymers. The relationship between the crystallinity and microhardness has been discussed previously. As can be seen from the figure, as the crystallization percentage increases, the microhardness increases. What is also interesting from these figures is that some correlation can be found for the microhardness and the relative fractional free volume of the amorphous phase. Essentially, the relative fractional free volume of the amorphous phase decrease as the microhardness increase. It is generally accepted that the increase in the microhardness is associated with the increasing crystallinity, but what this study shows is that at least part of the increase can also be attributed to the decreased free volume of the amorphous materials (as consequence of the decrease mobility of chains in the amorphous phase). It is not possible to give a quantitative correlation of the relative contribution of the increases in crystallinity and the decreased amorphous phase free volume.

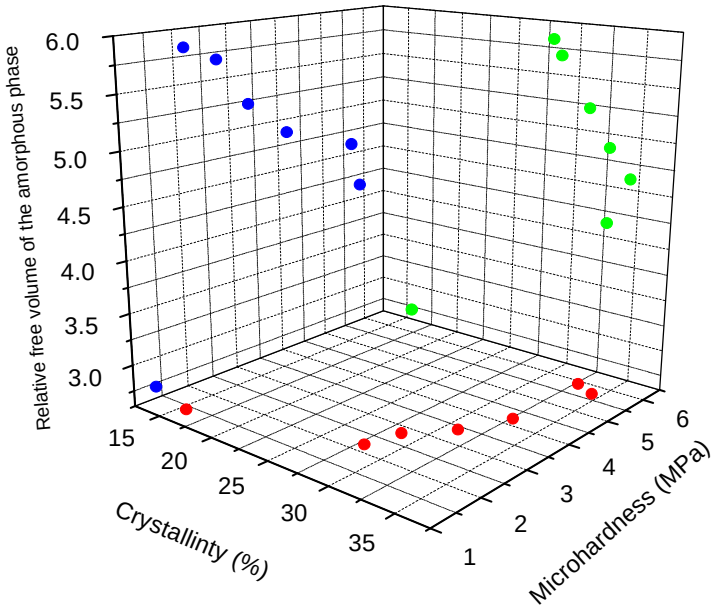

Figure 4.17 Variation in the relative fractional free volume of the amorphous phase as a function of crystallinity percentage and microhardness of PE1.

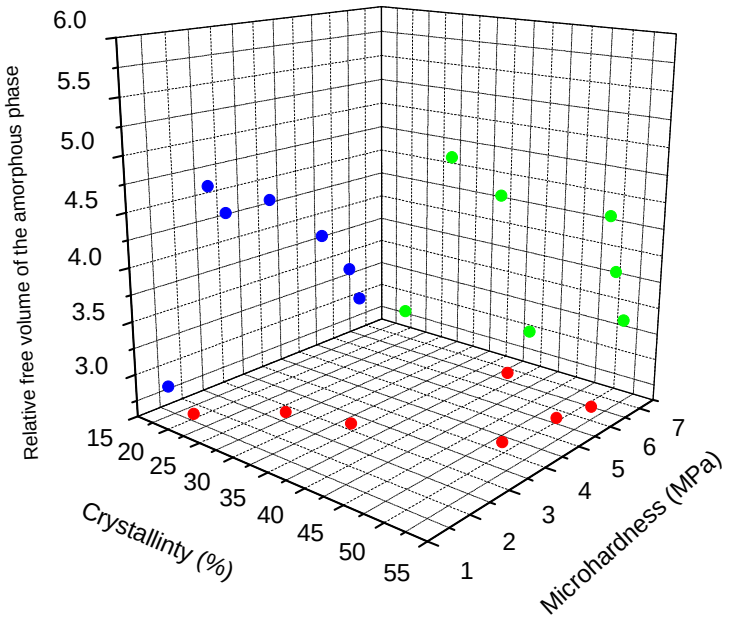

Figure 4.18 Variation in the relative fractional free volume of the amorphous phase as a function of crystallization percentage and microhardness of PE2.

Figure 4.19 shows essentially the same data presented in the previous two figures but in this case, the microhardness and relative free volume of the amorphous phases are plotted as a function of the crystallinity in both of the copolymers. (Again is should be noted that the high crystallinity point is omitted for reasons mentioned above.) What is remarkable about this figure is the almost direct inverse correlation between the microhardness and the relative free volume of the amorphous phase, with an increasing crystallinity. This degree of correlation is remarkable in that the microhardness and positron annihilation measurements are completely independent measurements. The inverse relation is most apparent in the higher crystallinity PE2 copolymer. In this case there is a relatively small increase in the crystallinity, but a very large increase in the microhardness. This dramatic increase in the microhardness is mirrored by a dramatic decease in the free volume of the amorphous phase (as a result of less chain branching as pointed out earlier). Such a high degree of correlation between the microhardness and nature of the amorphous phase for both copolymers suggests that this phase plays a very significant role in determining the overall bulk microhardness of

the sample. Indeed from the above figure, it could be argued that in fact there is a stronger correlation between the nature of the amorphous phase and microhardness than there is between the microhardness and the crystallinity. This argument needs to be treated with some caution of course, since the situation is more complex in that more crystallinity means less amorphous material (or the other way around). Therefore the relative contribution from each phase changes as the morphology changes.

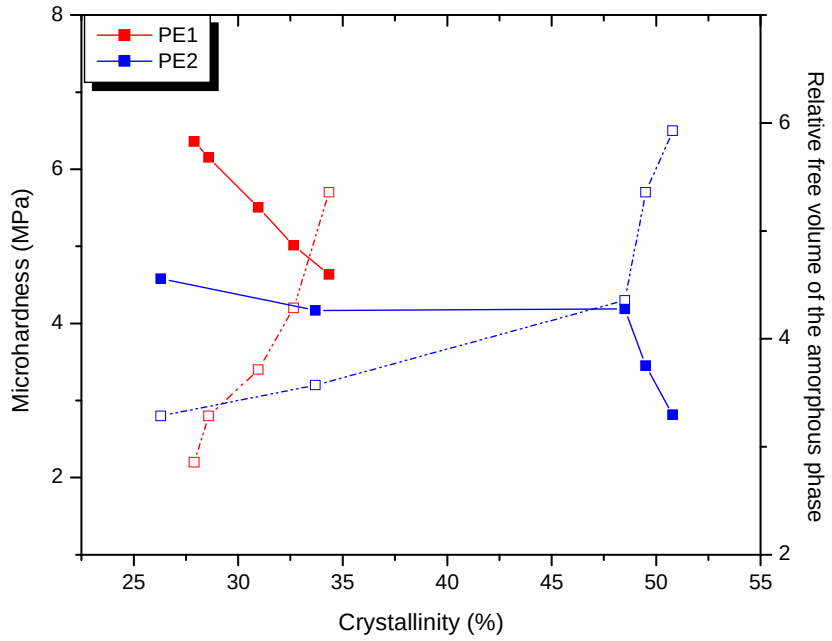

Figure 4.19 Sample microhardness (open symbols) and relative free volume of the amorphous phase (closed symbols) as a function of copolymer crystallinity.

In the above case, the correlation is clear for each of the individual copolymers, but the explanation for the difference between PE1 and PE is not clear. As mentioned in a number of places the octene copolymer has a higher relative free volume in the amorphous phase. Based on the amount of crystallinity relative to the PE2 copolymer, there is also relatively more amorphous material in the PE1 copolymer and less crystallinity, yet the microhardness values for this copolymer are higher than the PE2 copolymer. This is an apparent contradiction and most probably points to the fact there are different “scaling factors” for the two copolymers although it is difficult to justify this based on a physical argument. What is interesting is that when the data is plotted not with crystallinity but with TREF elution

temperature (as in Figure 4.8) the respective temperature fractions for the PE2 copolymer have higher crystallinity, higher microhardness and lower relative amorphous free volume than the corresponding PE1 copolymer.

From the above we conclude that the comonomer content and distribution is the main factor affecting the microstructure of the copolymer as well as the positron annihilation parameters (and subsequently the free volume parameters). This is also reflected in the crystallinity and mechanical properties of the copolymers.

The effect of microstructure on the properties of LLDPE was discussed for both bulk and fractionated copolymer, where a correlation between different microstructural parameters was observed by fractionation of the copolymer to isolate homogenous fractions.

The complexity of the interrelationship between comonomer content (chain branching) morphology and measured positron annihilation parameters has been highlighted. A second approach to study this complex relationship is the manipulation of the copolymer morphology by removal of certain fractions as opposed to the analysis of the individual fractions. It is well known that removal of certain polymer fraction can have a dramatic impact on the polymer primarily due to the dramatic change in the morphology (mostly crystalline structure) caused by removal of a certain fraction with a particular molecular composition [54].

The manipulation of the composition of the structural units is one of the most common methods by which to modify polymer behavior. In the following section, determination of the effect of removing one of the TREF fractions from the bulk material, and the determination of the effect of this on the overall properties, including melting, crystallization temperatures, microhardness and measured positron annihilation lifetime parameters, will be described.

4.3.5 Removal of a polymer fractions

There is more than one way in which a fraction can be removed from the bulk polymer. Removal of fractions can be either based on removal of homogeneous molar mass fractionations or by removal of homogeneously crystallizable fractions. In the present study, removal was done by crystallizability, because the removal of crystallisable fractions will have the greatest impact on the crystal morphology and hence provide samples series with

differing type and degrees of crystallinities. As has previously been discussed, the positron lifetime analysis produced two o-Ps lifetimes attributed to the crystalline and amorphous phases and this approach allows for the generation of a different series (with regards to crystallinity) with exactly the sample bulk material. A single fraction was removed from the bulk copolymers by TREF process in each case as is described in the Table 4.5.

Table 4.5: TREF fraction removal process

Experiment	Description of the process
1	Removal of the amorphous fraction (20-60 °C), and then collect on of the rest of the copolymer (without ‹ 60).
2	Removal of the 70–80 °C fraction (without 80).
3	Removal of the 90–100 °C fraction (without 100).
4	Removal of the 110–120 °C fraction (without 120).

4.3.5.1 Effect of the removal of TREF fractions on the melting, crystallization and microhardness properties of PE1 and PE2

Figure 4.20 illustrates the effect of the removal of respective TREF fractions on the T_m of the samples. In the figure, the size of the data point represents the relative amount of material in the fraction removed. In other words, a larger data point means more material is removed in that fraction. The general trend was that, when the lower crystalline material was removed, there was an increase in the melting temperature. This was the case for both copolymers, where the melting temperature increases as the amorphous fraction was removed. This is expected since as the amorphous fraction is removed a more perfect crystalline material is left behind because the amorphous fraction contains the highly branched (high comonomer) chains as is shown above. This will lead to an increase in the melting temperature. As the higher temperature fraction is removed, the melting temperature decreases compared to the bulk copolymers. Again this is expected because more crystalline material was removed (fraction with less SCB or lower comonomer content).

The differences between the two copolymers with regards to the comparable melting points has been discussed above, but it is also worth noting that the amorphous fraction (less

crystallizability) constitutes a large proportion of the PE1 material compared to the PE2 material.

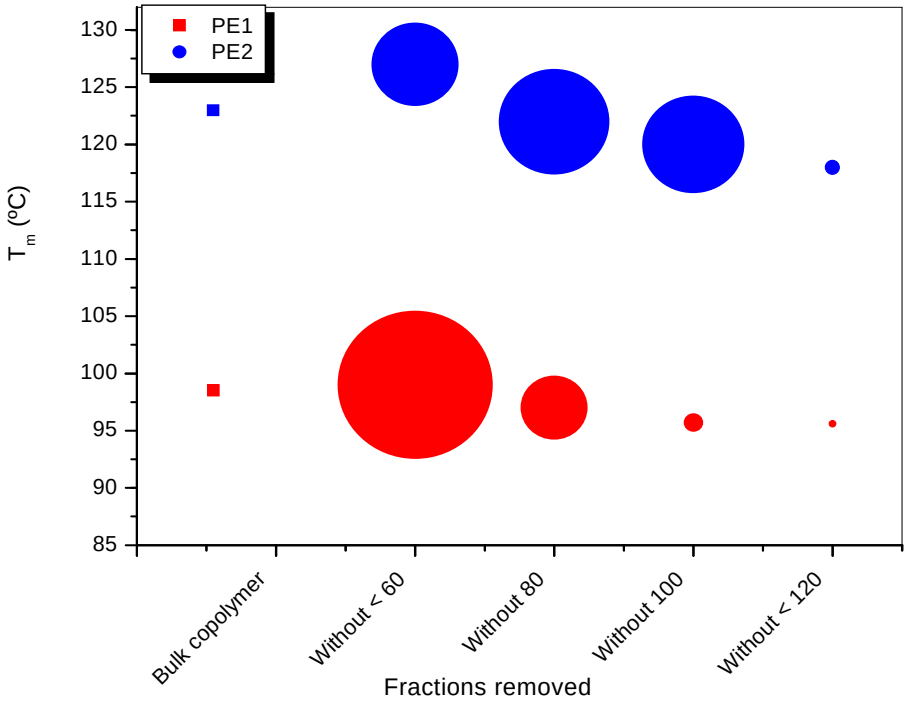

Figure 4.20 Melting temperature of the bulk and remaining material of PE1 and PE2.

Similar behaviour was observed for the crystallization temperature (T_c) (from DSC), where T_c increased compared to the bulk LLDPE as the lower temperature fractions was removed. As the higher temperature fraction is removed the T_c decreases compared to the bulk copolymer. This is due to the large amount of chain branching, which will tend to reduce the possibility of an ordered arrangement, leading to a reduced T_c.

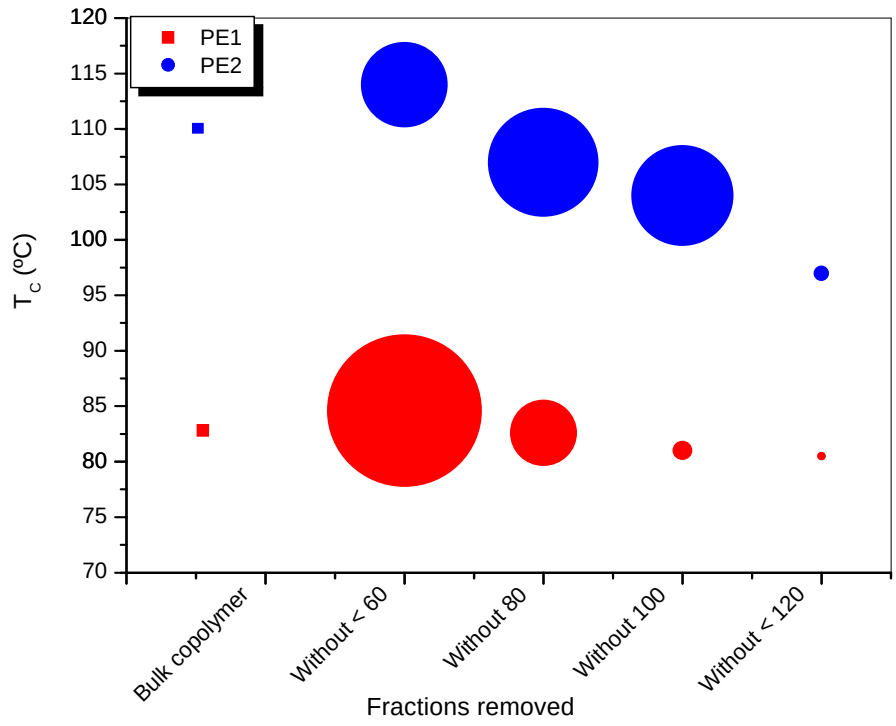

Figure4.21 Crystallization temperatures of the bulk and remaining material of PE1 and PE2.

Figure 4.22 illustrates the effect of the removal of TREF fractions on the degree of crystallinity. The general trend is that the crystallinity of the remaining material decreases as the temperature of the fractions removed increases. This can be attributed to the fact that by removing the lower temperature fraction, more amorphous and more short-chain branched material is removed, therefore the crystallinity of the remaining material will be higher than when the 100 °C fraction is removed for instance. In the case of the latter, more crystalline material is removed; therefore the crystallinity of the remaining material is lower. Again the overall higher degree of crystallinity in the PE2 copolymer is noted.

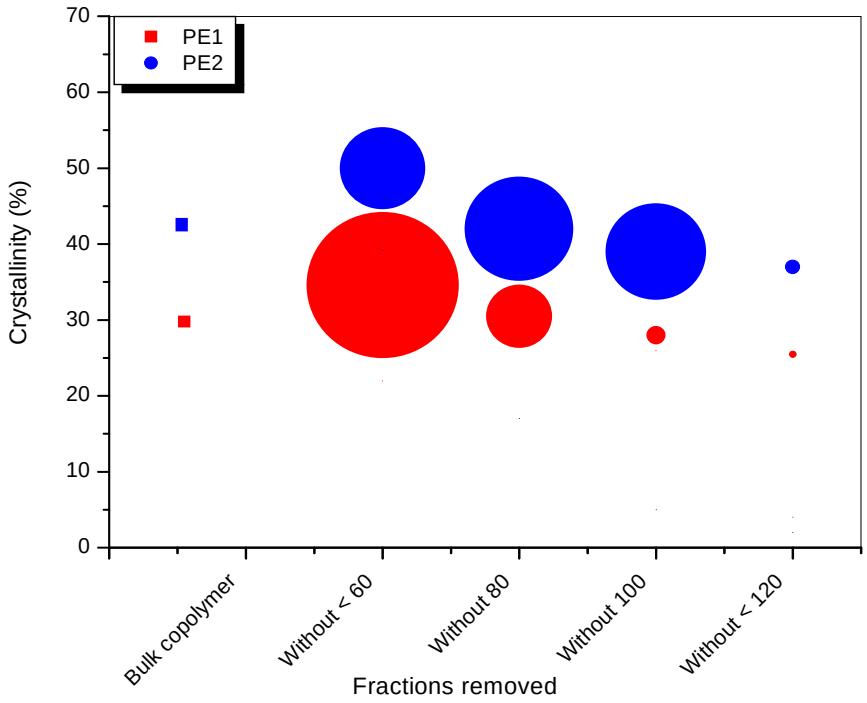

Figure 4.22 Degree of crystallinity (from density) of the bulk and remaining material of PE1 and PE2.

Figure 4.23 shows the microhardness of the materials. A similar trend to that seen for the crystallinity is observed. There is generally a decrease of the microhardness as the temperature of the removed fraction increases.

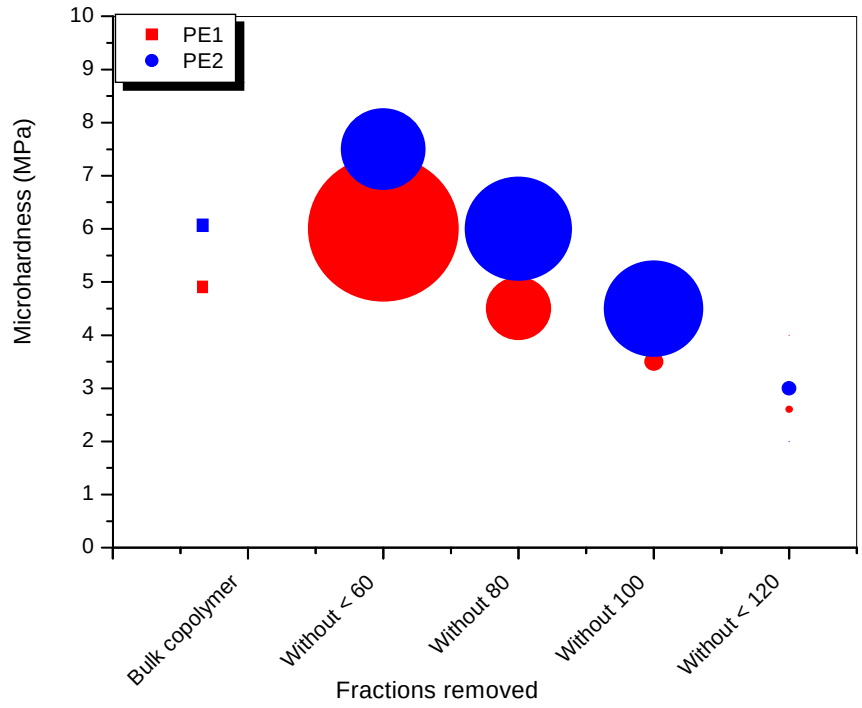

Figure 4.23 Microhardness values of the bulk and remaining material of PE1 and PE2.

It is clear from the preceding discussion that the technique of removal of the fractions has the desired effect on the crystal morphology and resultant physical properties. The next section describes the measurement of the positron annihilation parameters in this copolymer series.

4.3.5.2 Effect of removal of the TREF fractions on measured positron annihilation parameters.

Details of how the two longest o-Ps lifetimes and intensities for the bulk and remaining material of PE1 and PE2 after removal of TREF fraction are summarised in Table 4.6.

Table 4.6 The lifetimes and intensity values of the bulk and remaining material of PE1 and PE2

Fraction temperature	τ_3 (ns)		I_3 (%)		τ_4 (ns)		I_4 (%)	
(°C)	PE1	PE2	PE1	PE2	PE1	PE2	PE1	PE2
bulk	0.61±0.04	0.61±0.04	6.45±1.80	9.88±0.52	2.77±0.01	2.72±0.01	27.3±0.2	19.10±0.1
without ‹ 60	0.67±0.04	0.63±0.03	8.24±1.21	9.45±1.47	2.80±0.01	2.76±0.01	22.9±0.3	14.01±0.1
without 80	0.60±0.04	0.67±0.03	7.65±1.84	8.72±1.64	2.76±0.01	2.74±0.01	25.4±0.2	16.03±0.2
without 100	0.49±0.02	0.64±0.04	5.41±1.64	6.54±1.47	2.73±0.01	2.71±0.01	24.0±1.5	17.10±0.1
without 120	0.56±0.04	0.62±0.03	6.23±1.42	7.54±1.37	2.77±0.01	2.73±.0.01	22.8±0.2	18.80±0.1

Figure 4.24 shows the relationship between τ_3 and τ_4 values of the remaining material after removal of the individual TREF fractions. The results in the figure are very revealing especially with regards to the variation in the τ_4 (amorphous phase hole size). In the case of both copolymers, the removal of the low temperature fraction results in a dramatic decrease in the τ_4 values. The argument for this is analogous to the argument for the decrease in the τ_4 values in the case of the higher temperature fractions in the previous study. Effectively we are removing the "more branched" materials essentially from the amorphous phase which leads to a decreased average hole size in the amorphous phase. As is the case in the previous study, the changes in the τ_3 values are far less dramatic. Although in the case of the PE2 copolymer, there is a slight decrease with the successive removal of the higher temperature fractions.

Another feature of this figure is that the PE1 (octene copolymer) values are consistently higher than the PE2 (hexane copolymer). This is similar to the results on the fractions (Figure 4.11). It should also be pointed out at this point that in both of the two fractionation processes (measurement of fractions and removal of fractions) there are clear differences between the PE1 and PE2 copolymers. However, when the data is plotted with regards to the comonomer content or crystallinity these distinctions are not as apparent. This suggests that simply attributing the observed difference in the τ_4 values to the branching length is too simplistic. These are average values and this observation suggests that factors such as the differences in the short chain branching distribution are also important and need to be taken into account. Again, this highlights the potential short comings of some previous studies where completely different commercial samples have been studied.

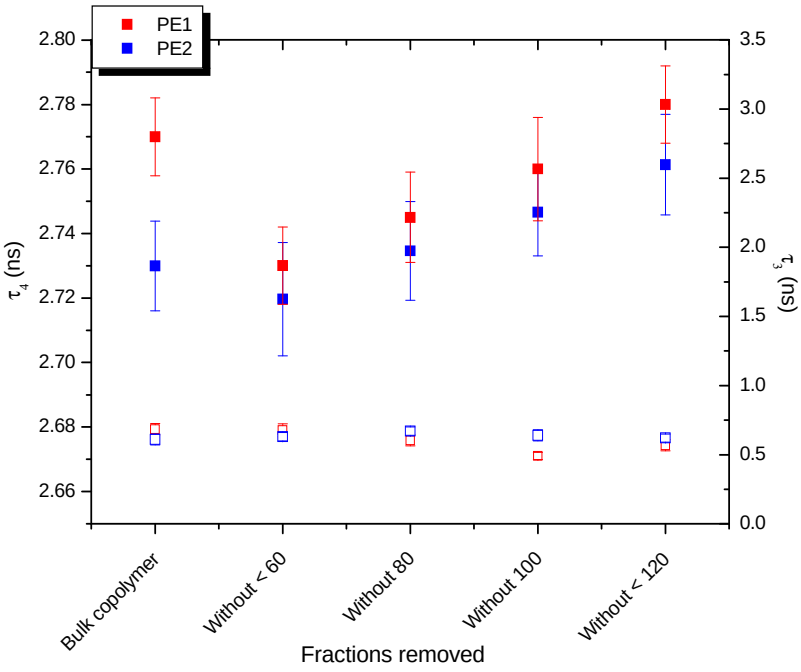

Figure 4.24 τ_3 (open symbols) and τ_4 (solid symbols) lifetimes for the remained material after removing TREF fraction.

Figure 4.25 shows the variation in the two o-Ps formation probabilities for the remaining copolymer material. The I_4 values show a relationship comparable to that observed in the previous study. As was the case previously, the PE1 copolymer has a higher I_4 value than the PE2 copolymer. The I_3 value shows a slight initial increase for the PE2 copolymer and both the PE1 and PE2 copolymers show a decrease as the temperature of the fraction removed increases with the exception of the highest temperature fraction. All of the variations observed in this figure can be argued in similar way as has been done in the previous study.

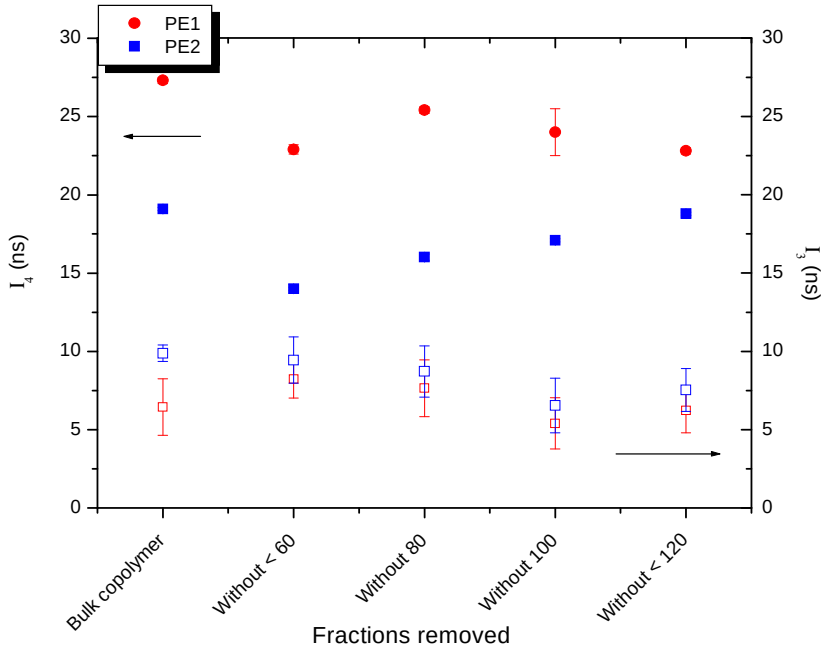

4.25. I_3 (open symbols) and I_4 (solid symbols) intensities for the remained material after removing TREF fraction.

Figure 4.26 shows the correlation between the relative free volume (calculated from equation 4.7) and recombined material after removal of the TREF fraction. The figure shows a significant decrease in the relative free volume of the amorphous phase as the lower temperature fraction is removed. After removing the lower temperature fraction, a slight decrease in the relative free volume is observed, however as the higher temperature fraction is removed, the relative free volume is increased.

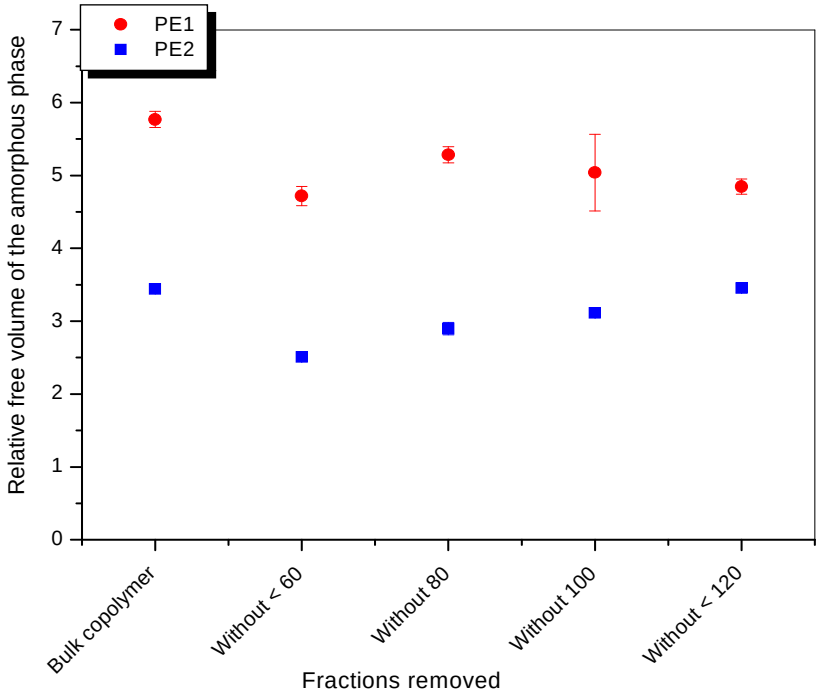

Figure 4.26 Effects of removed TREF fractions on relative free volume of PE1 and PE2.

Figure 4.27 shows the relationship between the measured crystallinity, the microhardness and the relative free volume of the amorphous phase of the copolymers after removal of the TREF fractions. Again a remarkably good correlation is found between the microhardness and the relative free volume in the amorphous phase. In the case of the PE2 copolymer the inverse relationship is clearly observed, but in the case of the PE1 copolymer the correlation between these two factors is not as clear.

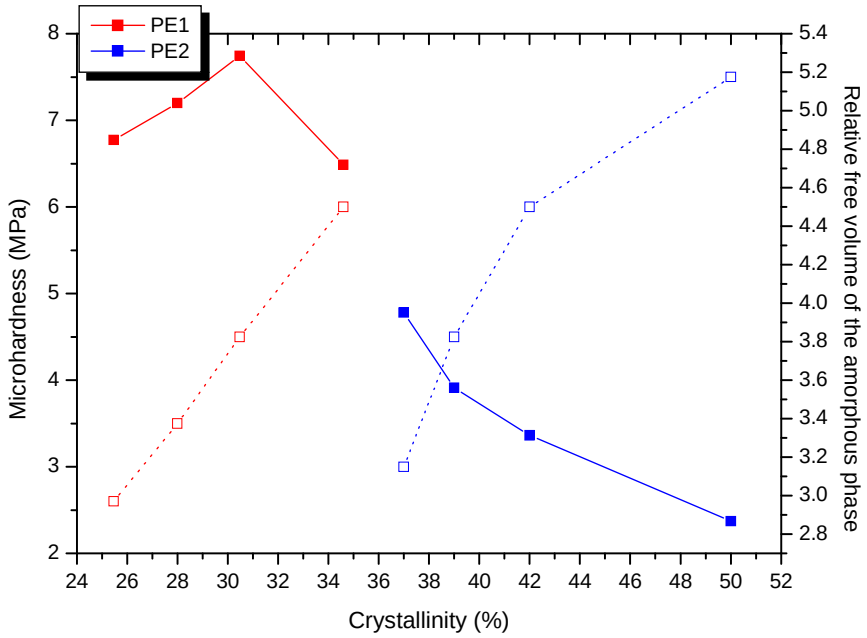

Figure 4.27 Sample microhardness (open symbols) and relative free volume of the amorphous phase (closed symbols) as a function of copolymer crystallinity for fraction removal samples.

4.3.5 Conclusion:

Two LLDPE copolymers were successfully fractionated according to crystallizability to produce a series of copolymer samples of differing degree of comonomer content, and consequently crystallinity. Each fraction was characterized on a molecular level by different techniques, such as DSC, NMR, CRYSTAF and PALS.

As has been extensively reported in literature, the chain branching plays a major role in preventing the polymer chains from packing together regularly and closely and has a predominant effect on the density and crystallinity of the copolymer. The results showed that as the comonomer content increases, the average number of consecutive ethylene units decreases and the crystallizable part of the copolymer becomes smaller. As a consequence, the crystallinity decreases and the amorphous and interfacial contents increase.

Variations in the free volume size of LLDPE with varying comonomer contents were observed by means of PALS measurements. A correlation between the relative free volume of the amorphous phase, crystallinity, microhardness and comonomer content was also established. It was found that the size of the free volume holes in the amorphous phase

increases with increasing comonomer content and related decreasing crystallinity. Therefore, these factors also affect the physical properties by dictating the molecular motions possible in the amorphous domains, which can be important, especially for low temperature properties. This is clearly seen in the microhardness results.

The study shows that in PALS analysis, the longest lifetime components τ_4 and I_4 show a strong dependence on the degree of SCB, the length of the SCB as well as the distribution as indicated by the greater dependence in the octene series relative to hexene series. The longer the alkyl branch, the higher the free volume present (in the amorphous phase), this was reflected in the higher τ_4 for the PE1 (octene comonomer) compared to PE2 (hexane comonomer). The type of comonomer therefore has a significant effect on the microstructure, and hence the final properties of the copolymer.

It is clear from the results that as the crystallization percentage increased the microhardness increased and simultaneously lamellar thickness increases; however the o-Ps lifetime τ_4 and intensity I_4 decreases. This decrease is associated with a decrease in the relative fractional free volume of the amorphous phase. This study has clearly illustrated for the first time, that in the case of LLDPE copolymers, the relative decease in the fractional free volume is at least partially responsible for the overall decrease in the microhardness although the increasing amount of crystalline material is the dominant factor determining this property.

It should also be noted that for the fractionated copolymers, any changes observed in the τ_3 value across the fractionation range or in the fraction removal study were very small.

This indicates that the interfacial region or defects are essentially the same for each fraction, and largely independent of the type or amount of comonomer. Essentially the "average size" of those defects or "free volume" is the same. In addition very small if any changes in the I_3 values are observed in the copolymers as a result of changes in the amount of crystallinity, although in some cases a clear increase is seen in higher crystallinity sample. If these values are considered to be proportional to the "number of defects" associated with the crystalline region then these results imply that there is little change in this number with changing crystallinity in the copolymers. In this particular study, the small changes may also be a result of the increasingly "more prefect" crystalline structures as a result of the fractionation, which goes hand in hand with the increased crystallinity of the higher

temperature fractions. This argument is somewhat supported by the fact that the greater changes are seen in the I_3 values in the fraction removal study relative to the fractionation study.

Further discussion on these issues is given in the concluding chapter.

4.4 References:

1. Lovisi, H., Tavares, M I B., da Silva, N M., de Menezes, S M C., de Santa Maria, L C. and Coutinho, F M B. Polymer 2001, 42, 9791-9799.
2. Bensason, S., Minick, A., Moet, S., Chum, A. and Hiltner, E. Journal of Polymer Science Part B: Polymer Physics 1996, 34, 1301-1315.
3. Zhang, M., Lynch, D T. and Wanke, S E. Polymer 2001, 42, 3067-3075.
4. Ibnelwaleed, A H. Polymer International 2004, 53, 1327-1335.
5. Islam, M A., Hussein, I A. and Atiqullah, M. European Polymer Journal 2007, 43, 599-610.
6. Kilburn, D., Bamford, D., Lüpke, T., Dlubek, G., Menke, T J. and Alam, M A. Polymer 2002, 43, 6973-6983.
7. Cerrada, M L., Perez, E., Perena, J M., Benavente, R., Misheva, M. and Grigorov, T. Macromolecules 2005, 38, 8430-8439.
8. Wang, H P., Ansems, P., Chum, S P., Hiltner, A. and Baer, E. Macromolecules 2006, 39, 1488-1495.
9. Gallo, R., Brambilla, L., Castiglioni, C., Ipsale, S., Severini, F., Quasso, F. and Consolati, G. European Polymer Journal 2005, 41, 359-366.
10. Benedikt, G. and Brian, G. Metallocene-catalyzed Polymers; Plastics Desing Library: New York, 1998.
11. Soares, J B P. and Hamielec, A E. Polymer 1995, 36, 1639-1654.
12. Monrabal, B. Journal of Applied Polymer Science 1994, 52, 491-499.
13. Soga, K., Toshiya, U., Takashi, A. and Shuji, N. Macromolecular Rapid Communications 1995, 16, 379-385.
14. Francis, M M. Journal of Polymer Science Part B: Polymer Physics 2001, 39, 2819-2832.

15. Edward, P S., George, B C., Christopher, M K., Michael, D M., Joseph, H M. and Brenda, J H. Journal of Applied Polymer Science 2003, 90, 722-728.
16. Britto, L J D., Soares, J B P., Penlidis, A. and Krukonis, V. Journal of Polymer Science Part B: Polymer Physics 1999, 37, 553-560.
17. Gabriel, C. and Lilge, D. Polymer 2001, 42, 297-303.
18. Nieto, J., Oswald, T., Blanco, F., Joao, B P S. and Benjamin, M. Journal of Polymer Science Part B: Polymer Physics 2001, 39, 1616-1628.
19. James, W. and David, C. Polyolefins: Processing, Structure Development and Properties; Hanser Gardner: USA, 2004.
20. Simanke, A G., Galland, G B., Freitas, L., da Jornada, J A H., Quijada, R. and Mauler, R S. Polymer 1999, 40, 5489-5495.
21. Al-Malaika, S., Peng, X. and Watson, H. Polymer Degradation and Stability 2006, 91, 3131-3148.
22. Peeters, M., Goderis, B., Reynaers, H. and Mathot, V. Journal of Polymer Science Part B: Polymer Physics 1999, 37, 83-100.
23. Wunderlich, B. Thermal Analysis of Polymeric Materials; Springer: Berlin, 2005.
24. Usami, T., Gotoh, Y. and Takayama, S. Macromolecules 1986, 19, 2722-2726.
25. Raúl, Q., Griselda Barrera, G. and Raquel Santos, M. Macromolecular Chemistry and Physics 1996, 197, 3091-3098.
26. Janimak, J J., Cheng, S Z D., Giusti, P A. and Hsieh, E T. Macromolecules 2002, 24, 2253-2260.
27. Cheng, S Z D., Janimak, J J., Zhang, A. and Hsieh, E T. Polymer 1991, 32, 648-655.
28. Peeters, M., Goderis, B., Vonk, C., Reynaers, H. and Mathot, V. Journal of Polymer Science Part B: Polymer Physics 1997, 35, 2689-2713.
29. Balbontin, G., Camurati, I., Tiziano, D O. and Zeigler, R C. Journal of Molecular Catalysis A: Chemical 1995, 98, 123-133.
30. Hosoda, S. Polymer 1988, 20, 383.
31. Razavi-Nouri, M. Polymer Testing 2006, 25, 1052-1058.
32. Starck, P., Rajanen, K. and Löfgren, B. Thermochimica Acta 2002, 395, 169-181.
33. Raul, Q., Jairton, D., Márcia, S., Rosângela, B. and Griselda, B. Macromolecular Chemistry and Physics 1995, 196, 3991-4000.

34. Raúl Q., Barrera, G., Raquel, G. and Mauler, S. Macromolecular Chemistry and Physics 1996, 197, 3091-3098.
35. Wilhelm, P. Modern Polymer Spectroscopy; Wiley: India, 2008.
36. Fei C., Robert, A. and Amarasinghe, S. Polymer International 2004, 53, 1795-1805.
37. Crist, B. and Howard, P R. Macromolecules 1999, 32, 3057-3067.
38. Huang, J., Lisowski, M S., Runt, J., Hall, E S., Kean, R T., Buehler, N. and Lin, J S. Macromolecules 1998, 31, 2593-2599.
39. Defoor F., Groeninckx, G., Reynaers, H., Schouterden, P. and Heijden, B V D. Journal of Applied Polymer Science 1993, 47, 1839-1848.
40. Vasanthan, N., Ozkaya, S. and Yaman, M. The Journal of Physical Chemistry B, 114, 13069-13075.
41. Fakirov, S., Krumova, M. and Rueda, D R. Polymer 2000, 41, 3047-3056.
42. Flores, A., Ania, F. and Baltá-Calleja, F J. Polymer 2009, 50, 729-746.
43. Calleja, J. and Fakirov, S. Microhardness of Polymers; Cambridge University Press: UK, 2000.
44. Flores, A., Baltá, C., Attenburrow, G E. and Bassett, D C. Polymer 2000, 41, 5431-5435.
45. Lopez, J. Polymer Testing 1993, 12, 437-458.
46. Swallowe, M. Mechanical Properties and Testing of Polymers; Kluwer Academic: Netherlands, 1999.
47. Flores, A., Mathot, V B F., Michler, G H., Adhikari, R. and Baltá Calleja, F J. Polymer 2006, 47, 5602-5609.
48. Mei-Ling, C. and Yi-Ming, S. Physica Status Solidi (c) 2007, 4, 3916-3919.
49. Borek, J. and Osoba, W. Polymer 2001, 42, 2901-2905.
50. Dlubek, G., Bamford, D., Henschke, O., Knorr, J., Alam, M A., Arnold, M. and Lüpke, T. Polymer 2001, 42, 5381-5388.
51. Wästlund, C., Eldrup, M. and Maurer, F H J. Nuclear Instruments and Methods in Physics Research Section B: Beam Interactions with Materials and Atoms 1998, 143, 575-583.
52. Lightbody, D., Sherwood, J. and Eldrup, N. Chemical Physics 1985, 93, 475-484.
53. Serna, J., Acaron, A. and Tre, C. Physica Status Solidi (a) 1989, 115, 389-397.

54. Keulder, L, The Effect of Molecular Composition on the Properties of Linear Low Density Polyethylene. Master Thesis, University of Stellenbosch, 2008.

55. Harding, G, The Fractionation and Characterisation of Propylene-ethylene Random Copolymers. Master Thesis, University of Stellenbosch, 2005.

Chapter 5
The effect of tacticity and short-chain branching on the free volume of polypropylene and propylene-1-pentene copolymer

5.1 Introduction

In the previous chapter, the free volume parameters were considered for relatively simple copolymers (from a molecular structure point of view). In this section considerably more complex structures are considered. Several polypropylene and polypropylene copolymers are studied. In these cases, the morphology is determined by tacticity, short-chain branching content and short chain branching distribution.

As was the case in the previous chapter, preparative (TREF) is used in order to isolate relatively homogeneous fractions and to produce copolymer series of differing morphology from the same bulk copolymer material. The TREF technique yields fractions with a narrow distribution of molecular species in comparison to the bulk copolymer, and each fraction is characterised by the fact that the chains present in that fraction all crystallise out of solution in the same temperature range of the fraction in question. This technique has developed into a standard method of analysis of the distribution of the crystallisable chains of semi-crystalline polymers. The most important factors affecting the fractionation of the homopolymers and copolymers of propylene are the stereoregularity of the chains and the comonomer content, respectively [1].

The current study aims to add insight to the understanding of the influence of the copolymer microstructure on the free volume of PP and propylene copolymers. To this end three different polymers, two grades of a propylene-1-pentene copolymers (PPA and PPB) and a polypropylene homopolymer (PPC), were fractionated by preparative TREF in order to isolate fractions of each material with specific characteristics and properties. The TREF fractions were analysed by ^{13}C NMR, HT-GPC, DSC, CRYSTAF, and PALS.

5.2 Experimental

The experimental details pertaining to this chapter are described in Chapter 3; only the most important points are summarised here.

5.2.1 Materials

Two propylene-1-pentene copolymers (PPA and PPB) were obtained from SASOL, South Africa. The polypropylene homopolymer (sample PPC) was obtained from Himont, Italy. Their characteristics are described in Section 3.2.2.

5.2.2 TREF

Preparative TREF was used to fractionate the bulk copolymers. Details of the fractionation method have been previously described by Harding and Van Reenen. [2]. The fractionation temperatures used in the current study were different. The two copolymers were fractionated at elution temperatures of 30, 40, 50, 60, 70, 80, 90, 100, 110, 120, 130 and 140 °C. The homopolymer was fractionated at elution temperatures of 25, 90, 100, 105, 110, 115, 120 and 140 °C.

5.2.3 Density measurements

Crystallinity was determined according to density by assuming a two-phase system with constant amorphous phase and crystalline phase densities, and by applying equation 4.1. The densities of a theoretical 100% crystalline and 100% amorphous were taken for PPA and PPB as 0.94 and 0.853 g/cm^3 respectively [3].

5.3 Results and discussion

5.3.1 The effect of tacticity on positron annihilation parameters

As was the case in the study described in the previous chapter, prep-TREF was used here to isolate fractions of relatively homogeneous crystallizability. In the case of polypropylene homopolymer, these effectively isolate chains with similar degrees of tacticity although tacticity distribution will also play a role. In the first part of the study, changes in the

measured positron annihilation parameters as a result of different tacticity is studied. Table 5.1 gives a summary of the analysis of the different TREF fractions of polypropylene homopolymer (PPC) as well as the bulk homopolymer.

As was the case for the LLDPE copolymers, the raw positron data was best resolved into four lifetime components. The results of the two longest o-Ps lifetimes from the polypropylene fractions (lifetimes τ_i and intensities I_i) are included in Table 5.1

Table 5.1 Fractionation and characterisation data of PPC

Fraction (°C)	Wt%	M_w [a] (g/mol)	PD[a]	T_m [b] $(°C)_{DSC}$	Cryst [c] $(\%)_{Density}$	*mmmm* [d] (%)	τ_3 (ns)	I_3 (%)	τ_4 (ns)	I_4 (%)
Bulk	-	6.9E±05	5.2	158.5	84.1	90.49	0.64±0.05	6.38±0.45	2.42±0.02	22.2±0.4
25	9.51	1.1E±05	5.4	-	-	14.08	0.52±0.02	7.24±0.32	2.56±0.02	22.9±0.2
90	8.31	1.7E±05	7.1	131.0	62.7	65.23	0.60±0.03	8.46±0.93	2.54±0.02	22.7±0.3
100	8.27	1.7E±05	3.6	148.1	70.9	91.10	0.68±0.03	7.60±0.22	2.39±0.02	20.9±0.3
105	9.91	2.3E±05	3.3	154.1	73.7	91.48	0.68±0.01	6.78±0.23	2.33±0.01	19.2±0.1
110	23.89	4.9E±05	3.1	159.6	76.3	94.48	0.70±0.04	5.47±0.42	2.33±0.02	22.7±0.4
115	25.65	7.0E±05	3.3	161.5	77.2	91.07	0.56±0.01	5.92±0.37	2.37±0.01	20.7±0.3
120	9.576	5.2E±05	3.0	159.9	76.5	84.41	0.58±.040	7.42±0.75	2.42±0.01	24.0±0.1
140	4.85	4.5E±05	2.9	159.1	76.1	82.45	0.69±0.04	8.49±0.25	2.43±0.02	18.2±0.1

a) Determined from HT-GPC
b) Determined from DSC
c) Determined from density using equation 4.1 (cryst : crystallinity)
d) Determined from ^{13}C-NMR

Table 5.1 confirms that the preparative fractionation does in fact isolate fractions of progressively higher isotacticity as determined by the increase in the mmmm% (pentade sequence percentage) determined from NMR with progressively higher fractionation temperature. The effect that varying the stereo-regularity of the chains has on the measured positron annihilation parameters was investigated by analysing the TREF fractions of the homopolymer PPC. Figure 5.1 illustrates the effect of tacticity on the τ_3 and τ_4 lifetimes. (The positron annihilation parameters can of course be plotted according to TREF elution temperature or crystallinity as well, but in the interest of space only the tacticity is highlighted here). Evidently there is little effect of tacticity on the τ_3 lifetime although there is possibly a very slight increase in the τ_3 lifetime with increasing tacticity. There is a far more well-defined relationship between the τ_4 lifetime and the tacticity of the chains. The higher the tacticity of the chains, the shorter the lifetimes become which implies that the samples with a high tacticity have smaller free volume holes in the amorphous phase. Since the τ_4 lifetime is associated with the pick-off annihilation of o-Ps in the amorphous phase, this relationship is

not altogether unexpected. The increased level of stereo-regularity of the chains results in smaller relative hole sizes in the amorphous phase. The I_4 and τ_4 values obtained are in good numerical agreement with a finding of a similar study described in the literature [4]. Hamielec *et al.* [5] observed an increase in the lifetime (hole size) with increasing randomness of the chain configuration in a series of polymers.

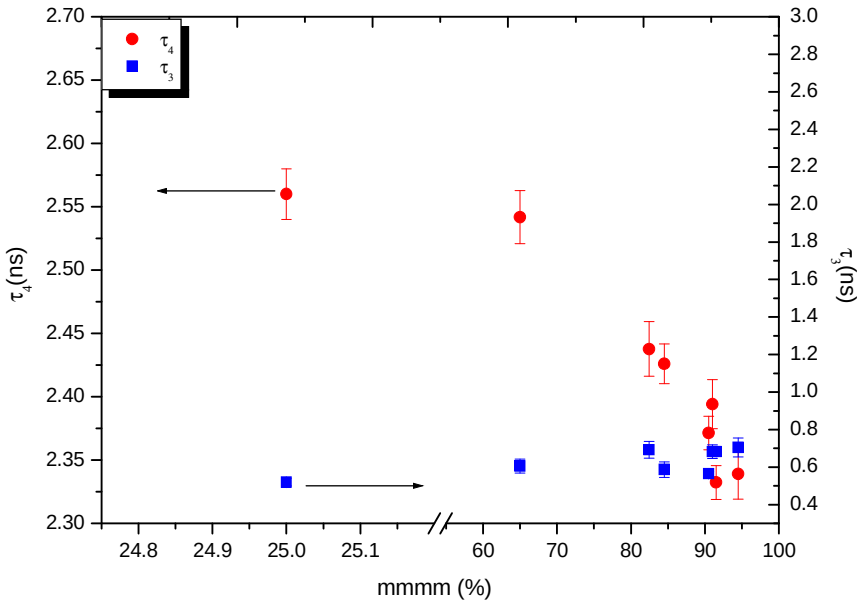

Figure 5.1 Effect of the tacticity of PPC on the τ_3 and τ_4 lifetimes.

5.3.2 The effect of tacticity and short chain branching on positron annihilation parameters

The effect of tacticity on the free volume properties of homopolymer PPC were described above. Now a more complicated system is considered and the effect of both short chain branching and tacticity will be discussed.

5.3.2.1 Fractionation

Whereas the homopolymer is heterogeneous in molar mass and tacticity, the copolymers have the added dominant effect of the comonomer to take into account. The effect of the comonomer is very important, not only in terms of the crystallisability of the chains and physical properties, but also in terms of the free volume of the copolymers. Two different PP copolymers (PPA and PPB) were fractionated and a full characterisation of each fraction was

conducted to be able to determine a relationship between the copolymer microstructure properties and free volume parameters.

A detailed study on the fractionation and characterisation of PP-pentene copolymers has been reported by Lutz [6] and only factors directly relevant to the present study are considered here. In the study by Lutz it was shown that preparative TREF fractionation of propylene-1-pentene copolymers showed a correlation between the 1-pentene content and the distribution of molecular species in the copolymers. Lutz concluded that both the tacticity and comonomer play the largest role in the fractionation process. Lutz found that the isotacticity of fractions increased with increasing elution temperature and the content of pentene units decreased monotonously. The focus of the present study is more on the measured positron annihilation parameters in relation to the microstructure and morphology of the semi-crystalline copolymers.

As mentioned earlier (Section 5.2.2), both copolymers were fractionated into twelve fractions. Figure 5.2 shows the weight fractions of the preparative-TREF fractions for PPA and PPB. It is immediately apparent that the introduction of a comonomer has a significant effect on the ability of the chains to crystallise. The majority of the homopolymer chains elute at 110 and 115 °C while those of the copolymers elute mostly at the lower temperature of 100 °C. There are also differences between the two copolymers as indicated by the TREF data. PPB consists of chains that generally elute at a slightly lower temperature than those of PPA. The data are consistent with the data for the bulk samples given in Table 3.1, which indicates that PPB has higher comonomer content than PPA and thus would be expected to elute at a slightly lower temperature than PPA.

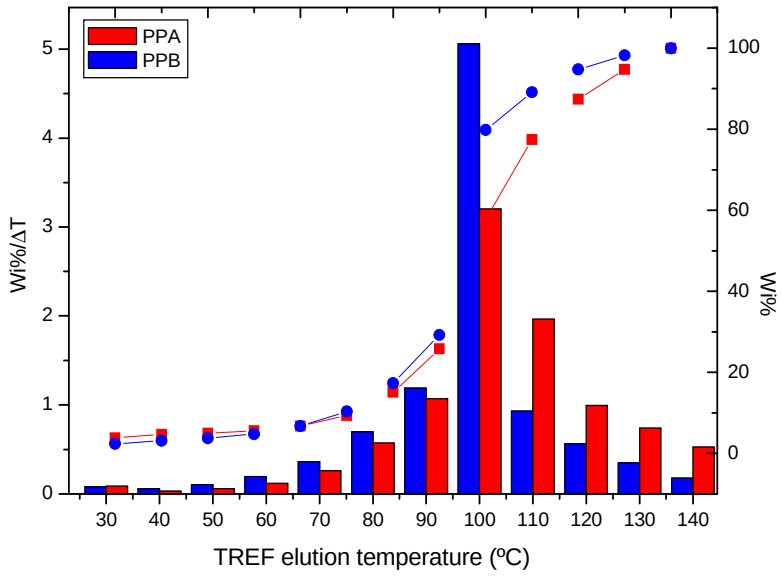

Figure 5.2 TREF profiles of PPA and PPB. (Tabulated data can be found in Appendix A)

The CRYSTAF profiles of the bulk and fractions are presented in Appendix B. CRYSTAF results show that each curve has a crystallization peak over a temperature range of about 20°C, which shows that homogenously crystallisation fractions have been isolated. This suggests that TREF is an effective technique to derive uniform samples required in the present study. The CRYSTAF results are very consistent with that of the TREF experiment as would be expected.

It is important to investigate the relationship between melting and crystallisation behaviour and the molecular microstructure of the copolymers. Tables 5.2 and 5.3 illustrate the properties of each of the fractions of PPA and PPB, respectively.

The comonomer content, tacticity and molecular weight, were investigated to understand how they would affect the melting and crystallisation temperatures of the copolymer with small amounts of pentene.

Soares and Hamielec [7], demonstrated that PP chains are principally fractionated based on their tacticity, which determines the longest crystallisable sequence length. The introduction of a comonomer generally decreases this sequence length and becomes the dominant factor affecting the separation of copolymer chains.

Table 5.2 Fractionation and characterisation data of PPA

Fraction (°C)	Wt%	M_w [a] (g/mol)	PD[a]	T_m [b] (°C)$_{DSC}$	Cryst [c] (%)$_{Density}$	1-pentene content[d] (%)	τ_3 (ns)	I_3 (%)	τ_4 (ns)	I_4 (%)
Bulk	-	4.9E±05	9.6	148.2	58.7	4.60	0.89±0.06	8.18±0.5	2.52±0.03	19.8±0.7
60	1.16	1.6E±05	6.3	104.9	40.2	15.38	0.63±0.03	7.16±0.5	2.58±0.02	22.2±0.5
70	2.60	2.1E±05	5.8	116.8	42.7	12.50	0.61±0.03	8.76±0.5	2.50±0.05	21.2±0.8
80	5.72	2.9E±05	5.4	128.6	46.0	11.11	0.57±0.03	9.96±0.5	2.45±0.01	21.8±0.3
90	10.69	4.4E±05	5.1	135.1	48.2	5.71	0.56±0.05	8.53±0.5	2.43±0.02	23.5±0.6
100	32.02	6.0E±05	4.8	143.7	59.7	4.20	0.58±0.04	8.22±0.6	2.42±0.01	21.0±0.3
110	19.64	3.3E±05	4.4	145.3	58.8	3.88	0.68±0.03	11.85±0.7	2.39±0.01	20.9±0.3
120	9.93	5.8E±05	4.4	140.2	58.6	3.88	0.66±0.03	8.73±0.6	2.46±0.01	19.9±0.3
130	7.37	4.9E±05	3.3	143.0	52.0	1.92	0.65±0.04	10.04±0.8	2.46±0.01	23.5±0.3
140	5.24	2.1E±05	3.7	139.7	54.1	1.65	0.69±0.04	8.72±0.8	2.43±0.02	18.2±0.3

a) Determined from HT-GPC
b) Determined from DSC
c) Determined from density using equation 4.1 (cryst : crystallinity)
d) Determined from NMR

Table 5.3 Fractionation and characterisation data of PPB

Fraction (°C)	Wt%	M_w [a] (g/mol)	PD[a]	T_m [b] (°C)	Cryst [c] (%)	1-pentene content [d] (%)	τ_3 (ns)	I_3 (%)	τ_4 (ns)	I_4 (%)
Bulk	-	4.3E±05	10.1	145.6	54.7	5.80	0.77±0.06	9.30±0.8	2.42±0.02	18.3±0.4
60	1.95	1.4E±05	4.8	110.3	38.5	10.61	0.59±0.07	6.72±0.9	2.47±0.02	22.1±0.6
70	3.61	2.2E±05	3.7	121.5	41.3	12.28	0.60±0.03	7.15±0.9	2.46±0.01	24.7±0.3
80	6.95	3.4E±05	4.7	127.7	47.1	10.61	0.52±0.00	9.21±0.8	2.44±0.01	23.0±0.2
90	11.90	2.9E±05	4.5	136.3	54.0	7.33	0.68±0.04	9.93±0.6	2.43±0.01	21.7±0.3
100	50.61	2.7E±05	3.3	144.7	50.5	3.80	0.75±0.04	12.15±0.9	2.43±0.02	24.0±0.4
110	9.32	2.4E±05	3.6	145.2	63.2	5.71	0.56±0.03	11.69±0.6	2.42±0.01	20.7±0.4
120	5.65	5.6E±05	3.8	144.5	63.8	3.80	0.69±0.04	9.01±0.6	2.41±0.01	22.4±1.2
130	3.47	2.3E±05	3.4	145.4	59.6	1.94	0.65±0.04	8.77±0.7	2.41±0.02	20.6±0.3
140	1.75	4.0E±05	5.9	145.3	57.4	3.84	0.71±0.04	8.60±0.7	2.42±0.02	20.8±0.3

e) Determined from HT-GPC
f) Determined from DSC
g) Determined from density using equation 4.1 (cryst : crystallinity)
h) Determined from NMR

5.3.2.2 Characterisation of copolymer fractions

The DSC curves of the TREF fractions of both copolymers are presented in Appendix C. As can be seen in Appendix C, all fractions exhibit only a single melting peak. The tables above show the gradual increase in T_m (DSC melting peak maximum) with an increase in the prep-TREF elution temperature of PPA and PPB. This indicates that the pentene content incorporation becomes smaller with an increase in the elution temperature. In other words, as the elution temperature increases the number of the comonomer segment becomes less and the

influence of the comonomer segments on the crystallisation of the PP segments becomes weaker. An increasing T_m may also indicate an increase of isotacticity or the length of isotactic sequences with an increasing elution temperature. The melting temperature is controlled by factors including lamellar thickness. (Increasing the lamellar thickness will increase the melting temperature of the copolymer).

It is evident that the melting temperatures, crystallisation temperatures, and degrees of crystallinity all increase as the elution temperature of the fractions increases. Simultaneously there is a decrease in the comonomer content in the case of the copolymers and an increase in the tacticity of the chains in the case of the homopolymer, as is shown in Figures 5.3 and 5.4.

Figure 5.3 shows the relationship between the comonomer content and TREF elution temperature. A linear relationship between comonomer contents and elution peak temperatures are generally observed for both copolymers. It is also noted that the comonomer content in the lower temperature fraction of PPA is higher than the case of PPB. However, at high fractionation temperatures the incorporation of the comonomer is higher for PPB than PPA. The variation in comonomer content with increasing fractionation temperatures is a familiar trend observed by a number of researchers [8-10] for the preparative TREF fractions of semi-crystalline copolymers. The chains are separated according to the longest crystallisable sequence length. It has been observed that only one regular sequence of sufficient length is required to enable a chain to crystallise out at a certain temperature and therefore elute in a given TREF fraction [11]. This of course means that there may still be considerable microstructural variation even in the collected TREF fractions.

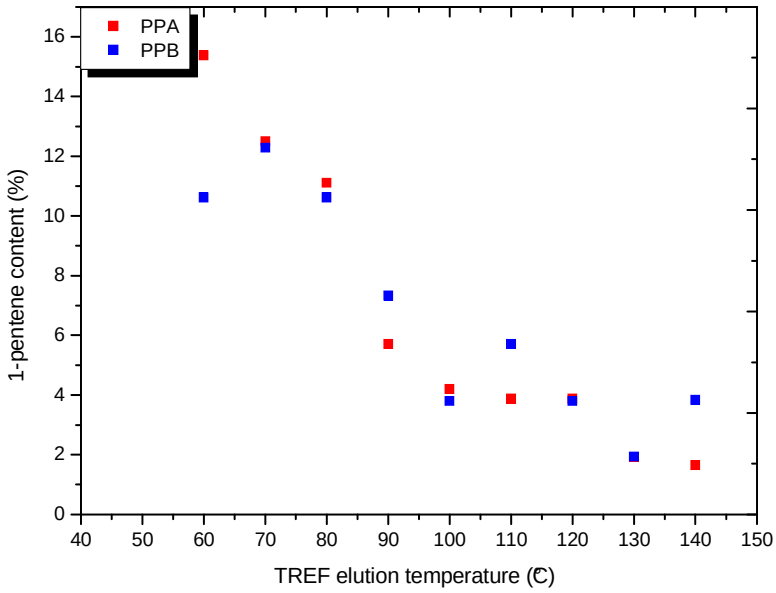

Figure 5.3 The 1-pentene content of the TREF fractions of PPA and PPB.

Determination of the tacticity of both copolymers was not an easy task, due to the overlap of the resonance signal of one of the methylene peaks in the 1-pentene side-chain. Sacchi *et al.*[12] describes an estimation method to calculate the tacticity based on the subtraction of the integrated signal area of a 1-pentene methylene carbon measured in a different spectral region from the total integrated signal area of the original 1-pentene methylene and the mrrr steric pentads. This method was used in the current study to determine the tacticity of the copolymers.

Figure 5.4 shows the evolution of *mmmm* % pentads (determined from ^{13}C NMR) for some of the PPA and PPB fractions as a function of elution temperature. As expected, isotacticity of the fractions increases with the elution temperature, confirming that the TREF of PP copolymers is conducted on the basis of both tacticity and comonomer content. However, an interesting outcome of this analysis is that the isotacticities of PPA fractions are systematically larger than those of PPB fractions, at a given elution temperature (except the fraction 60 °C). The tacticity of the fractions of PPA and PPB eluting at the same given temperature (and thus presenting the same crystallizability) is different. Greater differences are observed for the fractions collected in the low elution temperature range.

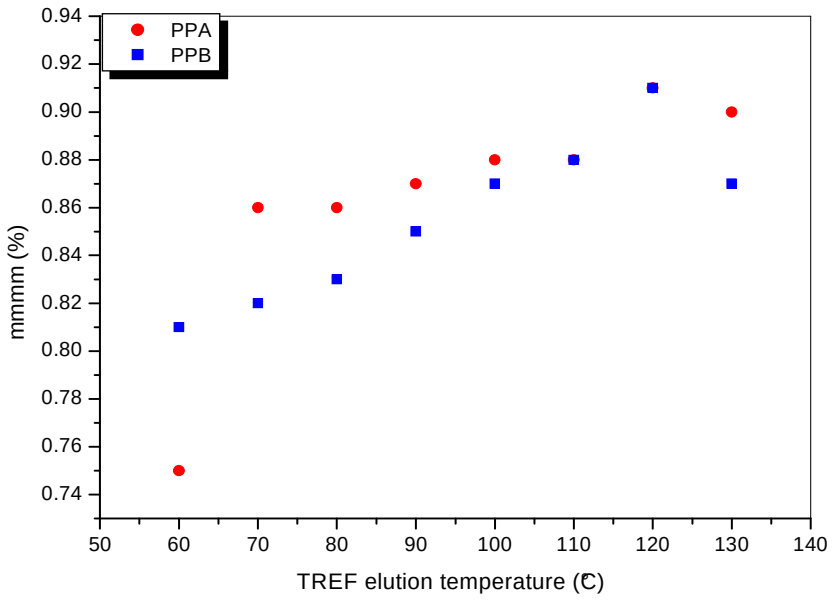

Figure 5.4 Evolution of mmmm % pentads for TREF fractions of PPA and PPB as a function of elution temperature.

Significant differences exist between the two resins in the way tacticity is distributed among the chains as is shown in the figure above. This effect is particularly clear when considering the large difference in the proportion of the fractions eluted at higher temperature, corresponding to the major fractions of PPA.

Figure 5.5 shows the crystallinity percentage calculated from the DSC melt enthalpy using ΔH for 100% crystalline polypropylene as 209 J/g [13-15], and from density using equation 4.1.

The crystallinity values calculated from density was consistently higher than the crystallinity from DSC melt peak. Using a somewhat lower value of 163 J/g [3] for ΔH reduced the discrepancy in the crystallinity value. Nevertheless, the difference between the crystallinity calculations remained significant. This is a results of the constant value taken for ρ_a in equation 4.1 not being strictly correct. The assumed value of 0.853 g cm^3 is taken from amorphous, atactic PP and it may not strictly be appropriate for the amorphous phase density where there is a high comonomer content. Nevertheless the values based on the density are used in the present study for the reason mentioned in the previous chapter, since the positron annihilation parameters were determined at room temperature as is the density measurement.

Despite problems in determining the absolute crystallinities, the relative crystallinity based on density should be reliable if we assume the change in the amorphous densities due to comonomer effects is relatively small.

Evidently, an increasing crystallinity and melting temperature are obtained with the increase in elution temperature. In particular, the linear relationship can be verified from the plots of crystallinity and melting temperature against elution temperature. These results are in accordance with those of Hosoda and Francis [9, 10].

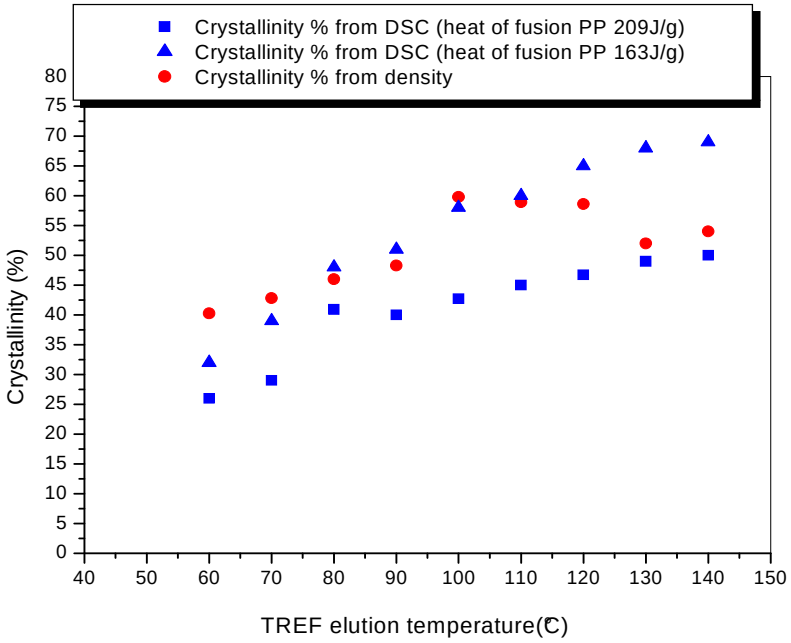

Figure 5.5 Crystallinity, determined using different techniques as a function of TREF fractions of PPA.

Figure 5.6 shows a definite increase in the percentage crystallinity of the fractions with an increase in elution temperature. This behaviour is expected, as TREF separation is based on differences in crystallizability according to chemical composition distribution. The percentage crystallinity decreased at the highest temperature fraction. This shows that the degree of crystallinity, and also the overall perfection of the crystals, is not as good for the highest temperature fractions as it is for the lower temperature fractions. Harding has observed this phenomenon in other copolymers [16].

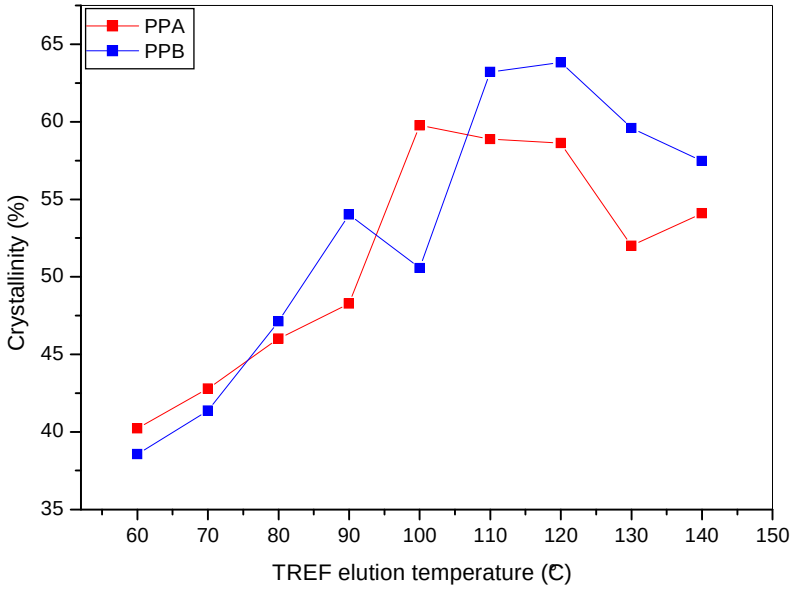

Figure 5.6 Crystallinity from density as a function of TREF fraction temperature of PPA and PPB.

5.3.2.3 Measurement of positron annihilation parameters

The PALS analysis was performed for the bulk and fractionated copolymers. Figure 5.7 shows a graphical representation of the τ_3 and τ_4 lifetimes as a function of the TREF elution temperature. The tabulated values can be found in Tables 5.2 and 5.3. Similar to what was observed in Section 4.3.4, the value of τ_4 (which is attributed to the pick-off annihilation of o-Ps in the amorphous regions of the polymer) shows a slight decrease as the fractionation temperature increases for the lower fractionation temperature region. However, in the higher fractionation temperature region the PPB copolymer shows no variation, while the PPA copolymer shows a slight increase. As was the case in the LLDPE copolymers, decreasing values can be attributed to the lower comonomer content in the amorphous materials. Again the higher the fractionation temperature, the lower the value of τ_4 which is due to a higher "packing density"of the chain in the amorphous region which will leads to a slightly smaller average free volume hole size within these amorphous areas and a decrease in τ_4 lifetime. In this case, however, the changes in the higher temperature fractions require further investigation.

The τ_4 lifetime of PPA is slightly longer than PPB for the lower temperature fractions. The trend is reversed for the higher temperature fractions, where shorter annihilation times are

found for PPA. These results correlate well with the results for the comonomer contents of the respective fractions. The lower temperature fractions of PPA contain relatively higher comonomer content than the low temperature fractions of PPB. This demonstrates the importance of the comonomer content in terms of chain mobility in the amorphous regions.

The τ_3 values also show a more complex relationship with the TREF elution temperature. This is discussed in later sections, but the variations are reflective of the very complex chain structure and morphologies in these copolymers

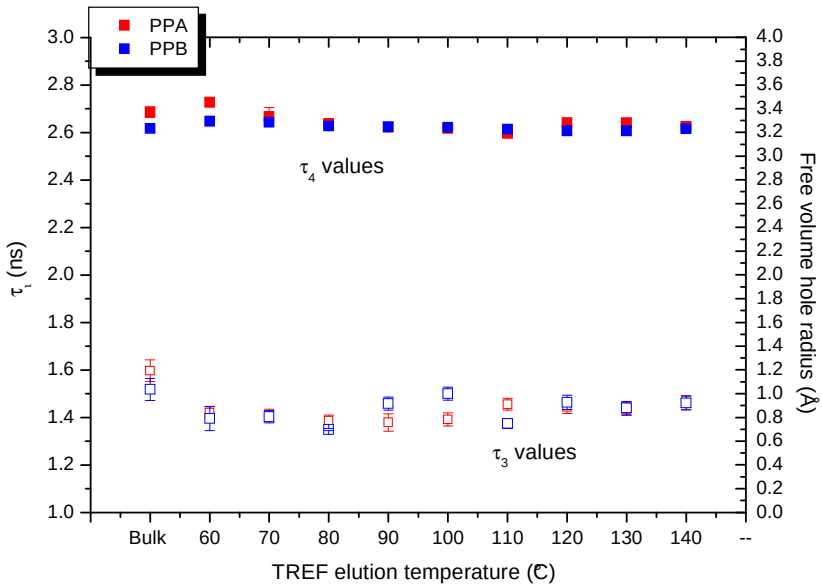

Figure 5.7 τ_3 (open symbols) and τ_4 (closed symbols) lifetimes for the bulk and TREF fractions of PPA and PPB.

Figure 5.8 show the o-Ps intensities, I_3 and I_4 for the bulk and fractionated copolymers. For clarity, the I_3 values are plotted on a shifted access on the right side. I_4, which is the annihilation probability of o-Ps trapped by the open spaces in the amorphous phase is expected to decrease upon decreasing the concentration of such spaces. Thus, the observed general decrease in I_4 is attributed mainly to the decrease in the concentration of the open spaces due to the successive decrease in the mobility of molecules and decreased degree of chain branching. A similar decrease was observed as described in Section 4.3.4, where the I_4 decrease as the TREF elution temperature increases. On the other hand the I_3 intensity (the component associated with annihilation at crystalline defects) once again shows a more complex relationship with the TREF fractionation temperature. It is also interesting to note that the I_3 values for the PPB copolymer are consistently higher than the PPA copolymer. This

must be attributed to the generally higher pentene content in this copolymer relative to the PPA copolymer at the same fraction temperature. Once again the variation in the o-Ps intensities shows a much more complex variation across the elution temperatures and the discussions above are much generalised observations which require further investigation in the next sections.

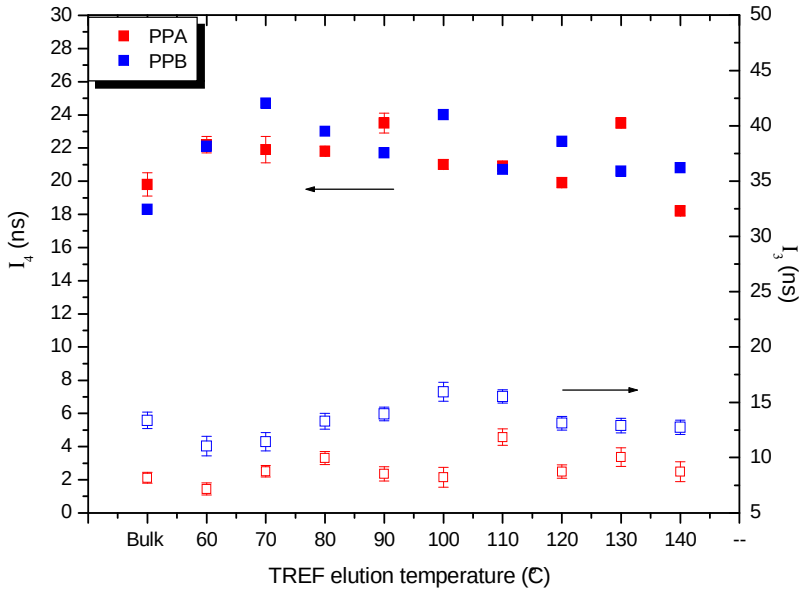

Figure 5.8 Intensities I_3 (open symbols) and I_4 (closed symbols) for the bulk and TREF fractions of PPA and PPB.

As discussed in Section 4.3.4, the relative free volume of the amorphous material can be calculated using equation 4.7.

Figure 5.9 shows the relative fractional free volume of the amorphous phase plotted against the τ_4 lifetime (hole size) of the amorphous phase. Very similar to what was observed in Section 4.3.4, it is clear that at a given o-Ps lifetime (τ_4), the relative free volume is larger for the PPB than the PPA copolymer which is due to the relatively higher I_4 value in most PPB fractions. The figure also illustrates the observation from Figure 5.7 that there is an overall bigger variation in the τ_4 value in the PPA copolymer series than the PPB series. This is once again attributed to the higher pentene content in the respective TREF fractions.

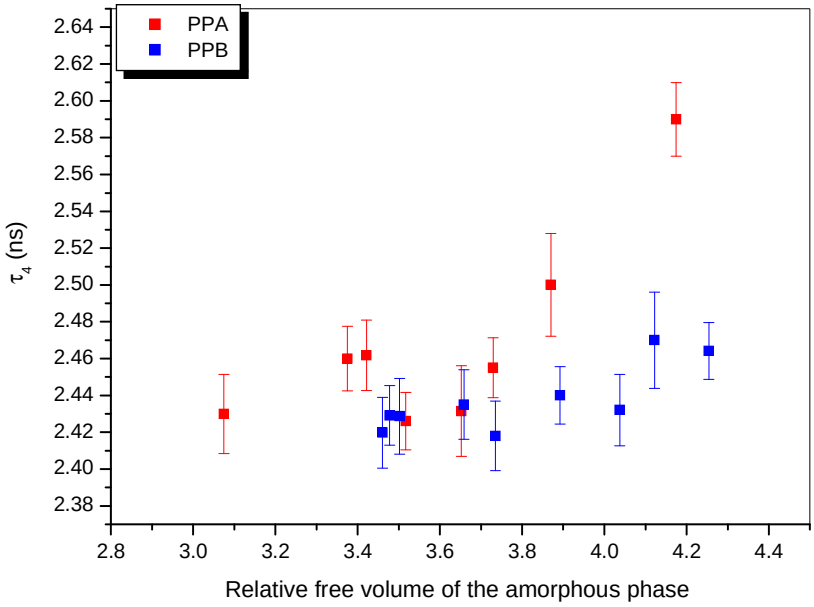

Figure 5.9 Changes in the relative free volume in the amorphous phase of fractionated PPA and PPB as a function of the o-Ps lifetime τ_4

A closer look specifically at the effect of the comonomer on the τ_4 lifetimes of PPA illustrates the effect the comonomer has on the mobility of the chains in the amorphous regions (Figure 5.10). The more comonomer present in the sample, the less defined are the crystalline regions, and also the lower the degree of order in the amorphous domains. This leads to larger free volume holes as implied by the longer o-Ps annihilation times. A similar increase in the longest lifetime with increasing comonomer content was also observed in the study presented in Section 4.3.4.

Figure 5.11 shows the relationship between lifetime and crystallinity for the copolymer fractions. The τ_4 lifetimes in particular are affected by the level of crystallinity in the sample (although not directly since the decrease is due to decreasing comonomer content in the amorphous region). The o-Ps lifetime is reduced from approximately 2.6 ns to 2.3 ns. The τ_3 lifetimes appear to be relatively unaffected. This is consistent with observations described earlier (Section 4.3.4) where the variation in τ_3 is minimal with an increasing TREF fractionation temperature.

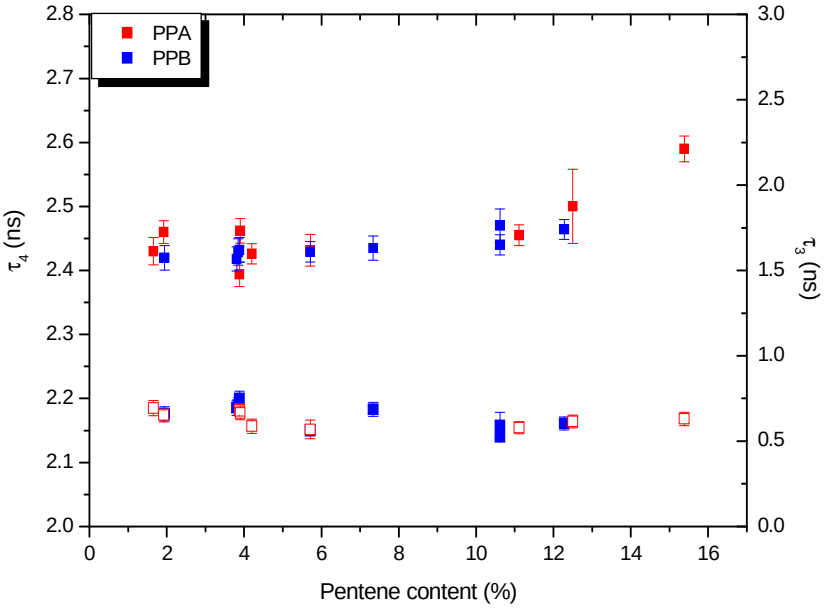

Figure 5.10 Comonomer content effects on τ_3 (open symbols) and τ_4 (closed symbols) lifetimes of TREF fractions of PPA and PPB.

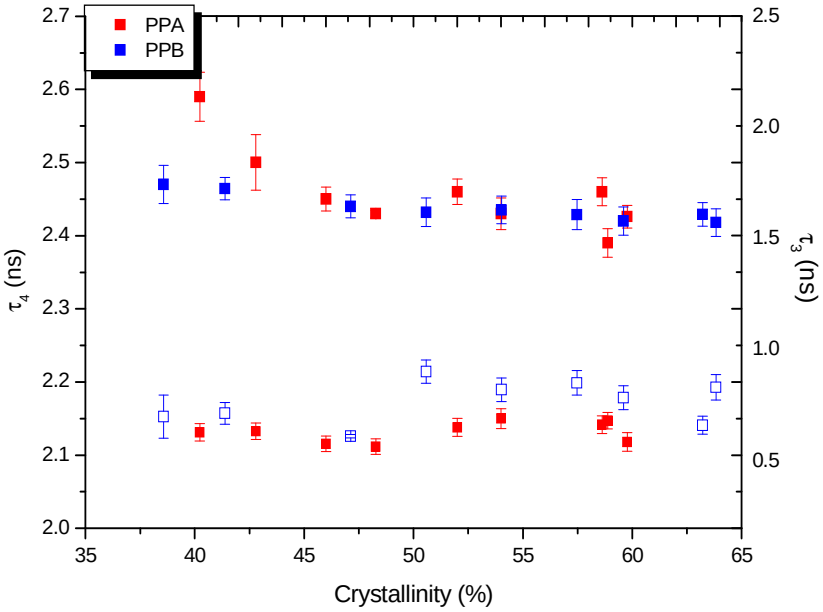

Figure 5.11 Crystallinity effect on τ_3 (open symbols) and τ_4 (closed symbols) lifetimes of TREF fractions PPA and PPB.

Similar results were observed for the o-Ps intensity (formation probabilities) with crystallinity, as shown in Figure 5.12. The figure shows that at higher amount of crystallinity the o-Ps intensity associated with the amorphous phase (I_4) is lower. A slight increase in I_3 (which gives information about the relative fraction of o-Ps annihilation) was observed as the

crystallinity increased. This is expected because I_3 is the intensity of the component associated with annihilation in the crystalline region and crystal interfacial region. This is consistent with observations described in Section 4.3.4. What is again observed, is that these increases are very small at best and do not show dramatic increases with crystallinity and while there is a general overall increase, the variation is by no means linear or direct.

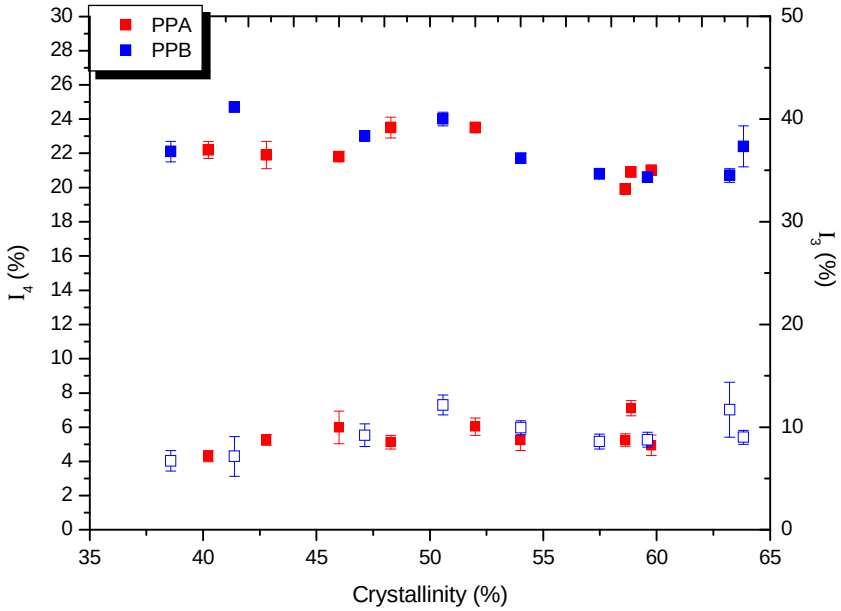

Figure 5.12 Crystallinity effects on I_3 (open symbols) and I_4 (closed symbols) of TREF fractions of TREF fractions of PPA and PPB.

Figures 5.13 and 5.14 show the combined effect of the crystallinity and relative fractional free volume of the amorphous phase on the microhardness of the samples. As was the case with the ethylene copolymer (and is well established), the microhardness shows a dramatic increase as the crystallinity increases. It is also clear that there is a relationship between the microhardness and the relative free volume of the amorphous phase. There is a clearer variation in the case of the PPA copolymer than the PPB copolymer which is illustrated in Figure 5.15.

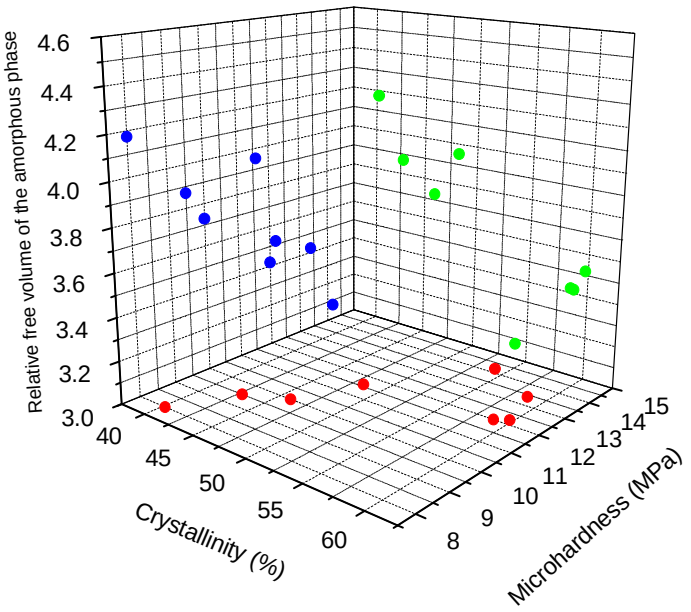

Figure 5.13 Variation in the relative fractional free volume of the amorphous phase as a function of crystallization percentage and microhardness of PPA.

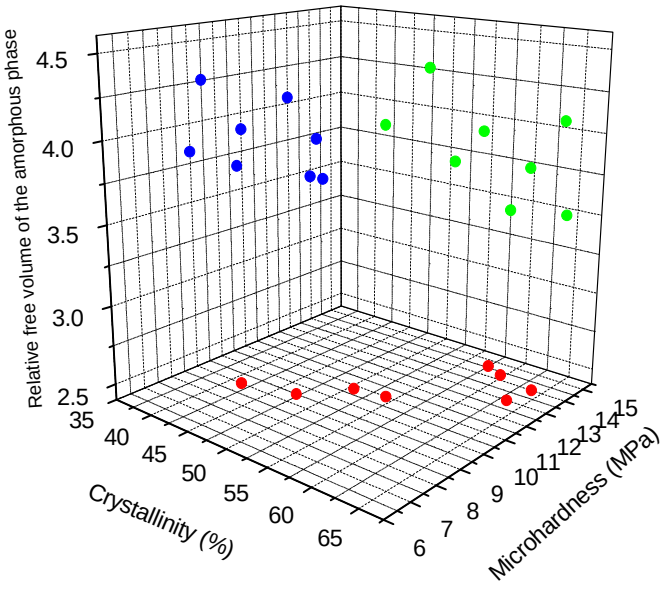

Figure 5.14 Variation in the relative fractional free volume of the amorphous phase as a function of crystallization percentage and microhardness of PPB.

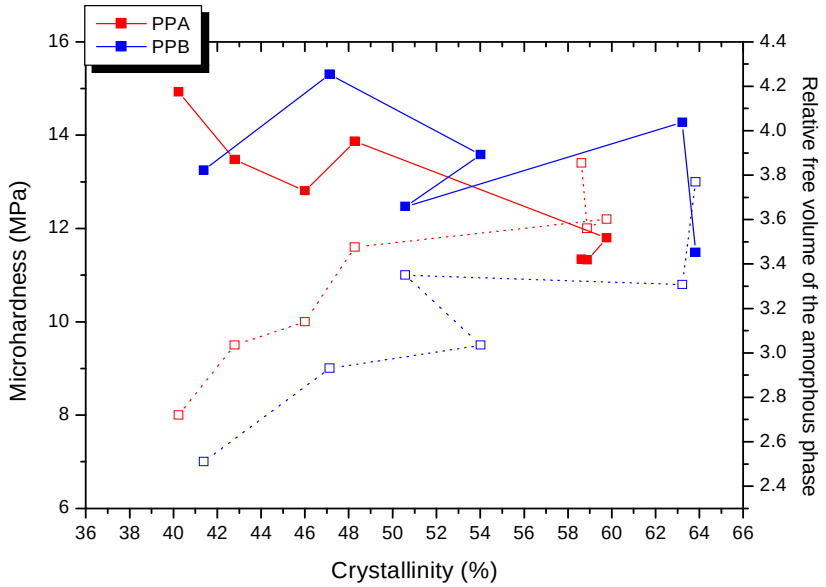

Figure 5.15 Sample microhardness (open symbols) and relative free volume of the amorphous phase (closed symbols) as a function of copolymer crystallinity. (Lines are added as a guide only)

Figure 5.15 shows the relationship between the microhardness, relative free volume of the amorphous phase and the measured crystallinity for the PP copolymers. Again it should be pointed out that in the figure the high temperature fractions have been omitted for clarity sake for the reason mentioned before. It can be seen that in the case of the propylene copolymers the relationship between the various parameters is not simple or as clear and direct as was the case for the ethylene copolymers. However, the same general trend can be observed for the inverse relationship between the relative fractional free volume and the microhardness as a function of crystallinity. Again for example, there is a direct correlation in the very high crystallinity fraction of the PPB copolymer between the dramatic increase in the microhardness of the sample and the corresponding dramatic decrease in the relative amorphous free volume fraction which is not simply apportioned to the small increase in the crystallinity for the samples. Again this highlights the contribution of the changes in the amorphous phase to the microhardness. However, as mentioned before we need to be cautious in interpreting this directly due to the fact the crystallinity affects both parameters, but once again we can conclude that there is some contribution to the microhardness from the changes in the natures of the amorphous phase.

5.3.3 Removal of polymer fractions

It has been pointed out previously that one way of producing additional copolymer series from the same bulk copolymer material is to use techniques where specific material fractions are removed from the bulk copolymer. A single fraction was removed from the copolymers after the TREF process as described in Section 4.3.5. These processes will allow for the analysis of the properties of the copolymer without that specific fraction, thereby revealing the influence that the fraction in question has on the properties. Table 5.4 describes the fraction removal process.

Table 5.4: TREF fraction removal process

Experiment	Description of the process
1	Removal of the amorphous fraction (20-60 °C), and then collect on of the rest of the copolymer (without ‹ 60).
2	Removal of the 70–80 °C fraction (without 80).
3	Removal of the 90–100 °C fraction (without 100).
4	Removal of the 110–120 °C fraction (without 120).
5	Removal of the 130–140 °C fraction (without 140).

5.3.3.1 Effect of the removal of TREF fraction on melting, crystallisation and microhardness properties of PPA and PPB

Figure 5.16 shows the effect of the removal of the of TREF fraction on the melting point of the remaining material. The size of the data point represents the relative amount of material in the fraction removed. In other words, a larger data point means more material is removed in that fraction. The figure shows that there is a decrease in the melting temperature of the remaining material as the amorphous fraction is removed. This is very different to the case of the LLDPE copolymers where an increase relative to the bulk copolymer is observed. Removal of the amorphous fraction from both copolymers resulted in a decrease in the melting temperature compared to the bulk copolymers. This can be explained by the fact that as the more highly branched (high comonomer content materials) is removed the size of the crystal may be effected and we end up with a very small crystal size due to the packing of shorter isotactic polypropylene sequences in the copolymer chains. This leads to a reduction in the melting temperature. It will, however, not affect the overall crystallinity percentage which increases as expected, as will be discussed later. As the higher temperature fractions

are removed, the melting temperature decreases compared to the bulk copolymer. This is expected since more crystalline material is removed in the higher temperature fractions.

The same effect on the melting temperature was observed for the removal of the 100°C to 140°C fractions of PPA. Essentially the melting temperature decreases relative to the bulk copolymer. However, there is a large difference in the size of the removed fractions. The 100 °C fraction constitutes a much larger proportion of the bulk material relative to the 120°C and 140 °C fractions or for that matter any of the other fractions.

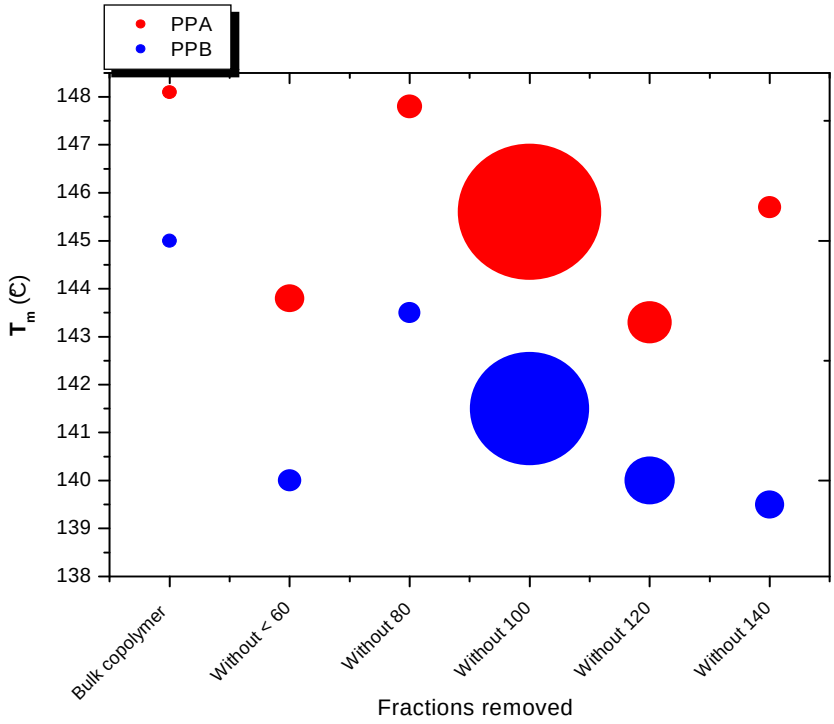

Figure 5.16 Melting temperature of the bulk and remaining material of PPA and PPB.

Figure 5.17 illustrates the effect of the removal TREF fractions on the degree of crystallinity. Besides the change in T_m, the crystallinity percentage also changes upon removing one TREF fraction. The general trend is that the crystallinity of the remaining material decreases as the temperature of the removed fractions increases. This can be attributed to the fact that when removing the low temperature fraction (without < 60), more amorphous material and more material with short-chain branches is removed, and therefore the crystallinity of the remaining material will be higher than when the 100 °C fraction is

removed for instance. This is because in the second case more crystalline material is removed, and therefore the crystallinity of the remaining material is lower.

Removal of the highly branch fraction results an increase in the percentage of crystallinity compared to the bulk copolymers. As the higher temperature fractions are removed, the percentage crystallinity starts to decrease, until it reaches the lowest value when the 140 °C fraction is removed. This is expected since the high temperature fraction constitutes the more crystalline material. Unlike the variation in the T_m, the crystallinity varies in a similar way with the fraction removal as was the case for the LLDPE series.

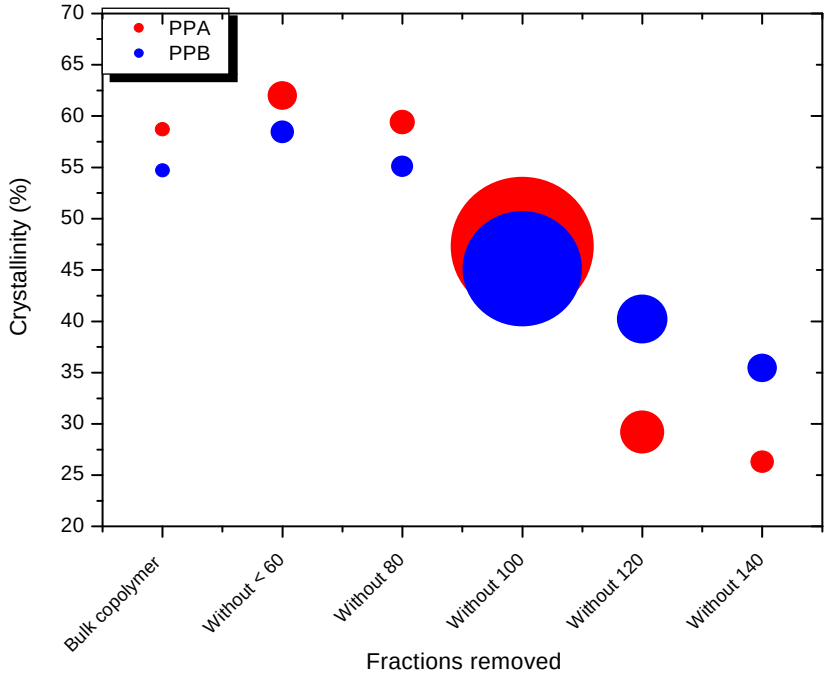

Figure 5.17 Degree of crystallinity (from density) of the bulk and remaining material of PPA and PPB.

Figure 5.18 shows the effect of the removal of the fractions on the microhardness of the remaining material. There is a general decrease in the microhardness as the temperature of the removed fraction increases. The reason for this is that after removing the low temperature fraction lower amounts of comonomer will be present, which will lead to less inhibition of the chain crystallisation. As the temperature of the removed fraction increases more comonomer will be present, which will affect the microhardness.

The above explanation for the relationship between the microhardness and the removed fraction is clearly shown in Figure 5.18. As the lower temperature fractions are removed, the microhardness of the remaining material increases compared to the bulk copolymer. This is because as the lower fraction is removed (amorphous fraction removed) there will be an increase in the crystallinity percentage which will increase the microhardness. As the higher temperature fraction is removed, the microhardness will decrease. From this we can conclude that the microhardness will always increase due to the hardening contribution of the developing crystal regions. However, this does not take into account any contributions there may be from the changes in the nature of the amorphous fraction. The next section considers this by presenting the positron annihilation data on the copolymers.

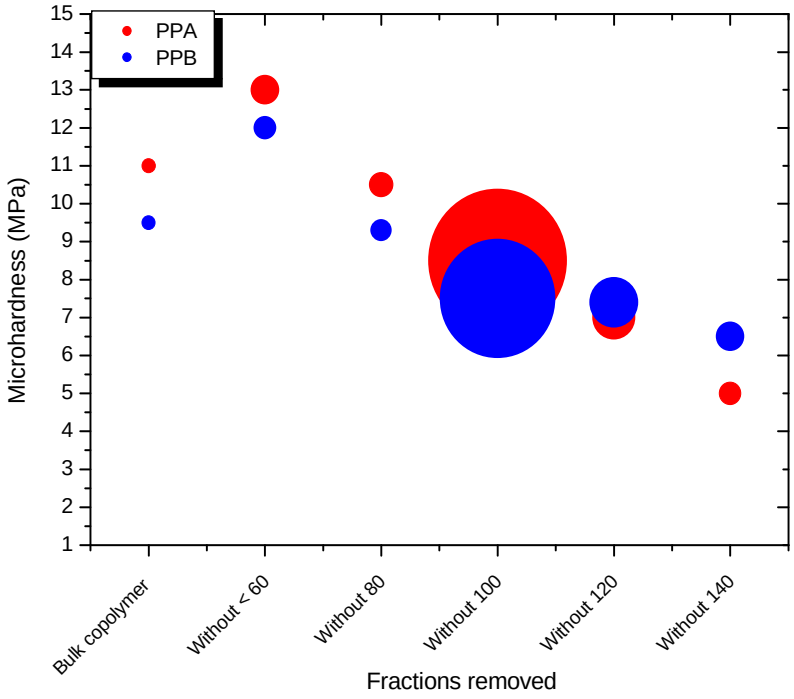

Figure 5.18 Microhardness values of the bulk and remaining material of PPA and PPB.

5.3.3.2 Effect of removal of TREF fraction on measured positron annihilation parameters of PPA and PPB.

Table 5.5 presents the lifetime and intensity values for the bulk and the remaining material after removal of the TREF factions.

Table 5.5 Lifetime and intensity values for the bulk and remaining material of PPA and PPB

Fraction temperature (°C)	τ_3 (ns)		I_3 (%)		τ_4 (ns)		I_4 (%)	
	PPA	PPB	PPA	PPB	PPA	PPB	PPA	PPB
bulk	0.99±0.06	0.77±0.06	8.18±0.5	9.30±0.8	2.52±0.03	2.42±0.02	19.8±0.7	18.30±0.4
without ‹ 60	0.58±0.03	0.45±0.04	14.54±2.2	8.90±0.8	2.41±0.01	2.37±0.01	24.4±0.9	22.11±0.3
without 80	0.66±0.04	0.48±0.02	11.50±1.0	9.34±1.0	2.45±0.01	2.39±0.03	21.3±0.3	20.72±0.2
without 100	0.62±0.03	0.59±0.03	9.74±0.9	9.22±1.3	2.53±0.01	2.43±0.03	19.2±0.3	19.85±0.1
without 120	0.83±0.05	0.61±0.01	9.82±0.6	13.13±1.1	2.52±0.02	2.44±0.04	18.9±0.5	18.62±0.4
without 140	0.87±0.05	0.64±0.03	12.52±1.1	10.56±1.1	2.64±0.02	2.48±0.03	17.6±0.4	17.58±.03

Figure 5.19 illustrates the values of the two longest o-Ps lifetimes of the bulk and the remaining material. The results presented in this figure are analogous with the results for the ethylene copolymers. There is a significant increase in the longest lifetime τ_4 (amorphous phase hole size) as the temperature of the removed fraction increases. This trend can be explained by the fact that by removing lower temperature fractions, more short chain branched material is removed which means decreased average hole size in the amorphous phase. This results in the free volume hole size of the remaining material being lower than that of the bulk copolymers. As the temperature of the removed fraction increases, less amorphous material and more crystalline material will be removed; which will lead to a progressive increase in the free volume hole size. Upon removing the 140 °C fraction, highly crystalline material is removed which means more lower free volume material will remain which will lead to a greater increase in longest lifetime τ_4 (amorphous phase hole size).

The changes in the τ_3 values are slightly less dramatic than τ_4, where it shows an initial decrease as the lower temperature fraction are removed and then increases as the temperature of the removal TREF fraction increases. What is significant in this case is that there is a clearer variation in the τ_3 lifetime across the series relative to the ethylene series shown in Figure 4.24. Noticeably there is a drop in the τ_3 value relative to the value for the bulk copolymer for the "without 60" fraction. The decrease in the τ_3 values can be interpreted as an effective decrease in the mean "hole size" of the holes probed by the o-Ps associated with the third component. Put differently, the mean hole size of the component associated with the crystalline phase (defects or interfacial) decreases. When the simultaneous dramatic decrease in the T_m (Figure 5.16) of the copolymers is considered, these results lend a great deal of support to the idea of a "more prefect" crystalline structure in these materials leading to the

decreased melting point and certainly lend support to the idea of the association of the third lifetime component to the "defects" associated with crystallinity. The trend in the value in relation to the T_m is not as apparent for the rest of the series, but nevertheless there is some similarity in the variation in these two parameters across the series although it is clear that it is not quantitatively so. This is most probably as a result of the complexity of the microstructure of the copolymers involved where it is not just the SCB or tacticity that changes across the series, but both. Both factors will affect the degree as well as the nature of the crystallinity (defects and interfacial region).

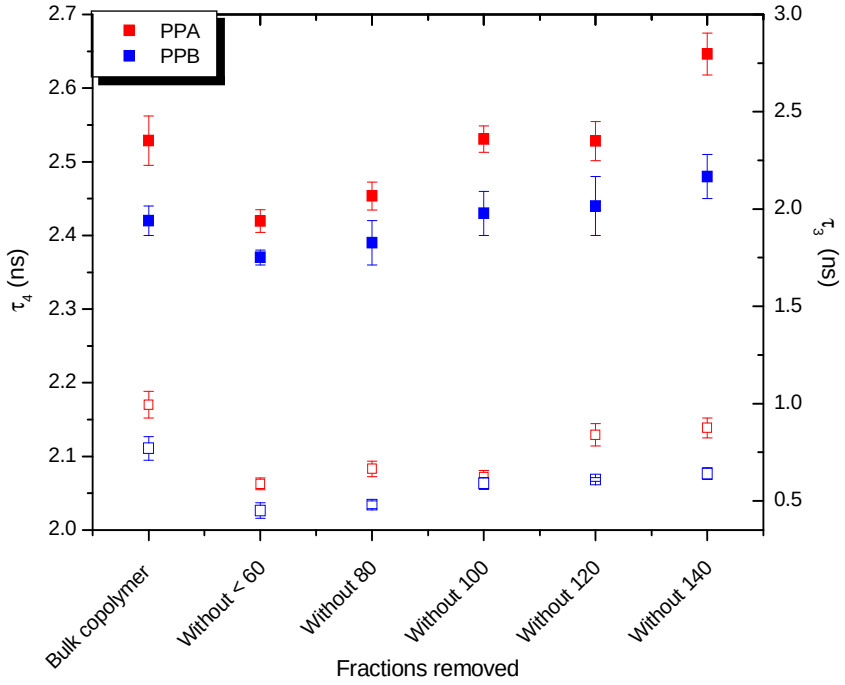

Figure 5.19 τ_3 (open symbols) and τ_4 (solid symbols) lifetimes for the remaining material after removing TREF fraction.

Figure 5.20 shows the variation in the two o-Ps formation probabilities across the series. There is a decrease in the I_4 values (which represent the annihilation probability of o-Ps trapped by the open spaces in the amorphous region) as the temperature of the removal fraction increases. This is somewhat different to case for the ethylene copolymers.

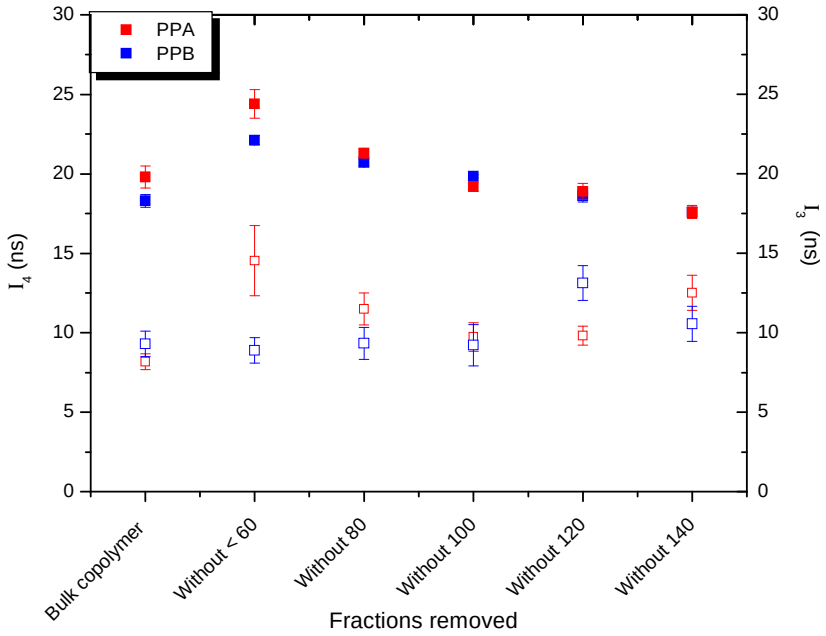

Figure 5.20. I_3 (open symbols) and I_4 (solid symbols) intensities for the remained material after removing TREF fraction.

The relative free volume was calculated according to equation 4.7. The correlation between the relative free volume and recombined material after removing individual fractions is displayed in Figure 5.21. The figure shows a significant decrease in the relative free volume as we remove higher temperature fractions. Again this is in contrast to the case of the ethylene copolymers. In the case of the propylene copolymers it should be noted that the τ_4 values (mean hole size) increase (Figure 5.19) but the overall relative fractional free volume in the amorphous phase decrease as a result of the decrease in the I_4 value increases. The reasons for this decrease are not immediately apparent. It is also noted that for all removal fractions, the relative free volume of the amorphous phase is higher for PPA than PPB which is due to the relatively higher longest lifetime τ_4 (amorphous phase hole size) largely because in the case of the PPB higher amounts of branched chains are removed.

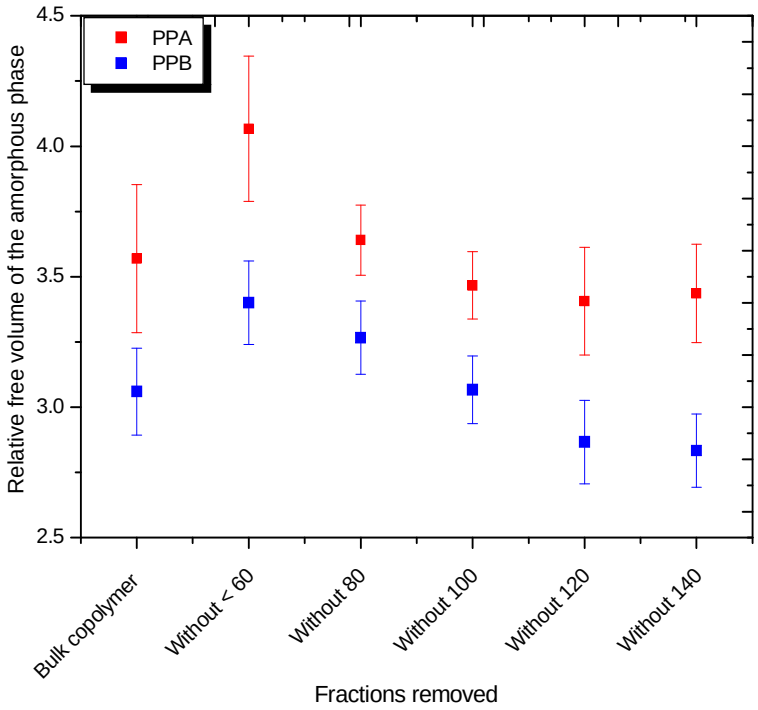

Figure 5.21 Effect of removal of TREF fractions on the relative free volume of PPA and PPB.

Figure 5.22 shows the relationship between the crystallinity, the relative fractional free volume of the amorphous phase and the microhardness of the remaining copolymer materials. Unlike all the previous cases where a more or less inverse relationship is observed between the relative fractional free volume in the amorphous phase and the microhardness, the opposite is true here. This is as a result of the opposite variation in the I_4 values to those observed previously. This would imply that in this case, it is clear that the nature of the crystalline phase is the dominant fact.

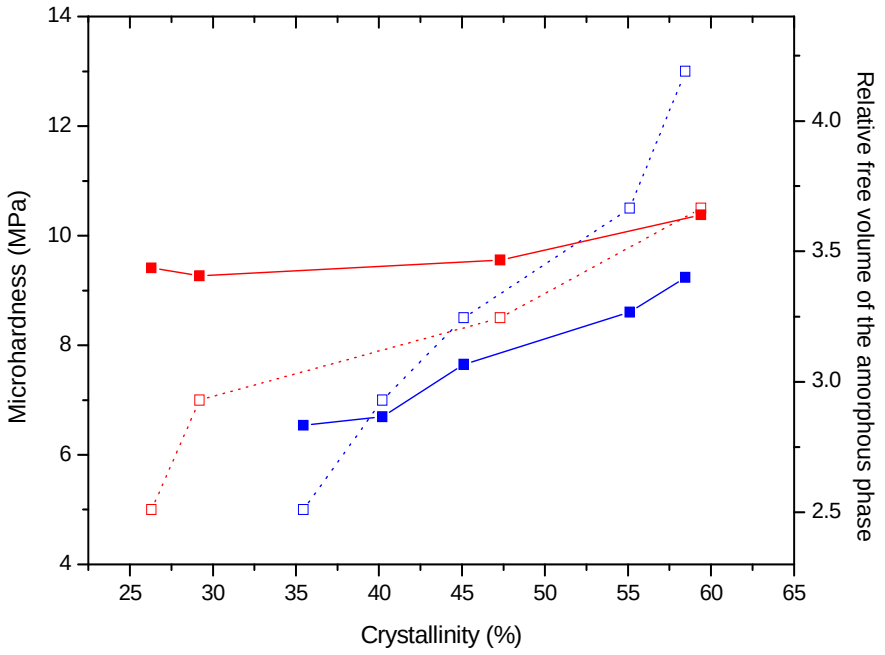

Figure 5.22 Sample microhardness (open symbols) and relative free volume of the amorphous phase (closed symbols) as a function of copolymer crystallinity for fraction removal samples.

5.4 Conclusions

PP copolymers with different chain (defects) structures provided the opportunity to study separately the influence of the amount and type of defects on the crystallisation, morphology and free volume behaviour of PP copolymers.

During the current study the different bulk copolymers were successfully fractionated into fractions with a narrower distribution of molecular species than the bulk materials. Characterisation and analysis of these fractions enabled the investigation of specific molecular characteristics of the free volume holes in the copolymers. It was observed that in the case of the homopolymer the *mmmm* pentad content affected the τ_4 lifetimes with the samples that had high tacticity having a reduced size of the free volume holes in the amorphous phase of the samples. In the case of the copolymer fractions the principal factor affecting the size of the free volume holes was the comonomer content; higher comonomer contents led to larger free volume holes in the amorphous phase. It was also shown that there is some relationship between the microhardness and the relative fraction free volume of the amorphous phase for the TREF fractions. Again this highlights that at least part of the change in microhardness is as a result of the amorphous phase. The results in the TREF fractional removal study do not

show this relationship. This is most probably illustrative of the fact that although the nature of the amorphous phase may play a role, it is still the crystalline phase that is dominant in determining the microhardness.

The results in the study on the removal of the TREF fraction, were similar to the results which was observed for polyethylene, where it is shown that the crystallinity of the remaining material drops as the temperature of the fractions removed increases. This can be attributed to the fact that by removing amorphous and more short-chain branched material, the crystallinity of the remaining material will increase. One of the most important finding in this study was that the T_m of the remaining material decreases when the lower temperature fractions are removed. Corresponding to this decreased T_m is a significant and noticeably decrease in the third lifetime component (τ_3). This provides strong evidence for the association of this lifetime component with the nature of the crystallinity in the sample at least in the copolymers studied. In general it is found that this third lifetime component and yield (I_3) showed more significant variations than in the case of the ethylene copolymers. In many cases the relationship with TREF elution temperature, crystallinity and other factors was not simple but showed more complex variations. This is most probably as a result of the more complicated chain structures where tacticity as well as short chain branching affect the degree and nature of the crystallinity, including the nature of the areas of crystallinity (defects or interface) were the o-Ps probes.

5.5 References

1. Anantawaraskul, S. Polymer Analysis, Polymer Theory; Springer: New York, 2005.
2. Harding, G W. and Van Reenen, A J V. Macromolecular Chemistry and Physics 2006, 207, 1680-1690.
3. Swallowe, M. Mechanical Properties and Testing of Polymers; Kluwer Academic: Netherlands, 1999.
4. Dlubek, G., Bamford, D., Henschke, O., Knorr, J., Alam, M A., Arnold, M. and Lüpke, T. Polymer 2001, 42, 5381-5388.
5. Hamielec, A E., Eldrup, M. and Mogensen, O. Journal of Macromolecular Science, Part C: Polymer Reviews 1973, 9, 305 - 337.
6. Lutz, M, Structure/Property Relationships of Commercial Propylene/1-Pentene Random Copolymers. PhD Thesis, University of Stellenbosch, 2006.
7. Soares, J B P. and Hamielec, A E. Polymer 1996, 37, 4607-4614.

8. Yonggang, L., Shuqin, B., Yejuan, Z. and Wenhe, Z. Journal of Applied Polymer Science 2005, 97, 232-239.
9. Francis, M M. Journal of Polymer Science Part B: Polymer Physics 2001, 39, 2819-2832.
10. Hosoda, S. Polymer 1988, 20, 383.
11. Lodefier, P., Jonas, A M. and Legras, R. Macromolecules 1999, 32, 7135-7139.
12. Sacchi, M C., Forlini, F., Losio, S., Tritto, I., Wahner, U M., Tincul, I., Joubert, D J. and Sadiku, E R. Macromolecular Chemistry and Physics 2003, 204, 1643-1652.
13. Chen, Z., Huang, W., Fang, P F., Wang, H M., Wang, S J., Xiong, J. and Xu, Y S. Nuclear Instruments and Methods in Physics Research Section B: Beam Interactions with Materials and Atoms 2008, 266, 117-122.
14. Greco, C., Mancarella, E., Martuscelli, G. and Silvesrte, C R. Polymer Engineering & Science 1982, 22, 536-544.
15. Vasile, C. Handbook of Polyolefins; Dekker: New York, 2000.
16. Harding, G, The Fractionation and Characterisation of Propylene-ethylene Random Copolymers. Master Thesis, University of Stellenbosch, 2005.

Chapter 6

Temperature dependence of PALS parameters in semi-crystalline polymers.

6.1 Introduction

In the previous chapters, various positron annihilation parameters have been discussed in relation to structural variations such as chain branching and tacticity.

In this chapter, the effect of the temperature on the measured positron annihilation parameters will be discussed. Selected bulk and copolymer fractions have been studied over the temperature range of (40-150 ºC) by positron annihilation lifetime spectroscopy. This has been done to gain better insight into the various positron parameters and how they relate to the morphology of the samples. One of the advantages of this approach over those presented in the previous chapters is that the morphology of the sample is manipulated by temperature while the other factors related to the chain structure remain the same. Unfortunately, however, the nature of the experiments also means that the samples are exposed to the positron source for much longer periods and therefore there is a potential that this may influence the measured parameters.

PALS studies of semicrystalline polymers studied at various temperatures have been reported [1-7]. In one such study, lifetime spectra for linear and branched polyethylene have been measured; it was observed that the longest lifetime decreases with decreasing temperature. Similar results were observed by Abdel-Hady and co-worker in their study [2]. They concluded that the hole size shows a small linear increase with temperature below glass transition temperature and a steeper increase above it in polyoxymethylene. It should be pointed out that in both of the studies mentioned, the raw positron data was only resolved into three components and no “intermediary lifetime”

associated with crystallinity is reported. While these studies have shed insight into the variation of positron parameters with temperature for semi-crystalline polymers, no detailed studies have been done on their correlation with morphology and chain structure.

6.2 Experimental

The experimental details of this chapter are summarised in Chapter 3, however a few points will be highlighted below.

6.2.1 Materials

1- Two different propylene-1-pentene copolymers (PPA and PPB). The details of both copolymers are listed in Table 3.1.

2- Two plastomers (PE1 and PE2). The details of both plastomers are listed in Table 3.2.

6.3 Results and discussion

6.3.1 The effect of exposure time on the PALS measurement

As has been mentioned in the introduction, there are certain advantages of doing thermal studies on samples where the chemical (structural) parameters remain the same. However, in order to do theses temperature measurements from a practical point of view requires that each individual sample is exposed to the positron source for a relatively longer period of time. It is well known that radiation-induced changes can occur in polymers as a result of prolonged exposure to the ^{22}Na positron source [8]. In the studies presented in the previous chapters, the length of exposure of the sample to the source was relatively short (about 1 hour) and the effects of the radiation exposure on the measured positron parameters can be assumed to be negligible. In temperature dependent studies, the effects of radiation exposure can be very important since the sample is exposed not just to a single measurement. The sample remains in contact with the source throughout

the temperature cycle. It is, therefore, important to establish the effect of the source exposure on the measured positron parameters.

Figure 6.1 shows the time dependent study of the effect of exposure on the intensities (I_4) and the lifetimes (τ_4) of o-Ps versus the time of exposure to the source for the two LLDPE samples. The results show that there is little to no change in the o-Ps lifetime (τ_4) with exposure time during the PALS measurements; however the o-Ps intensity I_4 decreased with exposure time. This is consistent with results that have been presented previously on the time dependent studies of the longest lifetime components and is generally referred to as inhibition of o-Ps formation due to source exposure [9, 10].

Figure 6.1 shows that the intensity I_4 dropped by 35% after 70 hours of exposure, however no change was observed in the lifetime τ_4 with the exposure to the source even after all this time. This indicates that in the successive measurements, only the Ps yield (I_4) and not the o-Ps lifetimes are affected by the irradiation. Several explanations for the decrease in o-Ps intensity with exposure time have been suggested. These include processes related to structural relaxation, formation of an electric field, cross-linking effects and the formation of free radicals [11-14].

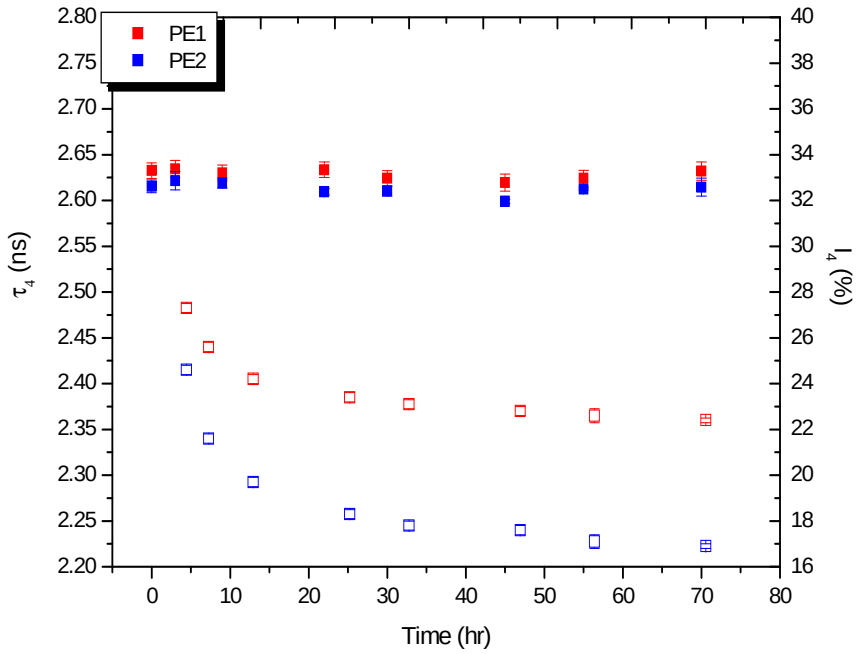

Figure 6.1 o-Ps lifetime τ_4 (solid symbols) and intensity I_4 (open symbols) as a function of time of exposure to the positron source for LLDPE copolymers

Similar behavior to the LLDPE polymers was observed for polypropylene copolymers. Once again I_4 dropped by 30% after 70 hours but no change was observed in the lifetime (τ_4) as is indicated indicted in the Figure 6.2.

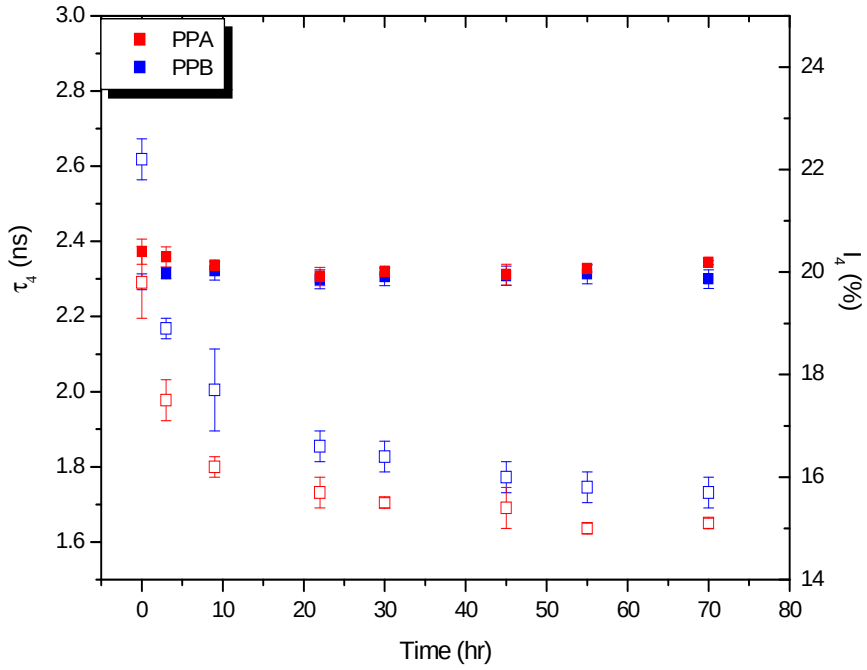

Figure 6.2 o-Ps lifetime τ_4 (solid symbols) and intensity I_4 (open symbols) as a function of time of exposure to the positron source for the propylene copolymers

Figures 6.3 and 6.4 show the effect of the source exposure on the third lifetime component and yield for the LLDPE and propylene copolymers respectively. It is clear that there is great variation of the τ_3 and in the case of the propylene copolymer the I_3 values with source exposure. Interestingly, unlike the longest lifetime intensity no clear decrease is observed in the I_3 value.

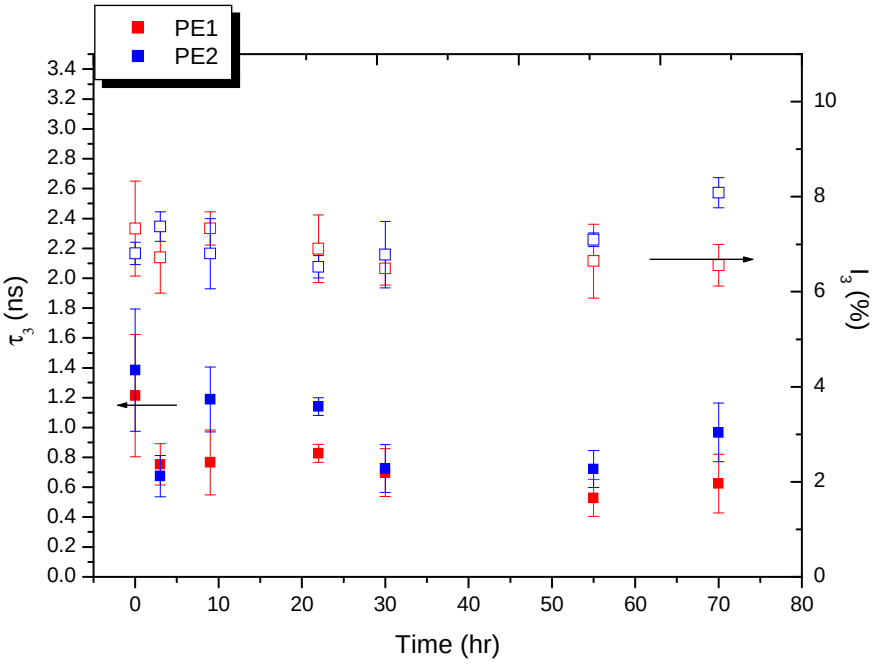

Figure 6.3: o-Ps lifetime τ_3 (solid symbols) and intensity I_3 (open symbols) as a function of time of exposure to the positron source for LLDPE copolymers

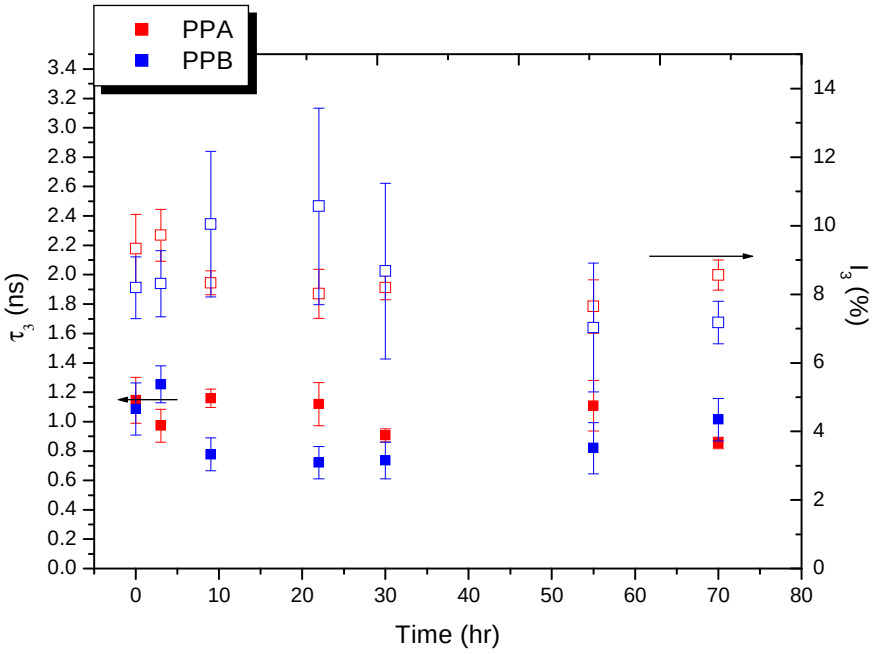

Figure 6.4: o-Ps lifetime τ_3 (solid symbols) and intensity I_3 (open symbols) as a function of time of exposure to the positron source for PP copolymers

The results of this exposure study indicate that while the τ_4 values are largely unaffected by source exposure, the I_4 values are. This means that the τ_4 values would be expected to be reliable while the I_4 values in the long term exposure studies must be treated with some caution. In addition, it should be kept in mind that several studies have shown that the decrease in the longest lifetime intensity I_i values due to source exposure can be annealed out with temperature[8, 15]. This provides a further complication in interpreting the I_i values in this study. This inevitably means that quantitative interpretations of the variation in the yield values need to be treated with some caution, as do the τ_3 and I_3 values.

6.3.2 The temperature dependence of positron parameters in the bulk polymers

As was the case in the previous room temperature isothermal studies, the PALS spectra were best resolved into four components using the PATFIT program. The lifetimes and intensity values obtained for the bulk LLDPE and polypropylene copolymers as a function of the temperature are listed in Tables 6.1 and 6.2 respectively. It should be noted that the sequence of the spectrum acquisition was from low to higher temperature. In other words the 40°C sample was measured first while the spectrum at 130° was measured last at least 24 hours after the first measurement.

Table 6.1 o-PS lifetimes τ_i, and intensities I_i values obtained for the bulk LLDPEs at different temperatures.

Measurement temperature (°C)	τ_3 (ns)		I_3 (%)		τ_4 (ns)		I_4 (%)	
	PE1	PE2	PE1	PE2	PE1	PE2	PE1	PE2
40	0.68±0.2	0.54±0.1	7.29±1.6	8.71±0.3	2.71±0.05	2.72±0.01	26.2±1.1	19.6±1.1
50	0.70±0.4	0.58±0.1	5.33±1.5	9.13±1.7	2.78±0.01	2.86±0.05	26.4±0.9	19.8±1.6
60	0.68±0.1	0.56±0.5	4.10±1.5	6.93±0.8	2.83±0.01	2.87±0.01	27.3±1.5	20.4±1.8
70	0.69±0.6	0.61±0.3	3.21±0.3	6.05±0.8	2.85±0.02	2.90±0.01	27.4±2.0	21.6±1.4
80	0.73±0.2	0.57±0.2	2.99±0.6	6.65±1.3	2.90±0.02	2.91±0.01	28.6±2.2	21.8±1.4
90	0.72±0.3	0.62±0.4	2.07±0.8	3.61±0.8	2.91±0.05	2.89±0.05	28.9±1.6	22.6±2.1
100	0.74±0.5	0.67±0.5	6.53±0.8	5.66±0.8	2.91±0.04	2.92±0.03	29.6±2.3	24.4±1.8
110	0.72±0.3	0.61±0.3	4.52±0.8	3.02±1.5	2.91±0.06	2.90±0.05	29.9±2.1	26.8±1.9
120	0.70±0.1	0.62±0.4	7.48±0.8	3.91±0.6	2.98±0.04	2.97±0.03	29.8±1.9	28.4±2.3
130	0.65±0.2	0.58±0.2	7.60±0.7	4.14±0.7	2.97±0.04	2.97±0.03	29.8±1.7	28.7±1.4

Table 6.2 o-Ps lifetimes τ_i, and intensities I_i values obtained for the bulk polypropylene copolymer at different temperatures.

Measurement temperature (°C)	τ_3 (ns)		I_3 (%)		τ_4 (ns)		I_4 (%)	
	PPA	PPB	PPA	PPB	PPA	PPB	PPA	PPB
40	1.03±0.2	0.98±0.4	7.41±0.6	9.01±0.5	2.52±0.05	2.97±0.06	16.4±1.2	19.2±0.2
50	0.97±0.3	0.92±0.1	6.90±0.8	8.22±0.6	2.67±0.06	3.16±0.07	19.1±1.3	21.1±0.1
60	0.95±0.1	0.87±0.2	8.03±0.6	8.46±0.6	2.73±0.09	3.16±0.04	22.6±0.9	22.2±0.8
70	0.98±0.1	0.84±0.5	6.76±0.5	7.12±0.4	2.79±0.04	3.25±0.04	23.2±0.8	23.3±0.7
80	0.84±0.2	0.83±0.3	7.01±0.5	5.75±0.4	2.87±0.03	3.27±0.04	24.4±1.3	25.2±0.3
90	0.81±0.3	0.85±0.4	5.35±0.5	4.48±0.5	2.91±0.04	3.24±0.03	24.4±1.5	26.6±0.8
100	0.72±0.2	0.86±0.2	5.31±1.3	5.04±1.1	2.98±0.06	3.25±0.03	24.4±0.9	25.8±0.9
110	0.68±0.3	0.79±0.3	5.20±0.9	4.69±0.9	3.12±0.07	3.16±0.03	26.1±0.8	26.3±0.4
120	0.66±0.2	0.74±0.3	4.25±0.6	4.92±0.7	3.18±0.06	3.29±0.04	27.1±1.2	27.4±1.1
130	0.68±0.1	0.81±0.2	5.52±0.6	5.59±1.1	3.21±0.08	3.43±0.04	27.1±0.7	27.5±0.9
140	0.72±0.2	0.86±0.4	6.38±1.9	4.58±0.5	3.19±0.06	3.44±0.03	27.1±1.1	27.8±0.7
150	0.73±0.1	0.80±0.3	5.54±1.4	6.43±0.7	3.22±0.7	2.97±0.04	27.1±0.7	28.1±0.6

Figure 6.5 shows the lifetime τ_3 versus the temperature of the four semicrystalline copolymers (For clarity purposes, the error bars have been omitted but it should be noted that these are relatively large relative to the changes observed). Interestingly, two different behaviors were observed. In the case of both the PP copolymers, the τ_3 value decreases with an increasing temperature, then increases at higher temperature. In the PE samples, however, a completely different behaviour is observed where a very slight increase in the τ_3 value is followed by a decrease. What is interesting is that the inflection points observed for both types of copolymers occur at the expected melting points in these materials. This behavior of τ_3 in the melting region may be due to the melting of the interface region or crystal reorganization as the melting point is reached, as τ_3 is attributed to o-Ps annihilation in the interstitial free volume in the crystalline defects and at the interface. What is interesting and discussed in detail later is that the data at and above the melting point is still best fitted with a four component analysis.

It is also noted that at lower temperature the τ_3 values of the PPB copolymer is lower than PPA, however at higher temperature the τ_3 values became higher in PPB. This behavior may be due to the reorganization of different crystal size as it reaches the melting temperature. The τ_3 values are also higher in the PP copolymers compared to the

PE copolymer. It is also noted that the variation in the τ_3 values for the PP copolymers is larger than the case of the PE copolymers which is consistent with the results presented in the previous chapters.

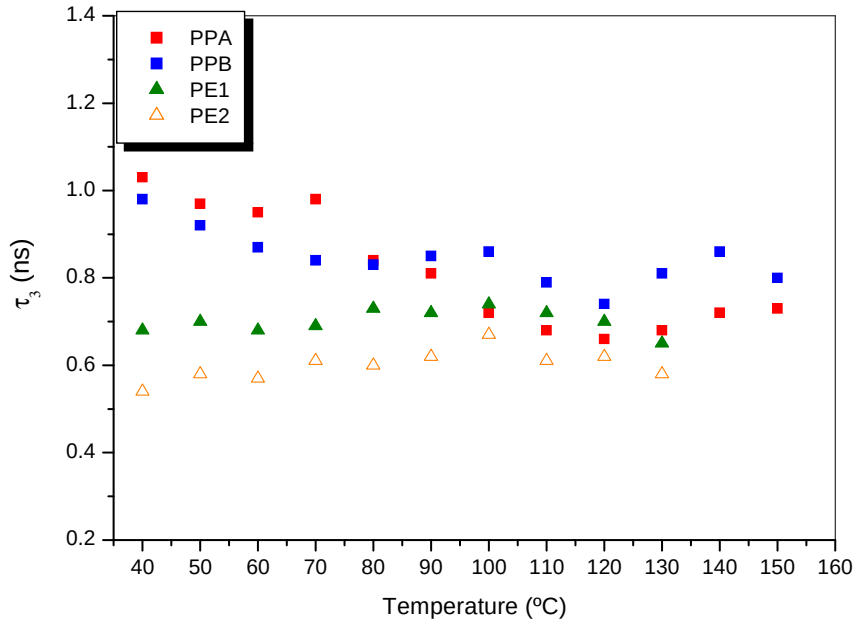

Figure 6.5 Temperature dependence of the τ_3 for all copolymers

Figure 6.6 shows the behavior of the longest lifetime τ_4 (amorphous phase hole size) as a function of temperature. It can be seen that as the temperature increases, the lifetime τ_4 generally increases. The increase of the longest lifetime gives information about the increasing dimensions of holes at which o-Ps is localized and annihilated. In other words, as the temperature increases, the molecular and segmental motions in the amorphous phase increase. This increase in the chain mobility with increasing temperature is associated with an increase in the mean local free volume as a result of the coefficient of thermal expansion [10]. In other words, the local segmental motion can occur due to the thermal expansion of the free volume providing the motional space, where any increase of temperature produces small effects on the thermal motion of the polymer chains. Therefore, small variations of τ_4 versus temperature must be expected

[16]. Similar increase of the radius in the amorphous phase with temperature was observed by others for different semicrystalline polymers [7].

It is also noted that the radius of the free volume cavity increases with temperature for all bulk copolymers as can be seen in Figure 6.6.

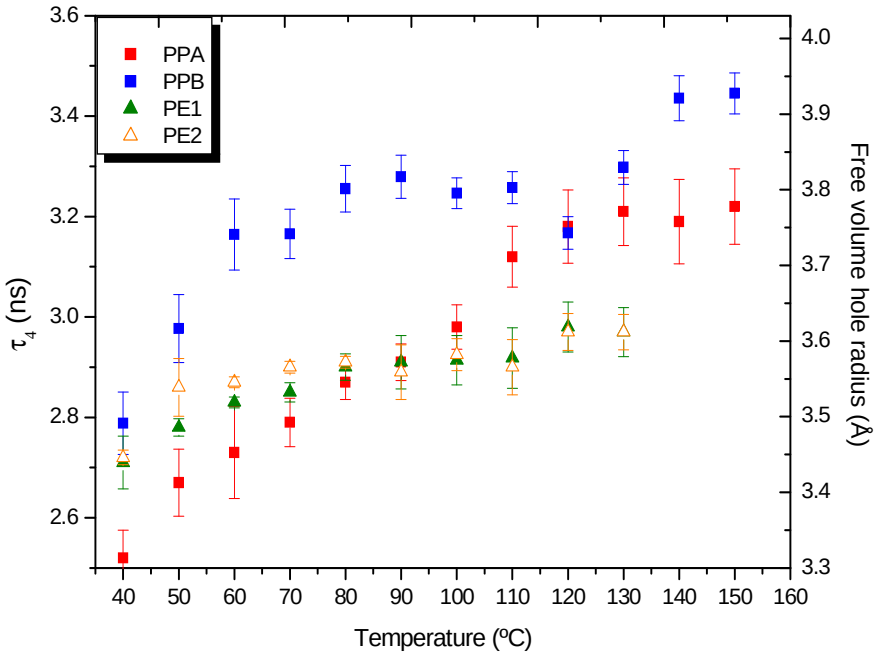

Figure 6.6 Temperature dependence of the longest component τ_4 for all copolymers

It is also noted that there is a steeper increase for the PPB copolymer (higher 1-pentene content). It is also interesting to note that the rate of the increase in the lifetime τ_4 value of the PE polymers is smaller than the PP copolymers across the entire temperature range. This is due to the different molecular structure of the two copolymers and consequent difference in chain mobility.

It is also noted that at higher temperature (close to the melting temperature of each copolymer); the rate of change of the lifetime τ_4 decreases (at about 100°C for the PE copolymers and at about 120°C for the propylene copolymers). In the case of the PPB

polymer a decrease is observed followed by a later increase at high temperature. This process is very clearly indicated in Figures 6.7 and 6.8 for the propylene copolymers and in Figures 6.9 and 6.10 for the ethylene copolymers. In the figures the DSC curves are included to indicate the melting points and melting ranges of the polymers. It should be remembered that the DSC curves are produced at a heating rate of 10°C/min, while the positron data is collected by first equilibrating at a specific temperature. The points from the positron data are, therefore, not directly comparable to the corresponding points on the DSC curves. Nevertheless, the comparisons do give an indication of the melt ranges of the respective polymers. In the figures both the τ_3 (B) and τ_4 (A) values are plotted.

Figure 6.7 shows the results for the PPA copolymer. The τ_4 value reaches a plateau value just slightly below the observed DSC melt peak of the polymer. The inflection point in the τ_3 values mentioned earlier is also observed.

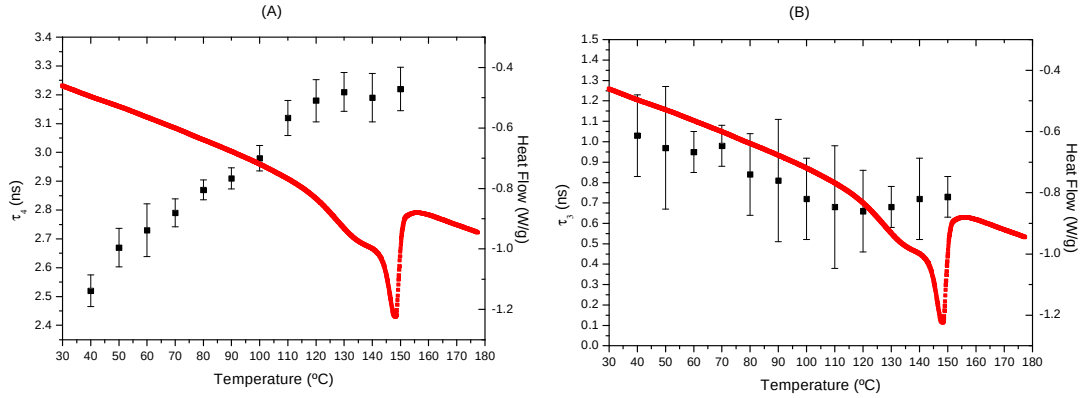

Figure 6.7 The longest lifetimes τ_4 (A) and the third lifetime τ_3 (B) with the DSC melting curve of PPA

Similar behaviour of the τ_4 value were observed for all copolymers as is shown in the Figures 6.8 to 6.10.The levelling off (or as in the case of the PPB copolymer the decrease) just below or at the melting point can be explained by the fact that as the crystals melt, more less branched (or more highly isotactic material) now forms part of the amorphous phase. This has the effect of counter balancing the increase in the amorphous hole size due to the thermal expansion.

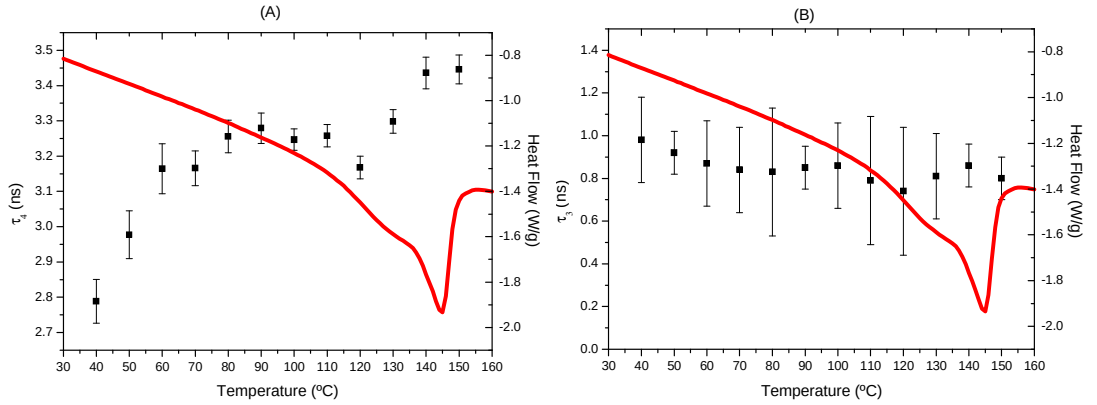

Figure 6.8 The longest lifetimes τ_4 (A) and the third lifetime τ_3 (B) with the DSC melting curve of PPB.

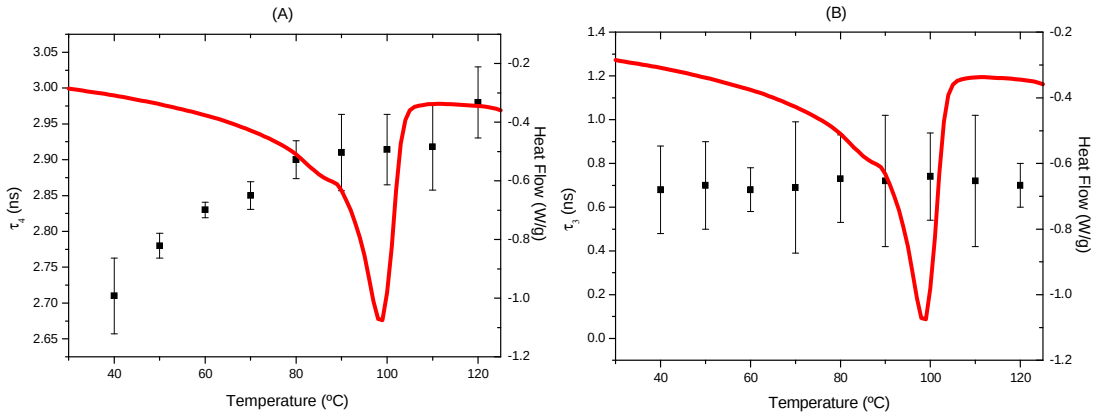

Figure 6.9 The longest lifetimes τ_4 (A) and the third lifetime τ_3 (B) with the DSC melting curve of PE1.

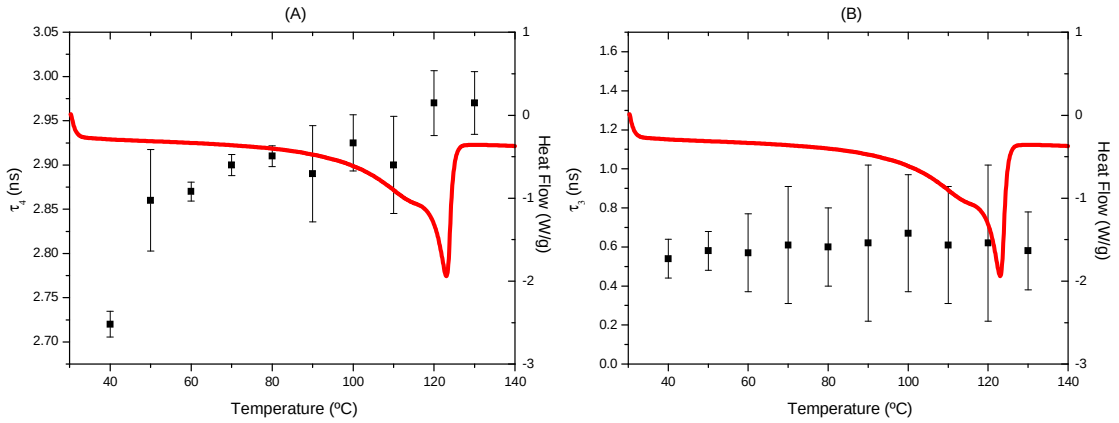

Figure 6.10 The longest lifetimes τ_4 (A) and the third lifetime τ_3 (B) with the DSC melting curve of PE2.

Again the difference between the variation of the τ_3 values between the PP and PE copolymers is highlighted with very little to no change observed for the PE polymers and bigger variation observed for the PP copolymers.

Figure 6.11 shows the variation of I_3 with temperature. The behavior of I_3 is similar to τ_3 where there is a decrease as the temperature increases. This decrease "levels off" at higher temperature (with the exception of the PE1 copolymer where a clear increase is observed as the temperature increases). This behavior supports the suggestion that the third lifetime component is attributed to o-Ps annihilation in the interstitial free volume associated with defect or crystal interfaces and the decrease would be consistent with the proposition that the variation in the third lifetime components is a result of crystal reorganization and melting. However, as mentioned previously the intensity data needs to be treated with some caution, due to possible source exposure effects. It addition is should also be mentioned that the raw data has been fitted with a four lifetime analysis across the entire temperature series and the later increase or "flatting" is an artifact of the analysis and really can not be interpreted as having any real physical significance above the melting point. This point is discussed further in the final part of this chapter and in the general conclusions of this study.

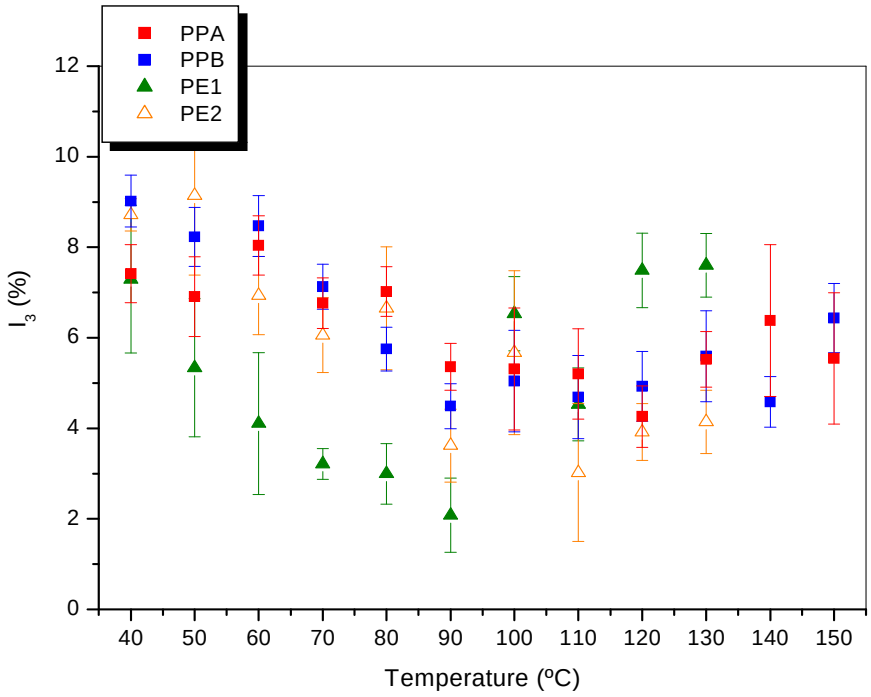

Figure 6.11 Temperature dependence of I_3 for all copolymers

Figure 6.12 shows the variation in the fourth lifetime intensity I_4. I_4 gives information about the relative fraction of o-Ps annihilation within the amorphous areas although again the values need to be treated with some caution due to the exposure effect. Nevertheless, a clear increase in I_4 values with temperature reflects the increase of the positronium formation probability in the amorphous regions, in other words the increase of the o-Ps intensity I_4 is due to the increase in hole concentration or the creation of free volume holes [17]. This behavior indicates that the number of free volume holes is strongly temperature dependent as is expected and has been reported before [18]. It is also worth noting that there is a general increase in the I_4 value with an increasing temperature, despite the observed decrease in this value with time of exposure to the sources (Section 6.3.1). This indicates that the general increase in hole number due to the temperature increase outweighs the decrease caused by source exposure. It should, of course, also be remembered that the o-Ps inhibition (as a result of source exposure) can

also be reversed by thermal annealing which may also be practically responsible for the apparent elimination of the exposure inhibition effect. It is also apparent that the ethylene 1-octene polymer (PE1) has the higher value across the entire temperature range.

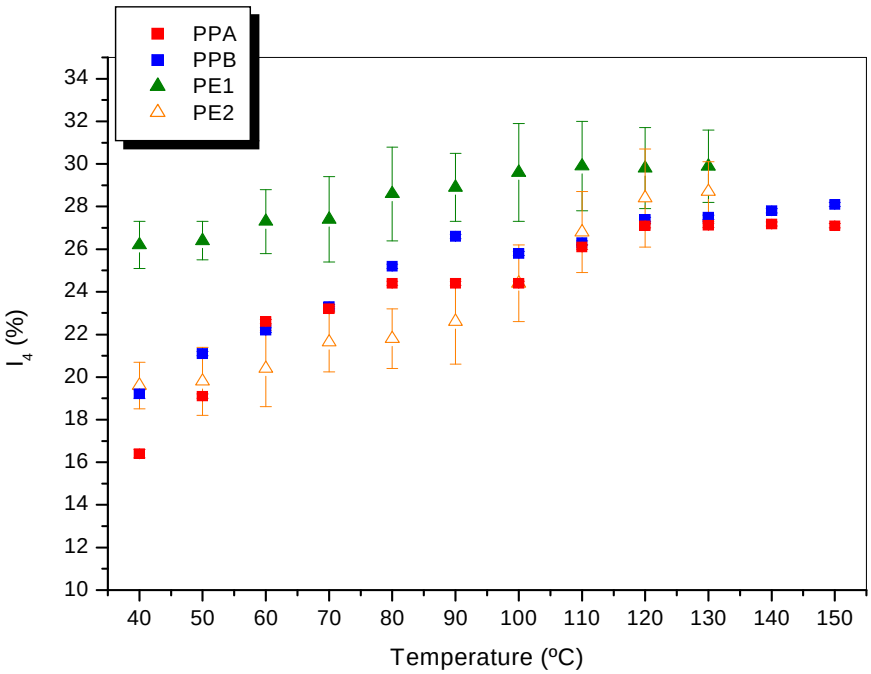

Figure 6.12 Temperature dependence of I_4 for all copolymers

Positron lifetime measurements in the copolymers allow for the estimation of the relative free volume. The results of the relative free volume for the copolymers based on the longest o-Ps lifetime (τ_4) and intensity (I_4) are presented in figure 6.13 as a function of temperature. As expected the results show that the relative free volume increases with temperature. This increase in the relative free volume with temperature is due to the increase of the positronium formation probability I_4 (despite any possible source exposure inhibition effect) as well as the general increase in the τ_4 values. It is also noted that although the PP copolymers have higher lifetime values (larger free volume hole sizes)

the relative free volume is lower in PP copolymers compared to PE1 especially at low temperature. This is generally due to the higher values of I_4 for the PE copolymers.

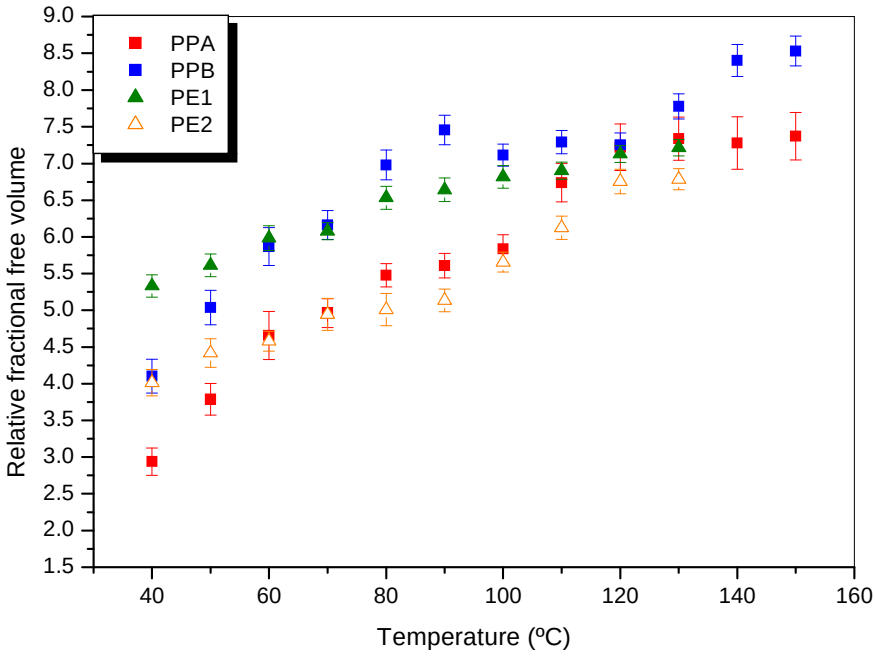

Figure 6.13 Relative fractional free volume as a function of temperature

The results show that as the temperature increases, the chain mobility will increase with a corresponding increase in the mean local free volume. Similar temperature dependencies of the lifetime of the longest component and its intensity have been reported previously for semicrystalline polymers [19, 20].

6.3.3 The temperature dependence of free volume in some TREF fractions.

In the proceeding section the two longest lifetime parameters were shown to vary with temperature and can be interpreted in terms of the change in the morphology of the polymer. A further temperature study was done on selected TREF fractions to provide further insight into the variation of the parameters as the crystalline morphology changes as a result of heating.

Similar results were observed in the case of the fractions as was the case for the bulk copolymers, where variation of the o-Ps lifetime with temperature was observed. There is once again a pronounced increase of the free volume hole size as we increase the temperature. Once again this indicates the thermal expansion of the free volume hole is extremely marked especially at higher temperature.

Figures 6.14 and 6.15 show the lifetime τ_3 and τ_4 versus the temperature for fraction 100 ºC of all four different copolymers.

The behavior of the lifetime τ_3 (which reflect the free volume in the crystalline and interface regions) of the 100 ºC fraction is different form the bulk where it shows that the lifetime τ_3 increases with temperature. This is attributed to the greater degree of homogeneity of the morphology of the fractions and the much greater degree of crystallinity compared to the bulk material. On the other hand, the behaviour of the longest lifetime τ_4 (which reflect the free volume in the amorphous region) is very similar to what was observed in the bulk material, where it shows an increase in the lifetime with temperature. It is also noted that there is a sudden decrease or a “flattening” in the longest lifetime at a temperature close to the melting temperature of the fraction which confirm the results observed earlier with the bulk.

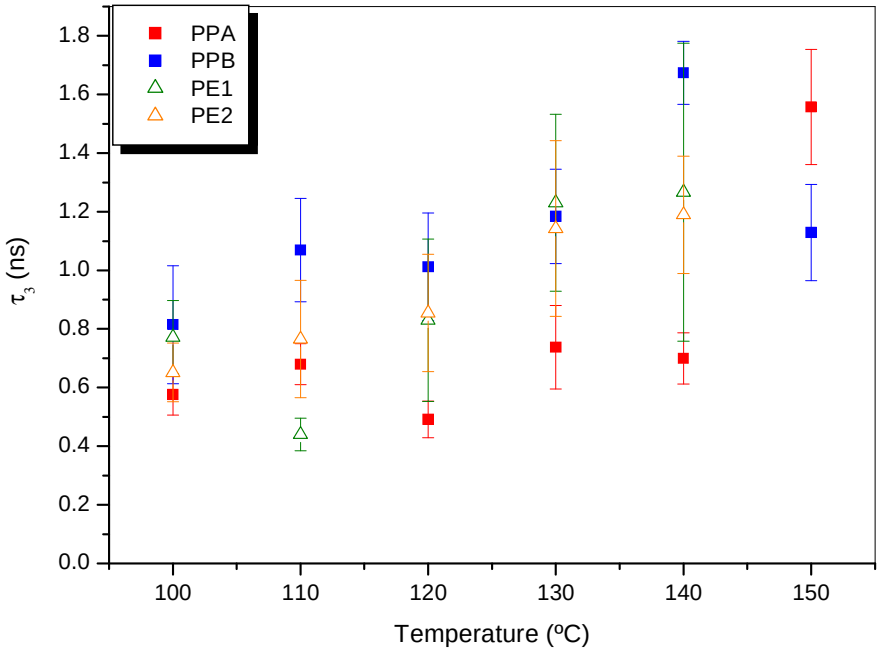

Figure 6.14 Lifetime τ_3 versus the temperature for 100 ºC fraction of all samples.

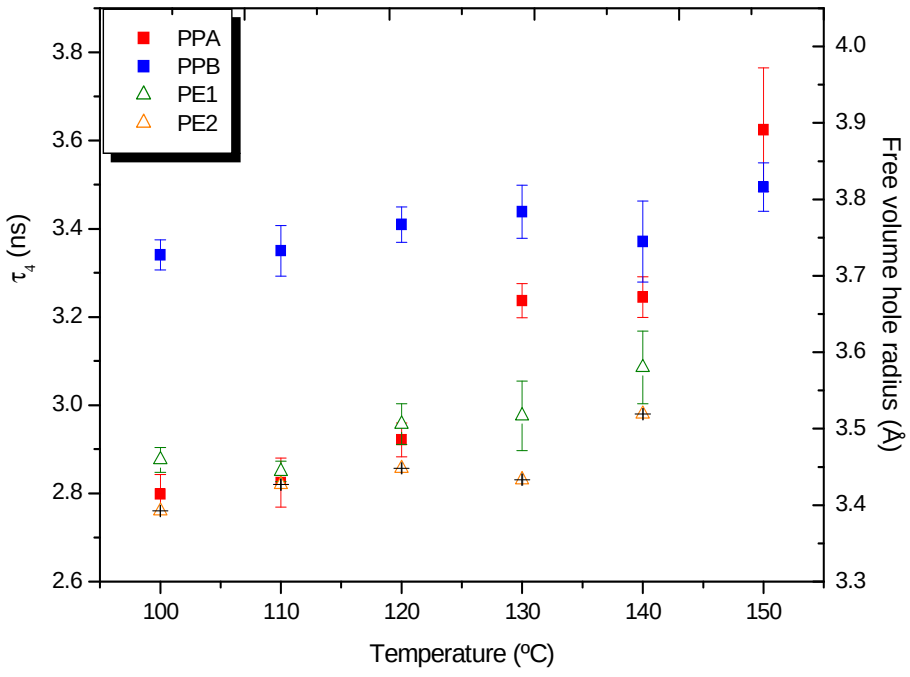

Figure 6.15 Lifetime τ_4 versus the temperature for 100 ºC fraction of all samples.

6.4 Conclusions

The effect of exposure time on the PALS measurement has been investigated; the results showed that there is no change in o-Ps lifetimes with exposure time during the PALS measurements; however the o-Ps intensity I_4 decreased with exposure time which indicates that only the Ps yield, the lifetime, are affected by the irradiation.

The temperature dependence of the positron annihilation parameters in the copolymers has been studied. This study presents an extension of those conducted previously, but in this case the positron annihilation parameters are measured for various morphologies by manipulation of the temperature. The results show that as the temperature increases, the lifetime τ_3 (the relative free volume hole size) associated with annihilation in crystalline regions), decreases for the propylene copolymers. This is most probably due to some degree of re-ordering in the crystalline regions. This process ultimately leads to a smaller mean hole size in these regions. In the case of the temperature study of the isolated fractions in the PP copolymers, τ_3 values generally increase in contrast to the bulk study. This attributed to the greater degree of homogeneity in chain structure and the resultant morphology in the fractions compared to the bulk samples and implied a lesser degree of reordering in these materials. The PE copolymers show very small increases (if any) in the τ_3 values. This implies that there is little change in the mean hole size in these regions as the melting temperature is reached. This observation can be extended to the studies in the previous chapters where it is seen that the τ_3 values in the ethylene copolymers shows little to no change with changes in crystal morphology as a result of fractionation or fraction removal. The propylene copolymers on the other hand, often showed complex variations across fractionation series or in the fraction removal studies and again in this study significant variations are seen. These variations are small and often within the limits of detection of the PALS technique as is indicated by the variation bars, but nevertheless the systematic variation in some cases implies that the changes are real and valid. The I_3 values in the present study show an

initial decrease with increasing temperature for all the copolymers, but interpretation of these values above the melting point of the materials becomes problematic.

The changes in the longest lifetime component associated with the amorphous phase show much larger change with changes in the temperature. There is a clear increase in the τ_4 lifetime (mean hole size) and intensity (I_4) with an increase in temperature. These increases can be associated with the "thermal expansion" of the amorphous areas and increased molecular motions. As the melting point is approached, the rate of increase in the τ_4 value decreases as crystalline areas begin to melt as a result addition of the less branched (or more isotactic) material to the amorphous phase.

Finally the issue of fitting a four component analysis to all the raw data in this chapter should be addressd. In this and other studies the third component of a four component fit is attributed to annihilation in regions associated with crystallinity. If this is the case, above the melting point it is clear that these values will have no physical significance. Arguably a three component fit should be used in the completely amorphous material where the third component now becomes the component associated with amorphous annihilation. In the present study attempts were made to delineate a point in the temperature profiles where a three component analysis gives a better fit than the four component analysis. This was largely unsuccessful. This is possibly due to the fact that there is not one single point (temperature) at which the complete transition from semi-crystalline to completely amorphous occurs. When the data is forcesd to a three component fit at some point based on a melting point, no definite trend can be observed. This highlights the challenges in analyzing and interpreting the significance of the various positron parameters. It also highlights why studies such as the present one are needed to be done in which systematic series of samples are analyzed.

The final chapter gives further discussion and insights into the reliability of the interpretation of the variation in the positron annihilation parameters in terms of the nature and type of crystallinity.

6.5 References:

1. Hsu, F H., Choi, Y J. and Hadley, J H. Radiation Physics and Chemistry 2000, 58, 473-477.
2. Abdel-Hady, E E., Mohamed, H F M. and Fareed, S S. Radiation Physics and Chemistry 2007, 76, 138-141.
3. Mohamed, H F M., Abdel-Hady, E E. and Mohamed, S S. Radiation Physics and Chemistry 2007, 76, 160-164.
4. Suzuki, T., Kondo, K., Hamada, E., Quan Chen, Z. and Ito, Y. Radiation Physics and Chemistry 2001, 60, 535-540.
5. Wang, J. and Quarles, C A. Radiation Physics and Chemistry 2003, 68, 527-529.
6. Djourelov, N., Suzuki, T., Shantarovich, V. and Kondo, K. Radiation Physics and Chemistry 2005, 72, 723-729.
7. Danch, A. and Osoba, W. Radiation Physics and Chemistry 2003, 68, 445-447.
8. Jean, Y C., Mallon, P E. and Schrader, D M. Principles and Applications of Positron & Positronium Chemistry; World Scientific: New Jersey, 2003.
9. Dlubek, G., Saarinen, K. and Fretwell, M. Journal of Polymer Science Part B: Polymer Physics 1998, 36, 1513-1528.
10. Nahid, F., Beling, C D. and Fung, S. Physica Status Solidi (c) 2007, 4, 3751-3754.
11. Chenze, Q., Dong, M., Youha, H F., Yan, H Z., Yang, X. and Zhou, T W. Journal of Polymer Science Part B: Polymer Physics 2001, 39, 332-336.
12. Hill, A J., Jones, P L., Lind, J H. and Pearsall, G W. Journal of Polymer Science Part A: Polymer Chemistry 1988, 26, 1541-1552.
13. Badia, A. and Duplâtre, G. Radiation Physics and Chemistry 1999, 54, 151-158.
14. Peng, Z L., Olson, B G., McGervey, J D. and Jamieson, A M. Polymer 1999, 40, 3033-3040.
15. Peng, Z L., Itoh, Y., Li, S Q. and Wang, S J. Physica Status Solidi (a) 1996, 155, 299-303.
16. Wang, B., Wang, Z F., Zhang, M., Liu, W H. and Wang, S J. Macromolecules 2002, 35, 3993-3996.

17. Abdel-Hady, E E., Hamdy, F M M. and El-Sharkawy, M R M. Physica Status Solidi (c) 2009, 6, 2420-2422.
18. Kluin, J E., Yu, Z., Vleeshouwers, S., McGervey, J D., Jamieson, A M. and Simha, R. Macromolecules 1992, 25, 5089-5093.
19. Uedono, A., Kawano, T., Tanigawa, S., Ban, M., Kyoto, M. and Uozumi, T. Journal of Polymer Science Part B: Polymer Physics 1996, 34, 2145-2151.
20. Uedono, A., Kawano, T., Tanigawa, S., Ban, M., Kyoto, M. and Uozumi, T. Journal of Polymer Science Part B: Polymer Physics 1997, 35, 1601-1609.

Chapter 7
Conclusions and recommendations

7.1 Conclusions

The purpose of this study was to conduct a systematic investigation of the variation in the positron annihilation parameters (via positron annihilation lifetime spectroscopy) with polymer structure and morphology in semicrystalline polymers. This is necessary due to the complex morphology of these materials and the resultant complications that arise in the analysis and interpretation of the positron annihilation lifetime data. This lack of clarity has at least partially been responsible for the fact that there is not consensus in literature as to the number and interpretation of the various o-Ps lifetimes in these morphologically complex materials. In this study a systematic approach has been taken to shed light on the analysis and subsequent interpretation of the positron parameters in semi-crystalline polyolefin polymers.

This study took the approach of producing systematic polymer series by using preparative TREF fractionation to produce homogeneously crystallizable materials. It was further expanded to study the same materials but varying the morphology by selective removal of specific crystallizable fractions. Lastly, a new temperature probe was designed and developed to study the temperature dependence of the positron annihilation parameter in the copolymer materials.

The conclusions of this study can be divided into specific observations and conclusions based on the material types (ethylene or propylene copolymers with variation in short chain length, short chain branching and tacticity) and more general observations and conclusions as to the reliability and ultimately the interpretation of the positron annihilation parameters and their significance in terms of real physical structural parameters.

Several polyolefin polymers of differing molecular structure were selected for this study. In the first part of the study, two LLDPE of differing comonomer type (a 1-octene and a 1-hexene) were selected to study the effects of short chain branching on the morphology and subsequent measurement of the positron annihilation parameters. Preparative TREF fractionation was used to provide systematic series of samples with differing branching contents. This approach was selected over using different LLDPE samples since it provides sample series with better control over branching content. In addition to the sample series produced by the preparative fractionation, several additional samples series with differing crystalline contents and morphology were produceed by removing selective TREF fractions from the materials.

In this study, clear differences in the variation of the longest o-Ps lifetime parameter (τ_4) and yield (I_4) were observed as a function of both the length, content and distribution of the short chain branching in the material. These two parameters give the mean free volume hole size and relative hole number of the amorphous phase respectively. In addition clear differences are seen for the 1-octene and 1-hexane series. These positron parameters can be used to estimate the relative free volume of the amorphous phase. It was shown that in the case of the ethylene copolymer series there is a remarkable correlation between the measured fractional free volume of the amorphous phase and the bulk physical property of the microhardness. This correlation is observed in the fractionation study as well as the fraction removal study (although to a lesser degree). This correlation suggests that the nature of the amorphous phase is at least partially responsible for changes in the microhardness although the crystallinity degree plays the dominate role in determining the microhardness. This is the first direct measurement of the contribution of the amorphous phase to the microhardness in semi-crystalline polymers. It is, unfortunately not possible to make a quantitative estimation of the amorphous contribution, but nevertheless these results show at least from a qualitative point of view there is a contribution.

The variation of the third lifetime component (which is attributed to o-Ps annihilation in region of crystallinity in this and other studies), shows far less dramatic variations with chain structural parameters or changes in the crystallinity. There are very

small (if any) changes in the τ_3 lifetime with changes in the nature (predominantly the amount) of crystallinity in both the fractionation and fraction removal studies where slightly larger values are determined for the higher crystallinity materials. This indicates that the relative size and nature of the defects remains the same across the various series. Minimal variation in the I_3 values is observed in these copolymers except in the heating study where a decrease is observed on heating. If the I_3 values is considered to be proportional to the "number of defects" associated with the crystalline region then these results imply that there is little change in this number with changing crystallinity in the copolymers. In this particular study, the small changes may also be a result of the increasingly "more prefect" crystalline structures in the PE copolymers as a result of the fractionation, which goes hand in hand with the increased crystallinity of the higher temperature fractions. This argument is somewhat supported by the fact the greater changes are seen in the I_3 values in the fraction removal study relative to the fractionation study.

In the second part of the study, a structurally far more complex polymer (and consequently far more complex morphology) is studied. Two polypropylene copolymers and a polypropylene homopolymer were selected in order to establish the effect of both tacticity and short-chain branching on the measured positron annihilation parameters. Once again preparative TREF fractionation was used to produce polymer series with different comonomer contents and tacticities. The effect of removal of selective TREF fractions from the materials was also discussed for this complex system.

It was shown that the tacticity of polypropylene has little to no effect on the third component lifetime, but the longest lifetime τ_4 show a clear dependence where the value decreases (decreased mean hole size of the amorphous region decrease) with a higher percentage isotactic sequences of the chains.

The degree of structural and morphological complexity in the propylene copolymers is reflected in the often complex variation in the various positron annihilation parameters in the fractionation study, the fractional removal study and the temperature study. Nevertheless, as was the case for the ethylene copolymers, the longest o-Ps

lifetime τ_4 and yield (I_4) showed clear variation in these copolymers as a result of tacticity as well as short chain branching differences in the amorphous phase of the materials. It is for example, shown that the higher pentene content of the PPB copolymer relative to the PPA copolymer in the same temperature fraction results in a higher relative fractional free volume. The shorter third component lifetime (τ_3) and yield (I_3) also showed often complex variations. In general, this component showed greater variation in the propylene copolymer series than the ethylene copolymer series. This is reflective of not only the far more complex chain structures, but also of the complexity of the morphology of the propylene copolymers relative to the ethylene copolymers.

One of the most important results in this study was the correlation of the change in the third lifetime component (τ_3) with the changes in the T_m values determined by DSC in the fraction removal study. This result provides compelling evidence for the interpretation of at least the lifetime of this component being associated with the crystal structure. In the heating study, this third lifetime component showed significant decreases particularly in the case of one of the copolymers and this is again consistent with possible changes occurring in the crystal structure as the melting point is reached.

A correlation between the relative free volume of the amorphous phase and the microhardness was also found for these copolymer series but in the case of the fraction removal study the opposite correlation is found. This is reflective of the fact that in this copolymer series the nature and amount of crystallinity is the dominate factor in determining the microhardness.

7.2 General conclusions and comments

The results of this study confirm that in the semi-crystalline polymers studied, positronium may be formed in both the crystalline and amorphous phases. Strong evidence is found for the correlation of the third lifetime component being associated with o-PS annihilation in the crystalline regions. This may take place in three possible regions. The first region is the open amorphous texture and interfaces in spherulites and secondly; the interlamellar phase and lamellar defects, and finally; interstitial cavity in

the crystalline unit cell. Evidence is found in this study to support at least the τ_3 values (hole size) being reliable as a measure of the mean hole sizes of these defect or interstitial region. On the other hand, there is little evidence of significant variation in the I_3 values with the amount or nature of the crystallinity although in some case there is a clearer variation. This may be a result of a number of reasons. Firstly, any variation in the defect number difference between samples is relatively small and beyond the detection limits of the I_3 intensities. Secondly, the more highly crystalline materials in this study are inevitably also the less branched materials and would of course be expected to have less "defects" in the crystal structure. Certainly this would be expected in the fractionation study.

Lastly it should be noted that in all cases the raw positron data was best fitted with a four component analysis. This is true even for the samples that are measured above their crystalline melting points. It is important to note that when there is no crystallinity present in the samples, it is difficult to attach any real physical significance to the third lifetime component and intensity. Attempts were made to delineate a point (temperature) in the analysis of the raw positron data at which the data is best fitted with a three component fit rather than a four component fit. This is, however, extremely difficult and no definite point or temperature could be determined. Intuitively it would be expected to occur when no crystallinity is present. In the present study the data was presented across the entire temperature series with a four component fit (variation in both τ_3, τ_4 and I_3 and I_4) partially because of the fitting parameters, but also on the grounds that the trends make sense. This point highlights the challenges in analyzing and interpreting the positron annihilation lifetime data.

It is clear that the often complex chain structures and resultant complex morphologies in polyolefin polymers results in sometimes complex variations in the positron annihilation lifetime parameters. The study has highlighted the dangers of simple interpretation of the positron annihilation parameters in isolated polyolefin samples. It is hoped that the results and insights presented in this study will contribute to a better

understanding and interpretation of the relationship between the chain structure, morphology, physical properties and the measured positron annihilation lifetime parameters.

7.3 References

1. José, C M., Glaura, G S., Fernando, C d O., Rodrigo, L L., Jacques, R., Pedro, L. and Dario, W. Journal of Polymer Science Part B: Polymer Physics 2007, 45, 2400-2409.
2. Dlubek, G., Stejny, J., Th, L., Bamford, D., Petters, K., Ch, H., Alam, M A. and Hill, M J. Journal of Polymer Science Part B: Polymer Physics 2002, 40, 65-81.
3. Hosoda, S. Polymer 1988, 20, 383.

Appendix

Appendix A

(The raw data of TREF fractions)

Appendix A1: The raw data of the PE1 obtained after fractionation

Temperature (ºC)	Mass (g)	Wi %	ΣWi %	Wi%/ΔT
20	0.14	6.49	6.49	0.32
30	0.12	5.54	12.0	0.55
40	0.09	4.14	16.1	0.41
50	0.11	5.45	21.63	0.54
60	0.37	17.45	39.08	1.74
70	0.52	24.6	63.69	2.46
80	0.37	17.39	81.09	1.73
90	0.23	10.56	91.65	1.05
100	0.11	5.06	96.72	0.50
110	0.037	1.69	98.41	0.17
120	0.024	1.14	100	0.11

Appendix A2: The raw data of the PE2 obtained after fractionation

Temperature (ºC)	Mass (g)	Wi %	ΣWi %	Wi%/ΔT
20	0.01	0.78	0.78	0.15
30	0.03	1.55	2.33	0.15
40	0.03	1.29	3.63	0.13
50	0.03	1.29	4.93	0.13
60	0.04	1.81	6.75	0.18
70	0.15	7.53	14.28	0.75
80	0.50	24.15	38.44	2.41
90	0.72	34.80	73.24	3.48
100	0.37	17.92	91.16	1.79
110	0.16	7.798	98.96	0.78
120	0.02	1.031	100	0.10

Appendix A3: The raw data of the PPA obtained after fractionation

Temperature (ºC)	Mass (g)	Wi %	ΣWi %	Wi%/ΔT
20	0.11	3.82	3.82	0.19
30	0.02	0.85	4.67	0.08
40	0.01	0.32	4.99	0.03
50	0.01	0.59	5.58	0.06
60	0.03	1.16	6.74	0.11
70	0.07	2.61	9.35	0.26
80	0.16	5.73	15.08	0.57
90	0.30	10.70	25.78	1.06
100	0.91	32.02	57.80	3.20
110	0.56	19.64	77.44	1.96
120	0.28	9.94	87.38	0.99
130	0.21	7.38	94.75	0.73
140	0.15	5.25	100	0.52

Appendix A4: The raw data of the PPB obtained after fractionation

Temperature (ºC)	Mass (g)	Wi %	ΣWi %	Wi%/ΔT
20	0.05	2.38	2.38	0.02
30	0.02	0.82	3.14	0.01
40	0.01	0.60	3.72	0.01
50	0.02	1.04	4.74	0.01
60	0.04	1.99	6.70	0.02
70	0.07	3.67	10.32	0.03
80	0.15	7.08	17.27	0.07
90	0.26	12.13	29.18	0.12
100	1.08	51.52	79.79	0.51
110	0.20	9.49	89.11	0.10
120	0.12	5.76	94.77	0.05
130	0.07	3.536	98.24	0.03
140	0.05	2.38	100	0.02

Appendix B

(CRYSTAF traces)

Appendix B1 : The CRYSTAF trace of bulk PE1.

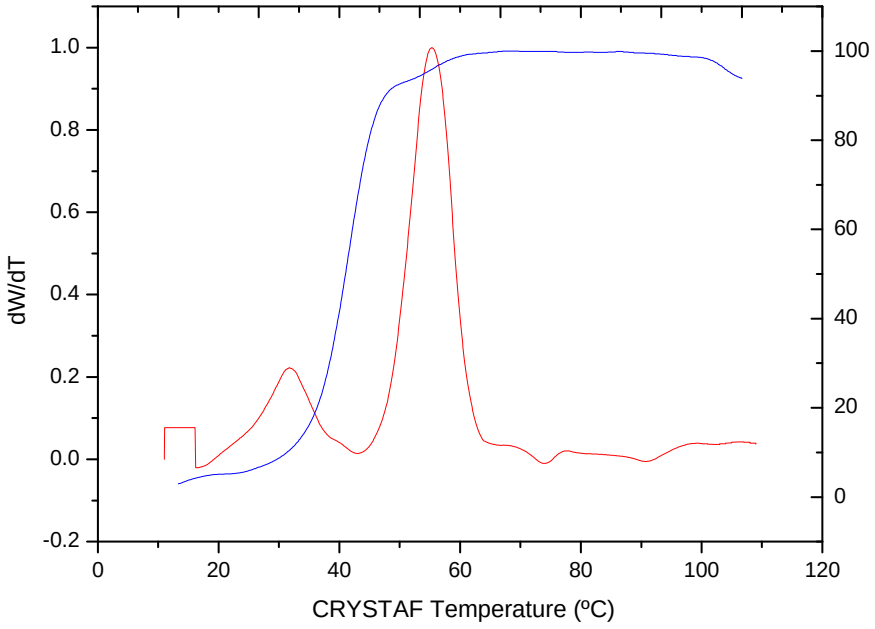

Appendix B2 : The CRYSTAF trace of bulk PE2.

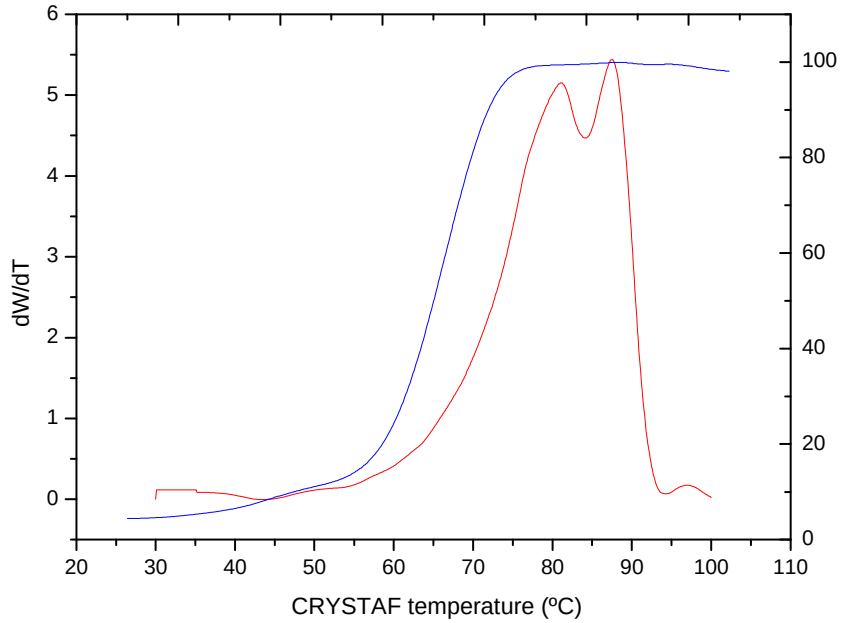

Appendix B3 : The CRYSTAF trace of bulk PPA

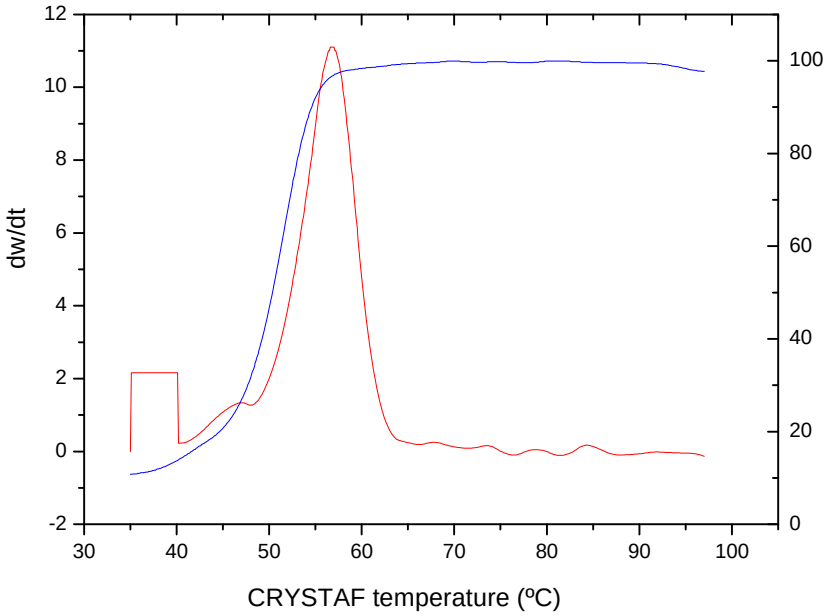

Appendix B4 : The CRYSTAF trace of bulk PPB

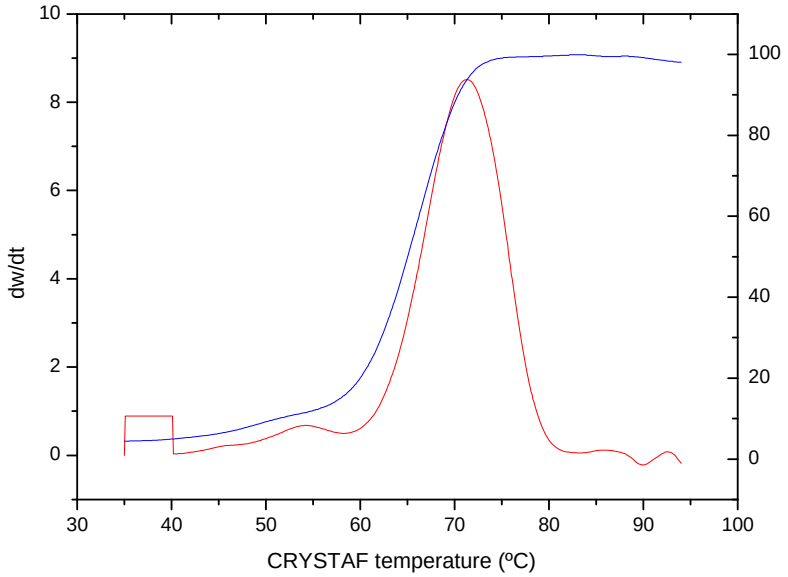

Appendix B5 : The CRYSTAF traces of the fractionated PE1.

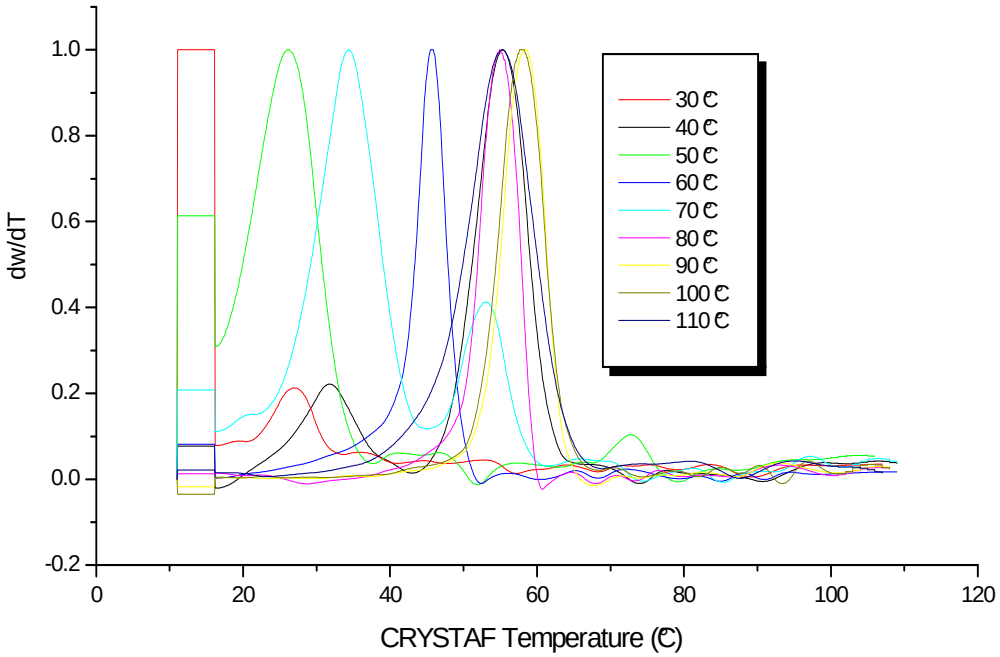

Appendix B6 : The CRYSTAF traces of the fractionated PE2.

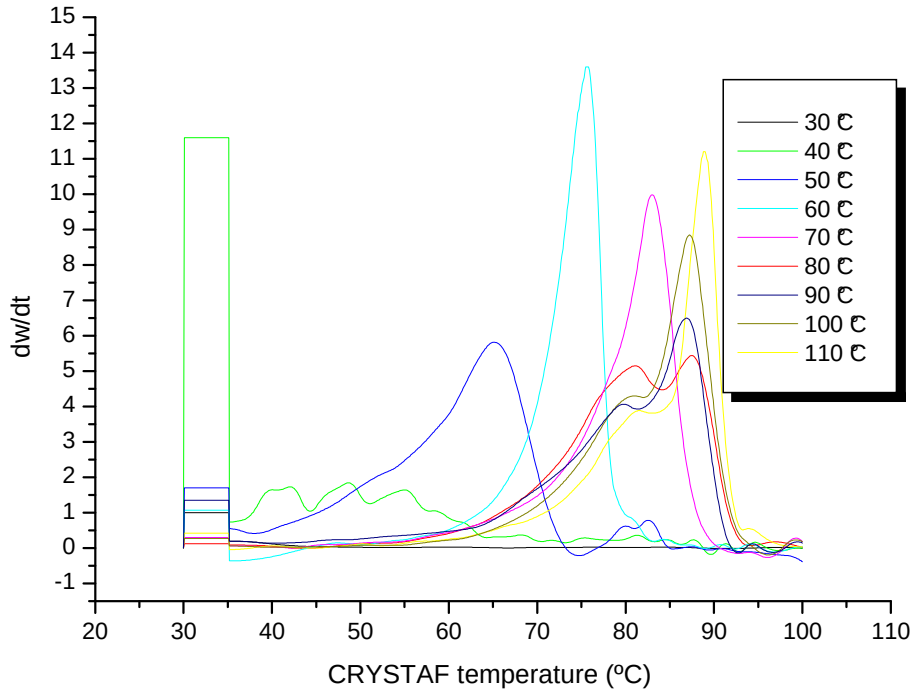

Appendix B7 : The CRYSTAF traces of the fractionated PPA.

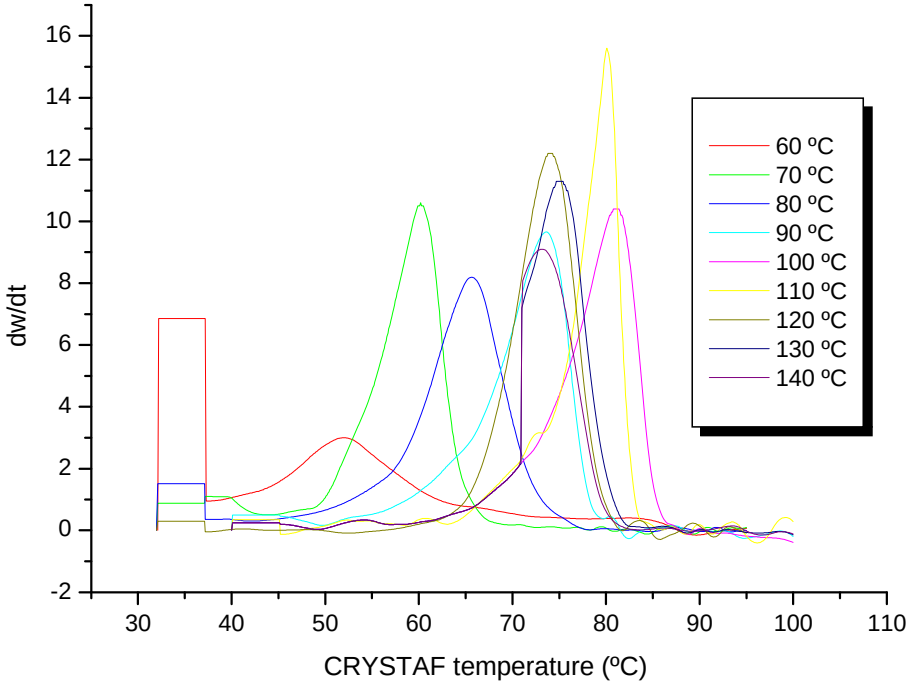

Appendix B8 : The CRYSTAF traces of the fractionated PPB.

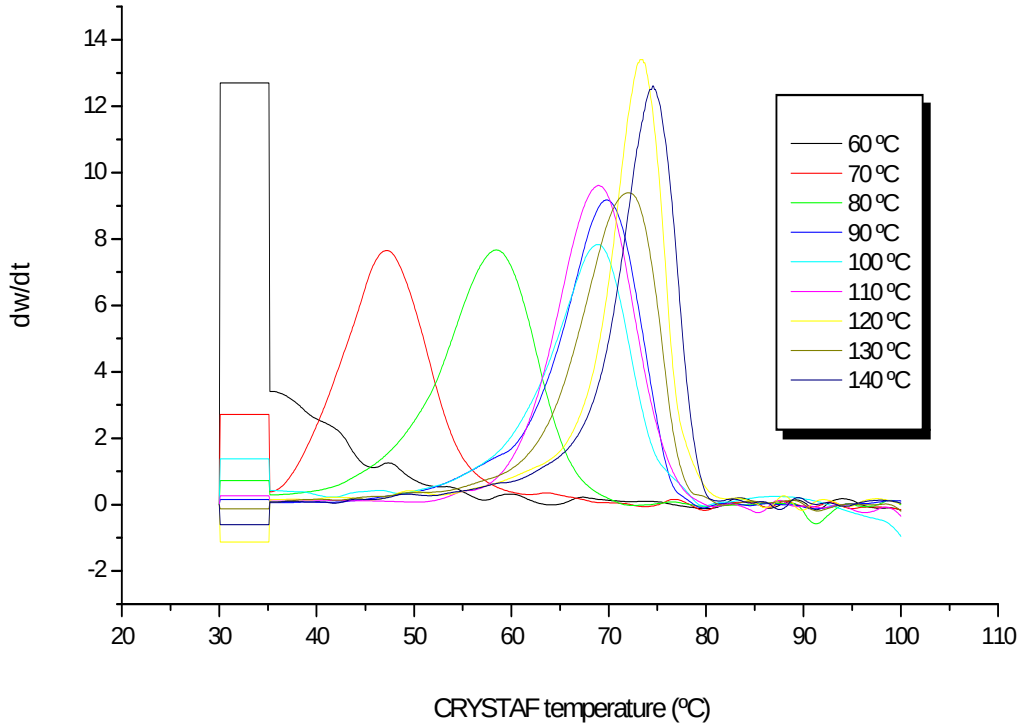

Appendix C

(DSC data)

Appendix C1: DSC heating and cooling curve of bulk PE1.

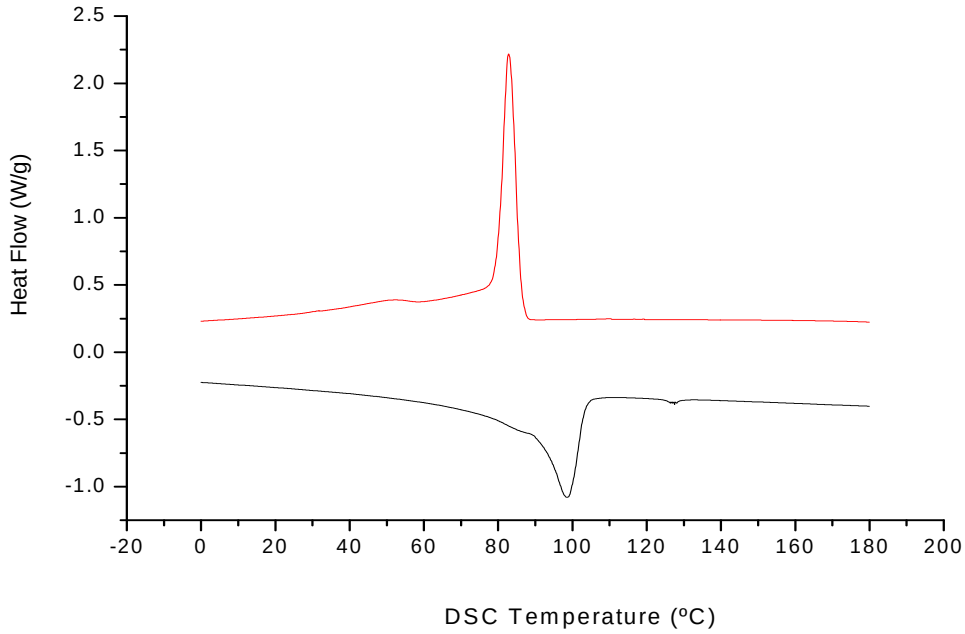

Appendix C2: DSC heating and cooling curve of bulk PE2

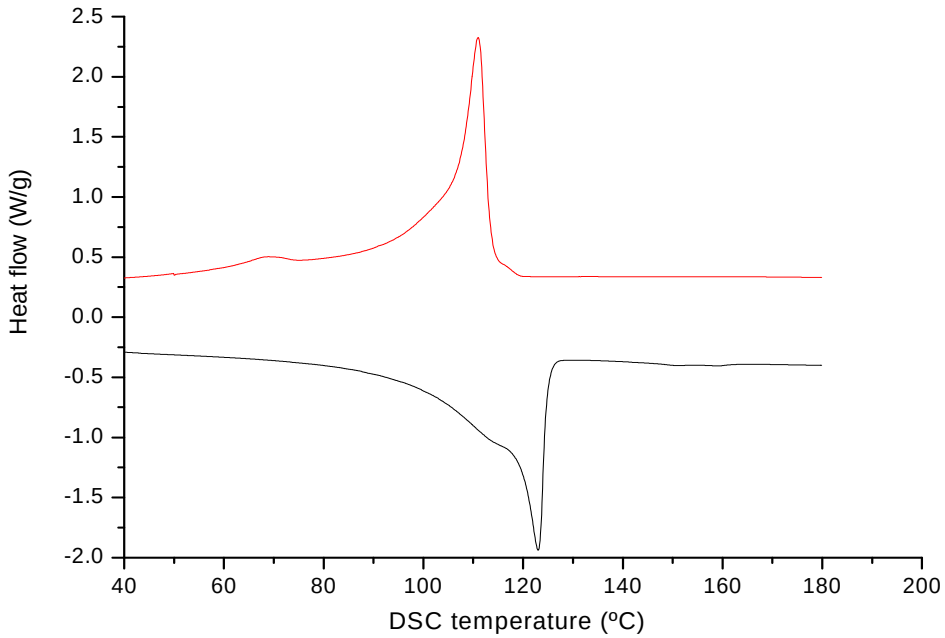

Appendix C3: DSC heating and cooling curve of bulk PPA.

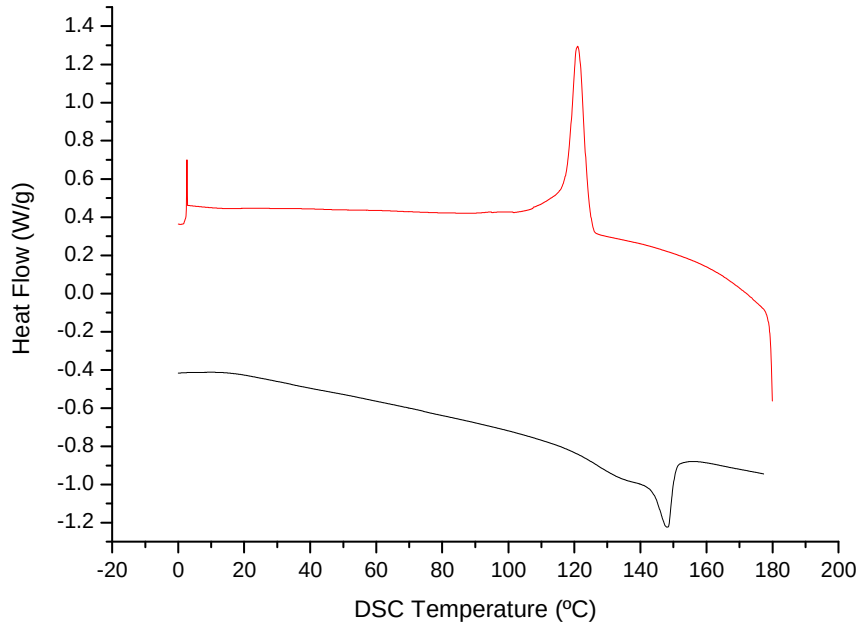

Appendix C4: DSC heating and cooling curve of bulk PPB.

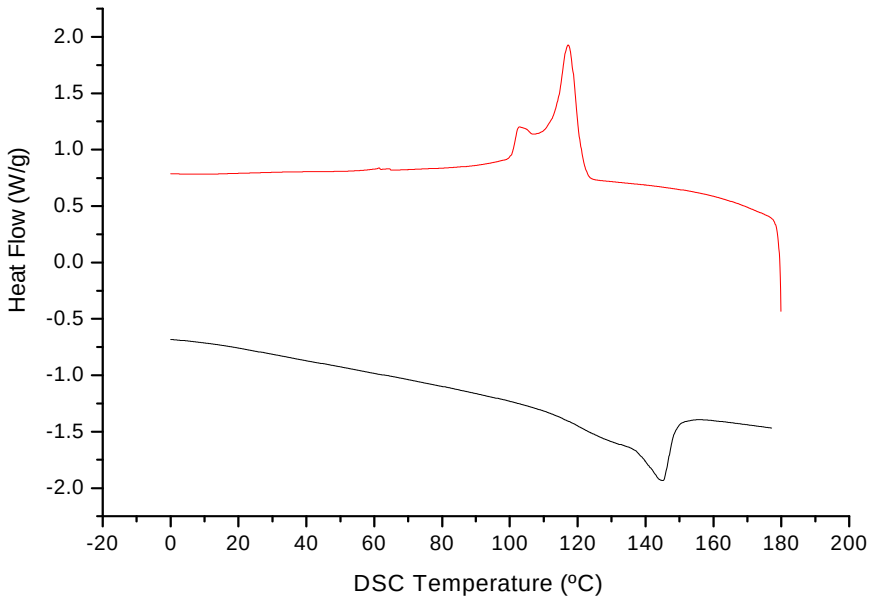

Appendix C5: The DSC melting endotherms for the PE1 fractions

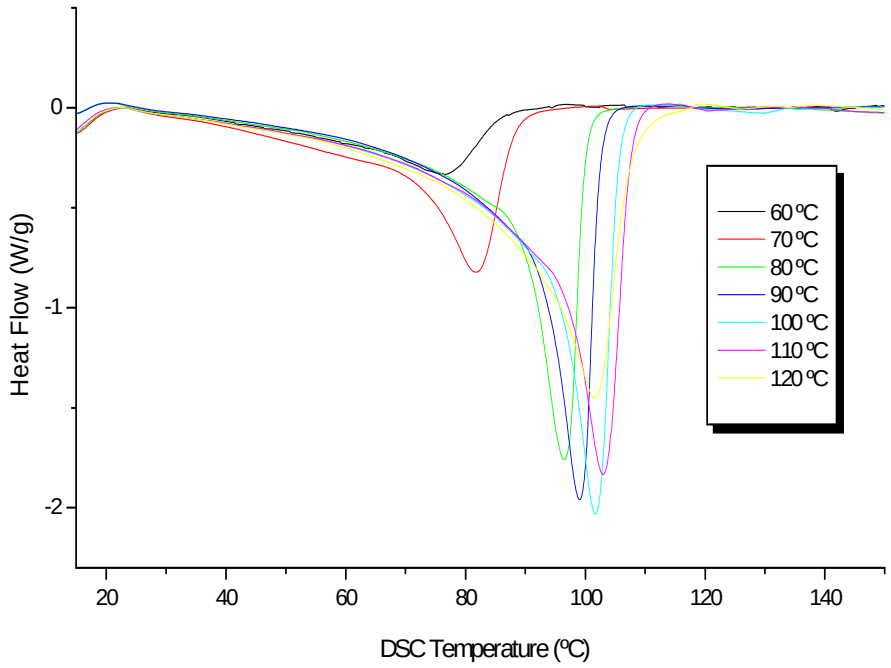

Appendix C6: The DSC melting endotherms for the PE2 fractions

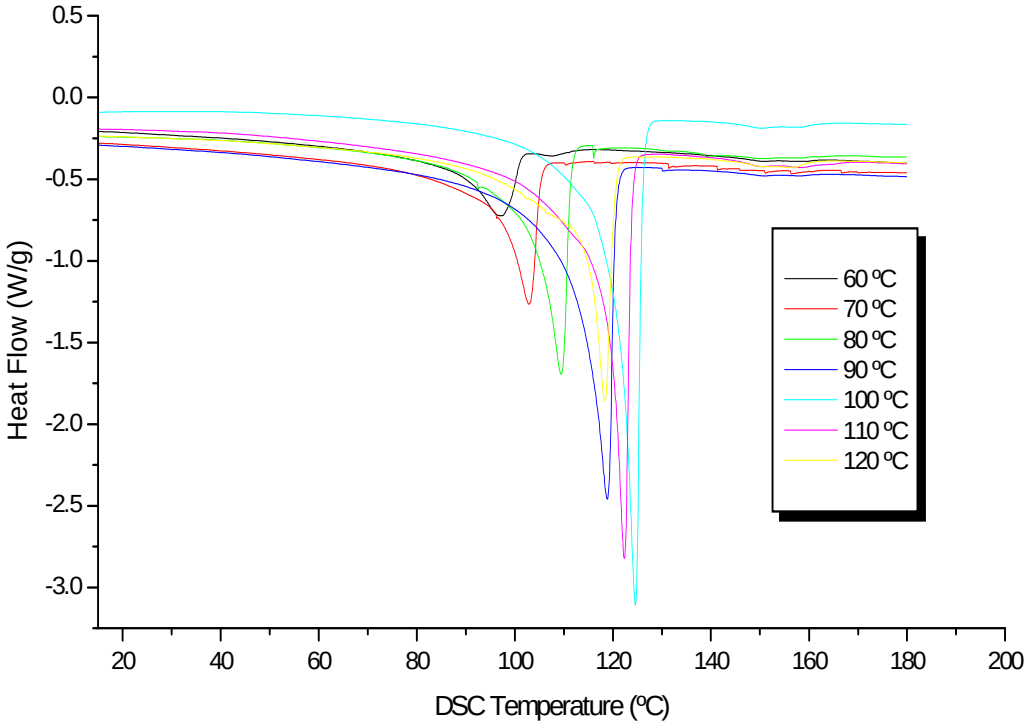

Appendix C7: The DSC melting endotherms for the PPA fractions.

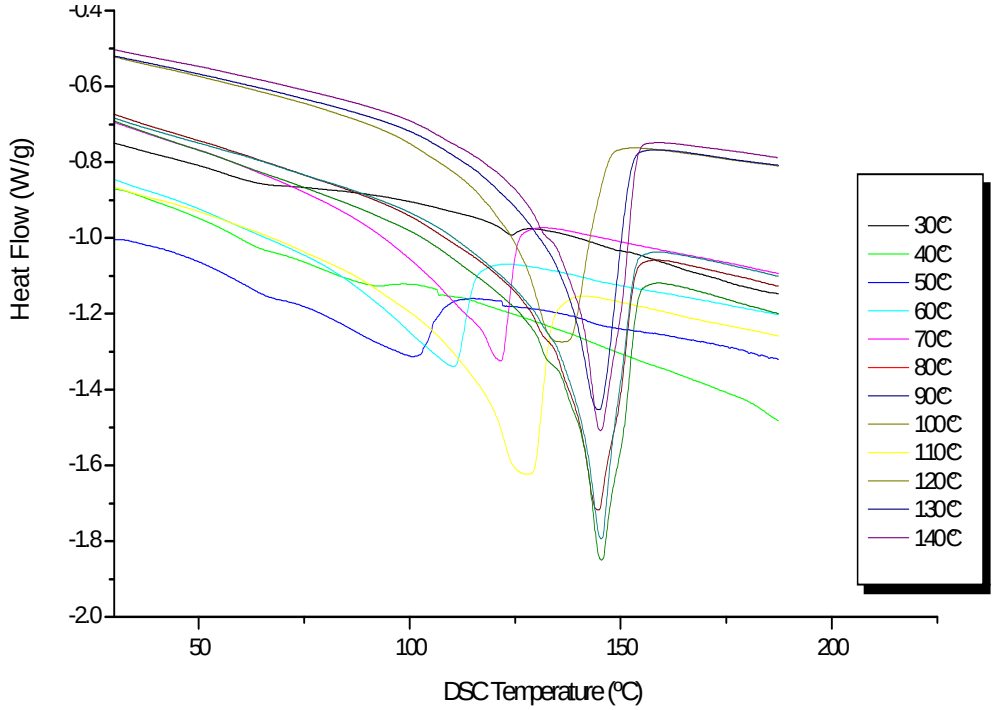

Appendix C8: The DSC melting endotherms for the PPB fractions.

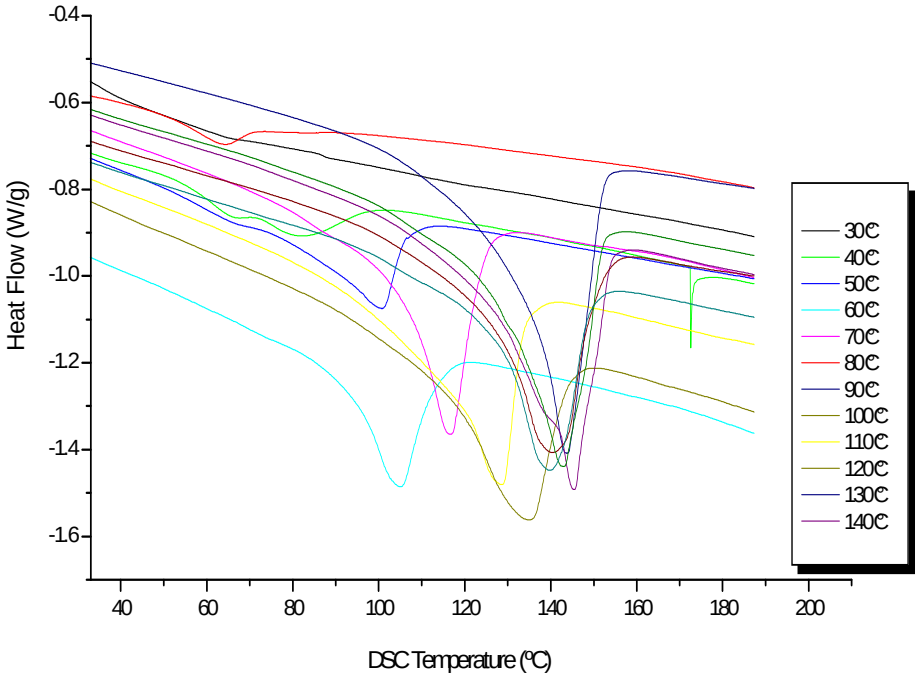

Appendix D

(NMR data and comonomer content)

Appendix D1 : The ^{13} C-NMR of the bulk PE1

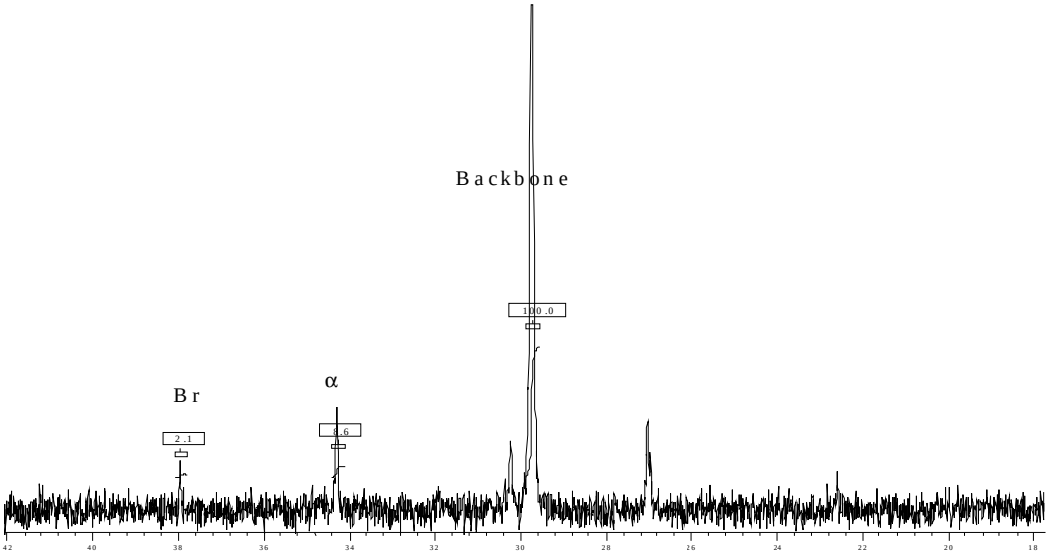

Appendix D2 : The ^{13} C-NMR of the bulk PE2

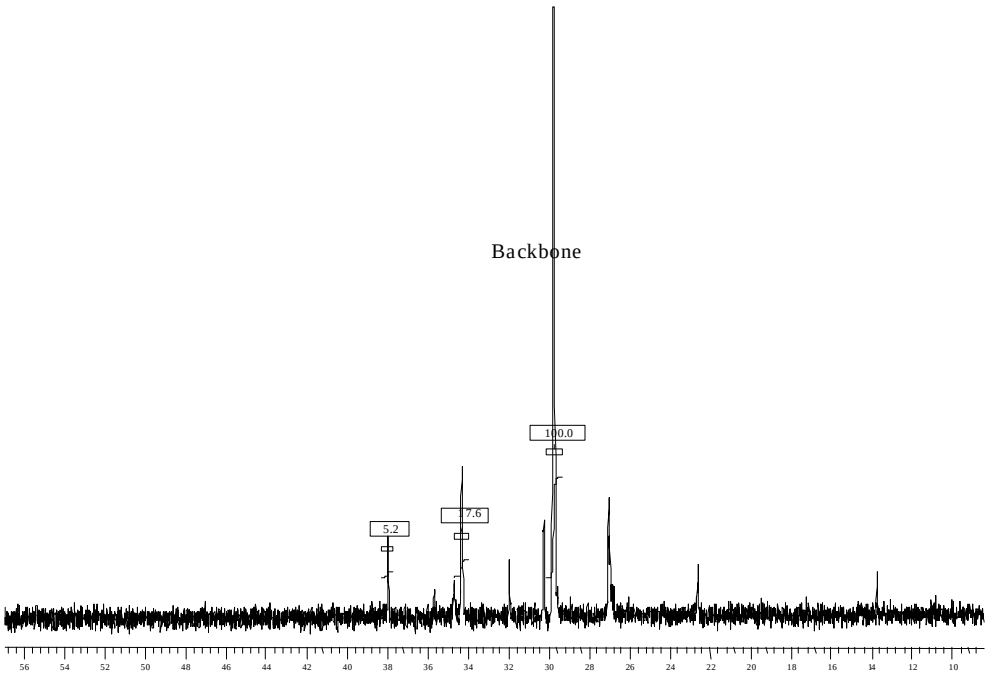

Appendix D3 : The ^{13} C-NMR of the bulk PPA

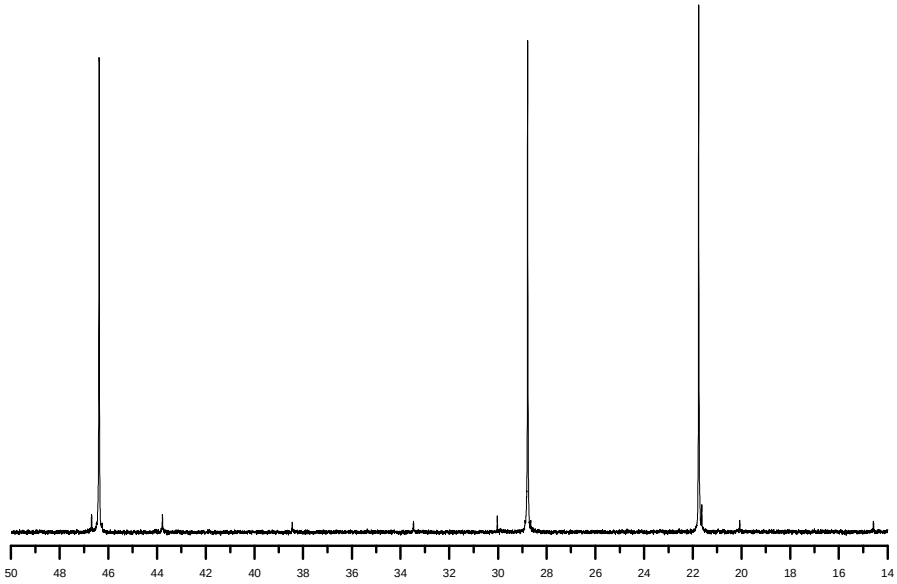

Appendix D4 : The ^{13} C-NMR of the bulk PPB

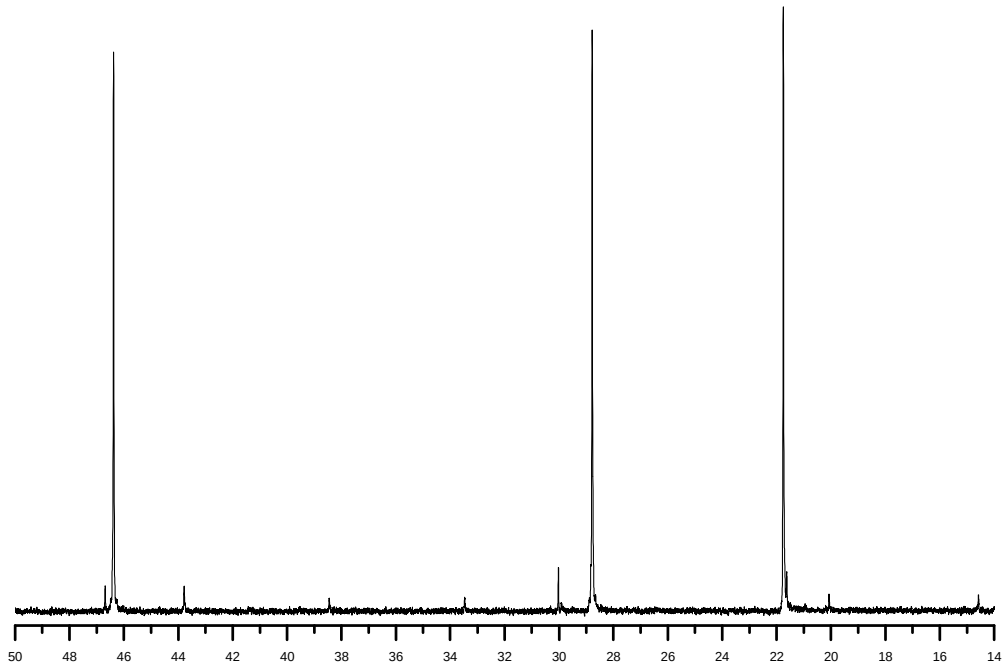

Appendix D5: Comonomer content as a function of the melting and crystallization temperature of PPA.

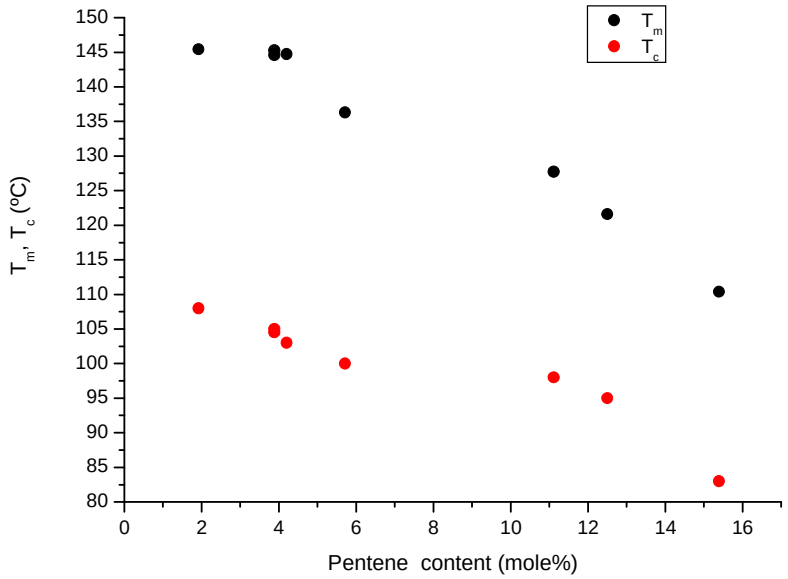

Appendix D6: Comonomer content as a function of the melting and crystallization temperature of PPB.

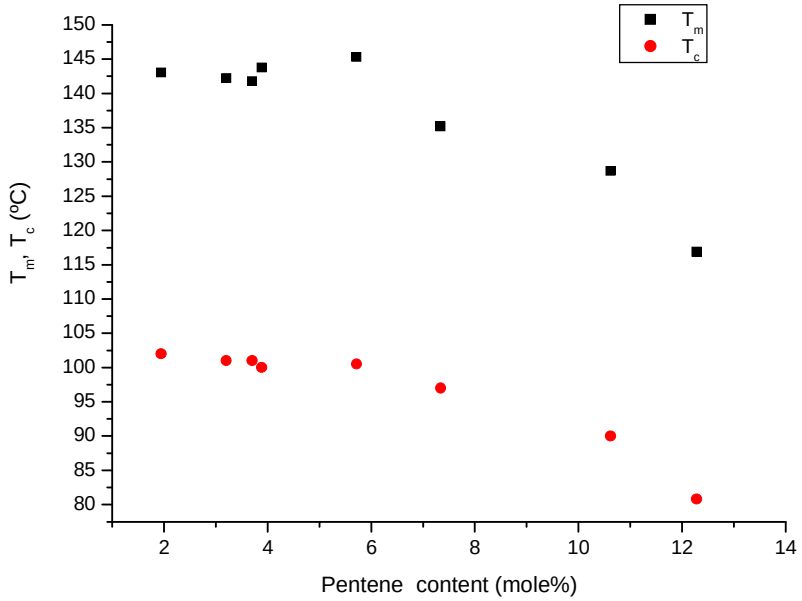

Appendix E

(Positron data)

Appendix E1: The output of PATFIT program

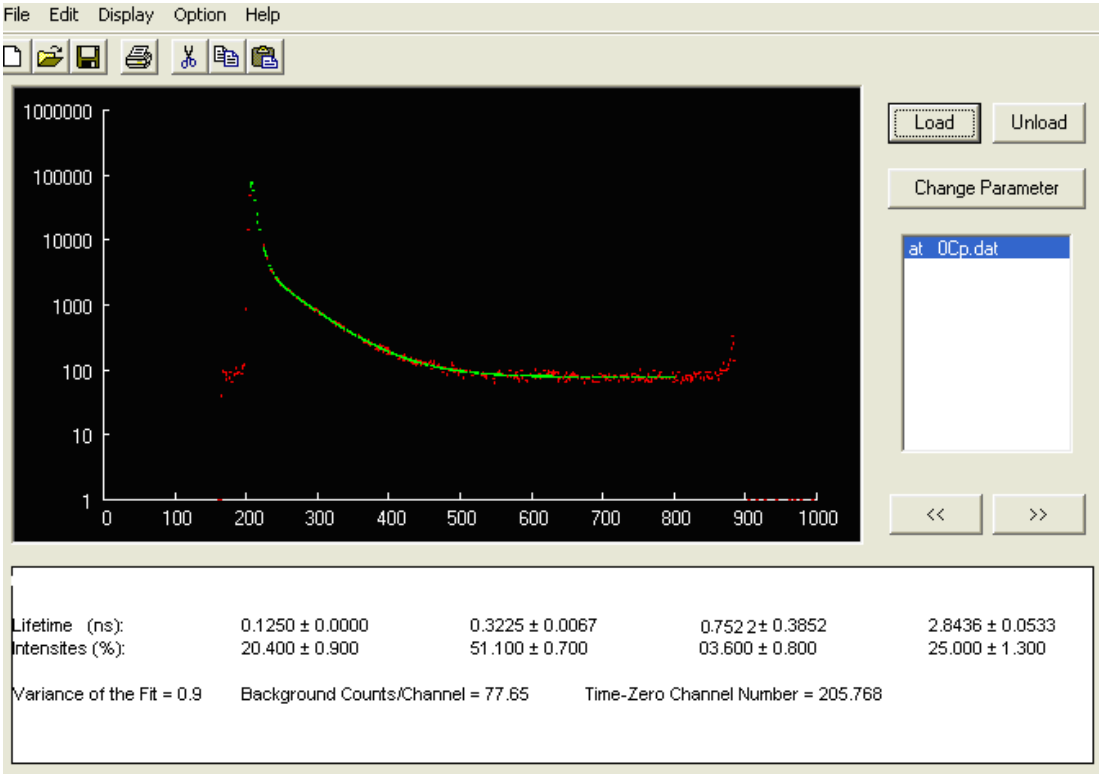

Appendix E2: Effects of removed TREF fractions on the free volume hole radius of PE1 and PE2

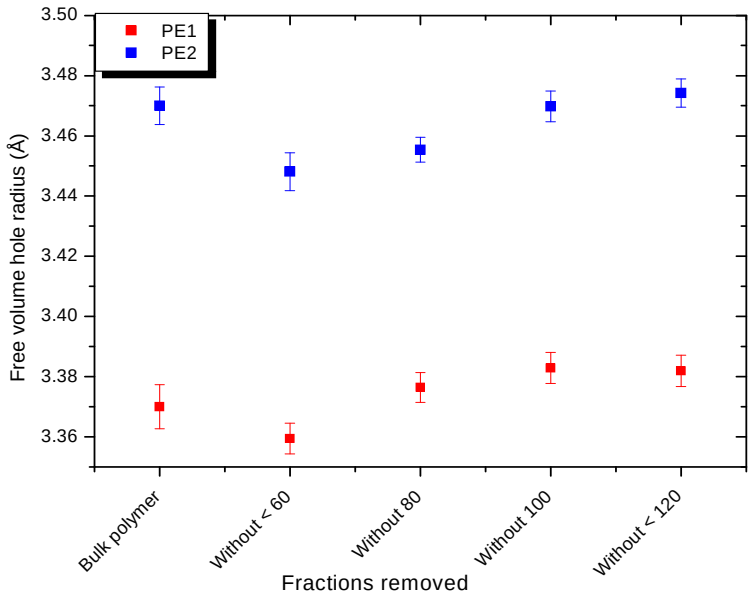

.

Appendix E3: Effects of removed TREF fractions on the free volume hole radius of PPA and PPB.